Research Article

Life Conflux

Transcription Factors as Early Diagnostic Biomarkers for Chronic Kidney Disease: A Comprehensive Analysis

Authors

Wei Zhou, Qingqing Jia, Shujun Wu, Hanyan Meng, Xinyu Wang, Mingzhu Jiang, Jianhua Mao

Correspondence

maojh88@zju.edu.cn (J. Mao)

Graphical Abstract

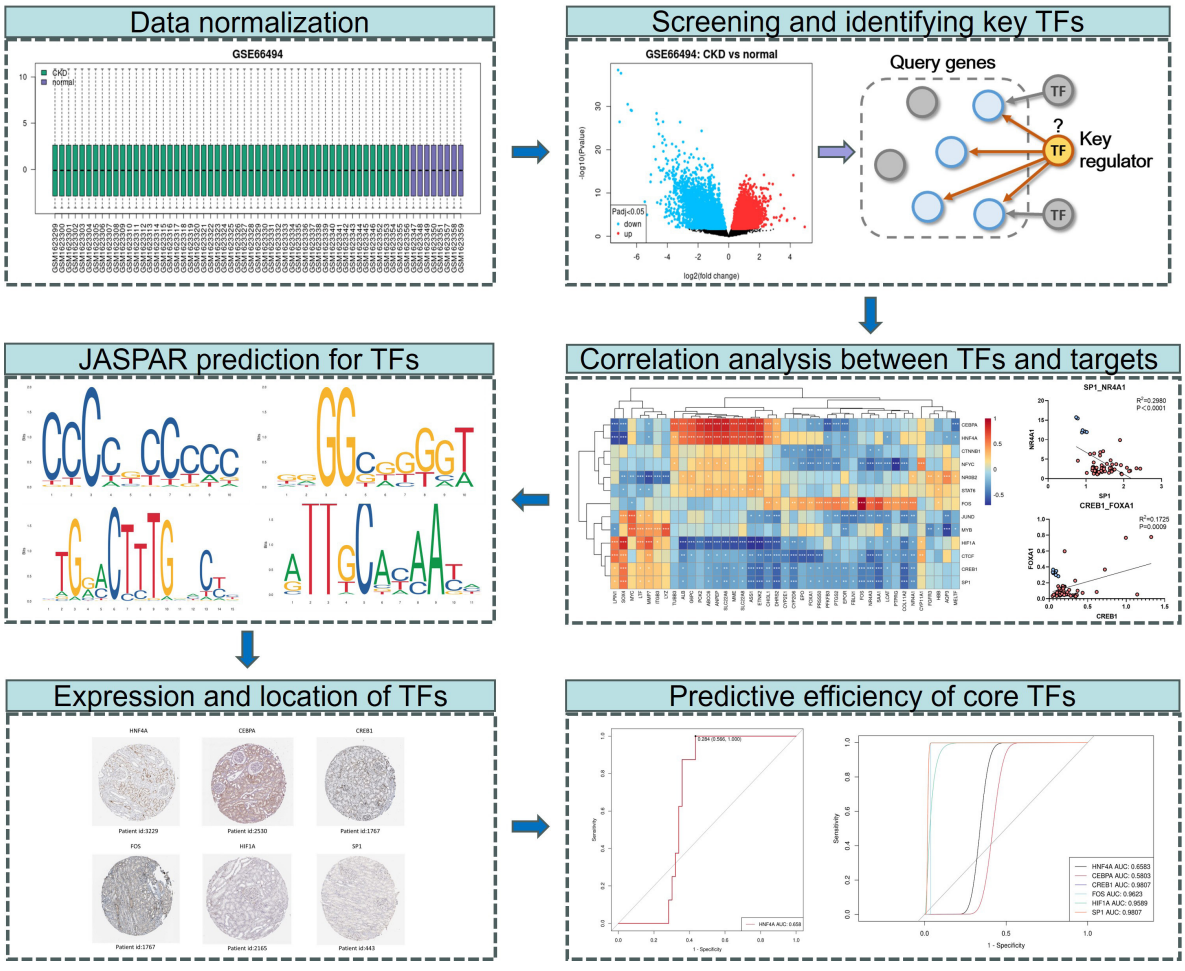

https://doi.org/10.71321/1pe9g186

Research Article

Life Conflux

Transcription Factors as Early Diagnostic Biomarkers for Chronic Kidney Disease: A Comprehensive Analysis

Wei Zhou [1†], Qingqing Jia [2†], Shujun Wu [3†], Hanyan Meng [1], Xinyu Wang [4], Mingzhu Jiang [3], Jianhua Mao [1*]

Received: 2025-03-12 | Accepted: 2025-12-11 | Published online: 2026-02-07

Abstract

Background: Chronic kidney disease (CKD) is a global health concern with significant implications for public health and mortality rates, projected to become the fifth leading cause of death by 2040. The search for early diagnostic targets for CKD is imperative. In this study, we concentrated on identifying key transcription factors (TFs) for the early diagnosis of CKD and established a regulatory network between these TFs and their corresponding target genes.

Methods: We conducted microarray data analysis and Gene Set Enrichment Analysis (GSEA) to identify differentially expressed genes (DEGs) and the associated pathways in CKD. We further explored the potential regulatory TFs among DEGs using the TRRUST v2 database and validated the TF-target regulatory relationships through correlation analysis and the JASPAR database. The protein expression of the identified TFs in renal tissues was also assessed.

Results: The analysis identified six TFs, namely HNF4A, CEBPA, CREB1, FOS, HIF1A, and SP1, which demonstrated potential as diagnostic biomarkers for CKD. These TFs showed differentially expressed patterns in CKD and were found to have multiple regulatory relationships with DEGs, indicating their crucial role in the disease process. ROC analysis revealed high predictive efficiency for four of these TFs (CREB1, FOS, HIF1A, and SP1), while the combined predictive efficiency of all TFs was exceptionally high.

Conclusion: Our findings highlight the role of transcription factors in the pathophysiological process of CKD and identify several key TFs with potential for clinical translation as early diagnostic biomarkers for the disease. Further validation and exploration are warranted to leverage the potential clinical utility of these TFs in the early diagnosis and prognosis of CKD.

Keywords: Chronic kidney disease; Transcription factor; Biomarker; Data analysis

Introduction

Chronic kidney disease (CKD) has emerged as a significant healthcare issue, affecting individuals across all age groups worldwide, which is expected to become the fifth leading cause of death by 2040 [1-2]. Despite the different etiologies of CKD, its prolonged and incurable process ultimately results in end-stage kidney disease (ESKD), which requires renal replacement therapy [3]. CKD is an independent risk factor for acute kidney injury (AKI), and AKI further aggravates the development and process of CKD [2, 4].

Renal fibrosis is the most important pathological feature of ESKD, which is characterized by glomerulosclerosis, interstitial fibrosis, and immune cell infiltration in the kidney [5-7]. Renal fibrosis is accompanied by pathological accumulation of extracellular matrix (ECM) proteins, including collagens and fibronectin [8]. However, excessive deposition of ECM in the kidney usually means the late irreversible stage of ESKD. A significant limitation of conventional renal function assessment, which depends on serum creatinine, BUN, and urine-specific gravity, is its inability to reliably detect subclinical renal dysfunction, despite its effectiveness in reflecting changes in glomerular filtration rate [9]. Therefore, the search for early diagnostic targets for CKD is urgently needed.

Transcriptional factors (TFs) play a crucial role in recognizing unique DNA sequences to regulate chromatin structure and

1 Department of Nephrology, Children's Hospital, Zhejiang University School of Medicine, National Clinical Research Center for Child Health, National Children's Regional Medical Center, Hangzhou, China.

2 Shanghai Institute of Infectious Disease and Biosecurity, Fudan University, Shanghai, China

3 Renal Division of Northern Jiangsu People's Hospital, Clinical Medicine College of Yangzhou University, Yangzhou, China.

4 Department of Pediatrics, The First Affiliated Hospital of Nanjing Medical University, Nanjing, China.

† These authors contributed equally to this work.

* Corresponding Author.

gene transcription, thereby establishing a complex system essential for controlling the expression of the kidney genome [10]. Recent studies have indicated that dysregulation of human TFs is closely related to the onset and progression of CKD [11-12]. It is well known that each TF, functioning as an upstream regulatory signal, can regulate multiple downstream target genes, which affects different biological processes and signaling pathways. Therefore, the changes in the expression of TFs deserve attention as potential early signals for CKD. Previous studies have identified some TFs mediating the pathogenesis of CKD, including RUNX2, HIF1A, KLF4, P65, IRF1, SMADs and so on [13-19]. Thus, some key TFs closely associated with CKD have the potential to be the biomarkers for early diagnosis.

In this research, we reanalyzed a classic microarray dataset from Nephroseq database (https://www.nephroseq.org/) to achieve TFs for early diagnosis of CKD [20]. In addition, we established the regulatory network between diagnostic TFs and corresponding target genes. Finally, we evaluated the diagnostic efficiency of these TFs.

Materials and Methods

Microarray Data Analysis

The microarray assay consisting of 8 control kidney samples and 53 CKD kidney samples (GSE66494) was reanalyzed using the online tool "GEO2R". The operation procedure was followed by the official instructions, as options were set to default settings. Differential expression genes (DEGs) were characterized by "adjust P value < 0.05".

Gene Set Enrichment Analysis (GSEA) Analysis

The gene symbols and corresponding $\log_2$FC values from GSE66494 were used for GSEA analysis based on the online tool [21]. GSEA analysis and plotting were performed using the clusterProfile package (version 3.10.1) and the enrichplot package (version 1.2.0).

Identification of differentially expressed transcription factors (TFs)

The top 500 DEGs of CKD patients were entered into TRRUST v2 [22] to obtain potential regulatory TFs in the next step. Among these TFs, some were also DEGs, which can be recognized by the venny tool as we described before [23]. In addition, the TF-target regulatory relationships were further validated by correlation analysis and the JASPAR database [24]. The correlation analysis was conducted by using two different online tools from omicstudio (https://www.omicstudio.cn/tool/59; The Spearman's method was employed) and hiplot (https://hiplot.com.cn/cloud-tool/drawing-tool/detail/646; Ward.D2 method was employed). The overlapping results from the above correlation analyses were used for subsequent validation.

Statistical analysis

The transcriptome expression value of selected genes was used for the linear correlation analysis based on the Graphpad software. The receiver operator characteristic (ROC) was performed by R software.

Results

Analysis Process

Firstly, DEGs were identified from microarray data from the GEO database. Then, GSEA analysis was conducted. Subsequently, the regulatory TFs of the top 500 DEGs were predicted by TRRUST database. Among these TFs, some were differentially expressed TFs, whose regulation of corresponding target genes was verified via linear correlation analysis and JASPAR database. Lastly, the diagnostic efficiency of the selected TFs was evaluated using ROC curve.

Identification of DEGs Between Normal and CKD Samples and KEGG Analysis

We selected GSE66494 dataset to conduct deep data mining, because many DEGs from the dataset had been proved to be important pathogenic genes related to CKD, such as PXR, ROCK2, as our research team and other researchers identified before [25-27]. Gene expression levels were compared between the CKD and control samples. The results from GEO2R were shown in Figure 1 A-D. Considering the continuous updates of the KEGG database, we conducted functional analysis based on the newest background genesets using GSEA method. A series of up-regulated and down-regulated pathways were shown in Figure 1E, and these can be summarized be summarized as four categories, including down-regulated energy metabolism, up-regulated proinflammatory and immune infiltration, profibrotic and proliferative pathways and renal dysfunction. As is widely known, renal interstitial fibrosis is the most significant pathological manifestation in CKD patients at the end stage [28]. Activated TGFβ/smads signaling and wnt/β-catenin signaling are canonical pathways associated with renal fibrosis [13, 29-30]. The CKD cluster is characterized by a pronounced pro-fibrotic and pro-inflammatory transcriptomic signature. Therefore, the dataset met the standard for further analysis.

Screening and Identifying Key TFs among DEGs

As the microarray dataset reflects changes in transcription levels, we looked up the upstream regulatory TFs for these mRNA changes. TRRUST2.0 is a manually curated database containing 8,444 TF-target regulatory relationships of 800 human TFs [22]. All of the regulatory networks were from recorded literature, which meant they were more reliable than bioinformatics prediction and high-throughput sequencing data. Then, 38 probable regulatory TFs were achieved from TRRUST meeting the criteria "p < 0.05" (Supplementary Figure 1). Among these TFs, 20 were differentially expressed in CKD group (Figure 2A). Furthermore, the above TFs with less than 3 target genes were excluded, only 13 TFs were used for the next validation (Figure 2B).

The Expression of Screening TFs and the Linear Correlation Between TFs and Matching Targets

Among these 13 TFs, heatmap showed that 7 were significantly up-regulated, while the others were significantly down-regulated (Figure 3A). Each TF had its own target gene, which was achieved from TRRUST database. Furthermore, we adopted two ways to conduct the correlation between TFs and corresponding target genes (Figure 3B & C). Each TF directly inter-

acts with the promoter region of one or multiple target genes, thereby influencing the expression of mRNA in those genes. This suggests a potential linear correlation between the TF and its corresponding target genes. We found that many TFs had positively or negatively related target genes (Figure 3D-R) containing HNF4A, CEBPA, CREB1, FOS, HIF1A and SP1. Among these TFs, HIF1A, SP1 and CREB1 were up-regulated in human CKD kidney tissue, while the others were down-regulated.

Figure 1. Differential gene expression in the GSE66494 dataset and the KEGG pathways involved. A. Boxplot of dataset. **B.** UMAP plot of dataset. **C.** Volcano plot of dataset. **D.** The amounts of differential genes of dataset. **E.** The up-regulated and down-regulated pathways of dataset based on GSEA analysis.

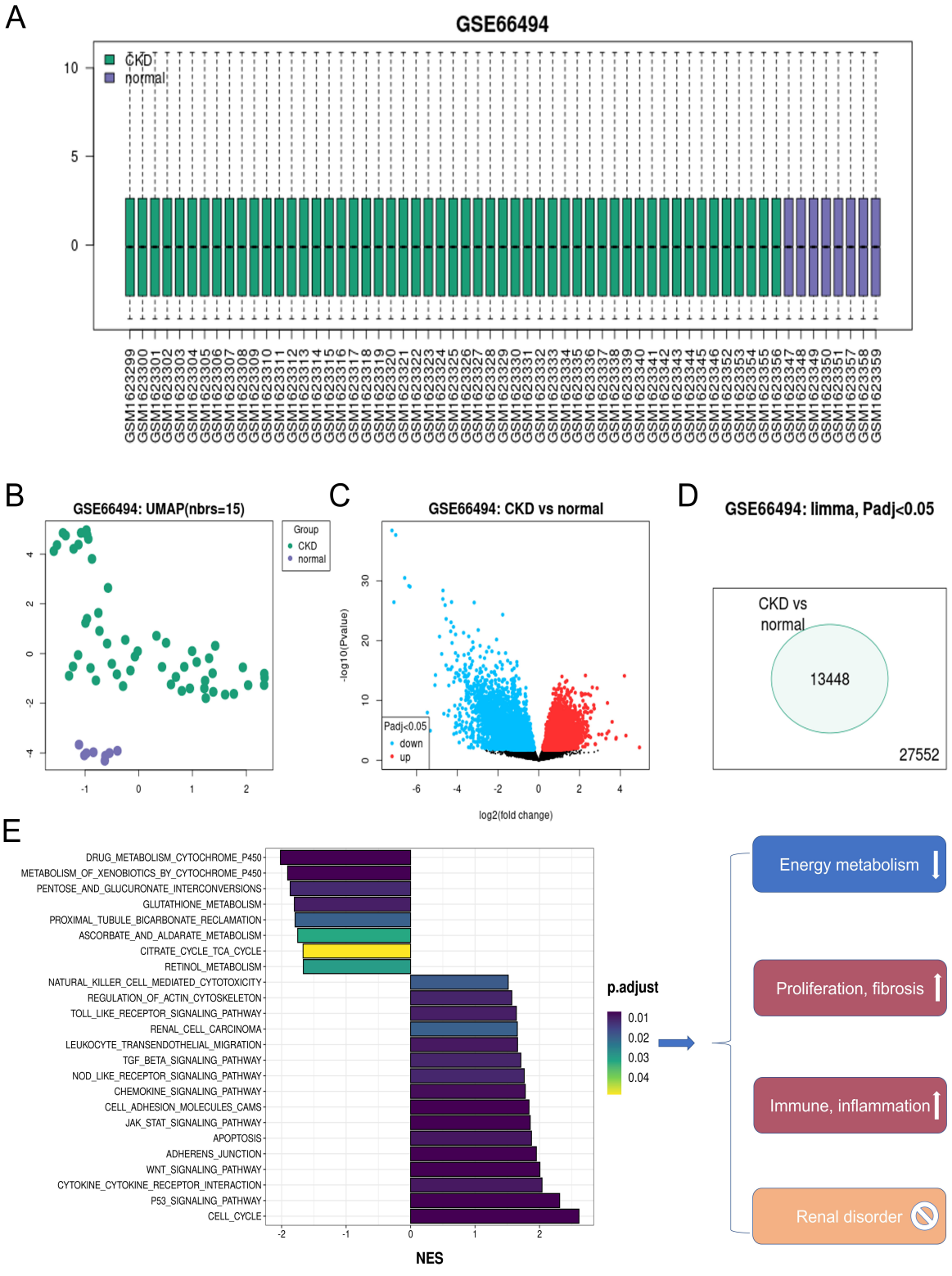

https://doi.org/10.71321/1pe9g186

The Potential Binding Sites of Key TFs

JASPAR database provided potential binding sites between TFs and target genes. According to the previous analysis, we focused on the specific TFs and their corresponding binding sites. From Figure 4A, SP1 had 6 binding sites with the promoter region of FOS, 5 binding sites with COL11A2, 1 binding site with PRSS50, 2 binding sites with NR4A1, 1 binding site with CHI3L1, 3 binding sites with FBLN1, 2 binding sites with EPOR and 5 binding sites with LCAT. CREB1 had only 1 binding site with FOXA1. HNF4A had 2 binding sites with the promoter region of ABCC6, 1 with SLC22A6, 1 with MMP7. CEBPA had 2 binding sites with PCK2. FOS had 1 binding site with FOXA1. HIF1A had 5 binding sites with ASS1. The high-frequency bind-

Figure 2. The differentially expressed TFs in CKD kidney. A. The venny diagram between predicted TFs and DEGs in the CKD kidney. **B.** Differentially expressed TFs with more than 3 target genes and their corresponding protein coding in the UniProt database.

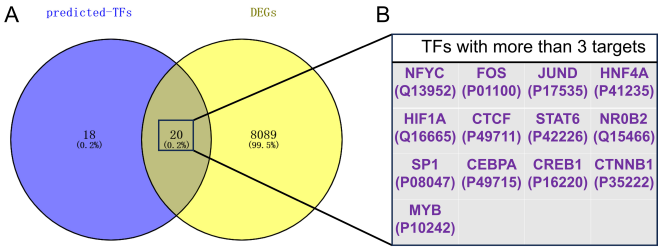

Figure 3. The up-regulated and down-regulated TFs in CKD and their relative linear analysis with corresponding target genes. A. Heatmap based on Nephroseq database reveals the up-regulated and down-regulated TFs in CKD. **B-C.** The linear analysis between TFs and their corresponding targets via two different methods. **D-R.** The linear analysis between each TF and each target gene.

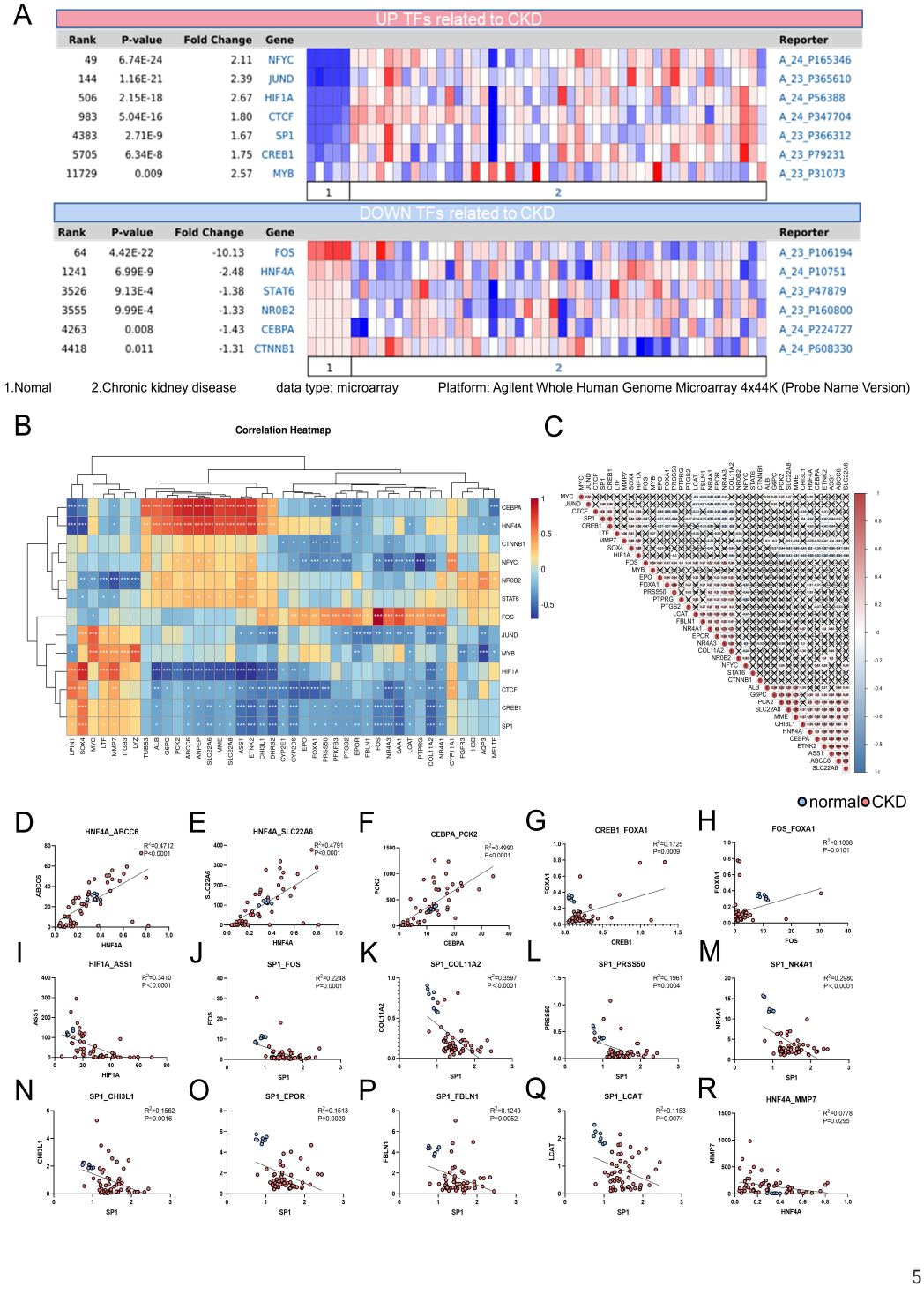

ing base sequences corresponding to each transcription factor were shown in Figure 4B-K.

The protein expression of hub TFs in renal tissues

We observed hub TFs in the normal kidney tissue based on the Human Protein Atlas Database. All of the selected TFs were expressed at a protein level in the normal kidney. However, they were distributed in different areas of the kidney. HNF4A was located mainly in the nuclear area of renal tubules (Figure 5A). CEBPA was expressed in both nucleus and cytoplasm of

Figure 4. The binding sites between selected TFs and target genes. A. The combing prediction between TFs and target sequences by JASPAR. **B-E.** The binding sites information for SP1. F. The binding sites information for CREB1. **G-H.** The binding sites information for HNF4A. **I.** The binding sites information for CEBPA. **J.** The binding sites information for FOS. **K.** The binding sites information for HIF1A. The larger the letter, the greater the frequency of the corresponding base.

A

Transcription factor	Target gene	Score	Relative score	Sequence ID	Start	End	Strand	Predicted sequence
Total 18 putative site(s) on the positive strand were predicted with relative profile score threshold 95%								
MA0079.2.SP1	FOS	14.453586	0.995298923	NC_000014.9:75276828-75278828	1582	1591	+	CCCCTCCCCC
MA0079.3.SP1	FOS	15.43146	0.975286119	NC_000014.9:75276828-75278828	1581	1591	+	TCCCCTCCCCC
MA0079.2.SP1	FOS	13.213753	0.964074552	NC_000014.9:75276828-75278828	159	168	+	CCCCGCCTCC
MA0079.2.SP1	FOS	13.213753	0.964074552	NC_000014.9:75276828-75278828	1601	1610	+	CCCCGCCTCC
MA0079.3.SP1	FOS	14.486494	0.963397361	NC_000014.9:75276828-75278828	158	168	+	TCCCCGCCTCC
MA0079.3.SP1	FOS	14.459636	0.963059453	NC_000014.9:75276828-75278828	1600	1610	+	CCCCCGCCTCC
MA0079.1.SP1	COL11A2	11.045893	0.972161372	NC_000006.12:c33162694-33160694	1783	1792	+	GAGGCGGGGT
MA0079.1.SP1	COL11A2	11.045893	0.972161372	NC_000006.12:c33162694-33160694	1801	1810	+	GGGGCTGGGT
MA0079.3.SP1	COL11A2	15.093589	0.971035308	NC_000006.12:c33162694-33160694	869	879	+	CCCCCGCCCCT
MA0079.3.SP1	COL11A2	14.962341	0.969384064	NC_000006.12:c33162694-33160694	874	884	+	GCCCCTCCTCC
MA0079.2.SP1	COL11A2	13.027086	0.959373479	NC_000006.12:c33162694-33160694	875	884	+	CCCCTCCTCC
MA0079.3.SP1	PRSS50	13.716568	0.95371081	NC_000003.12:c46712117-46710117	1392	1402	+	TTCCCTCCCCC
MA0079.2.SP1	NR4A1	14.453586	0.995298923	NC_000012.12:52020832-52022832	1093	1102	+	CCCCTCCCCC
MA0079.3.SP1	NR4A1	15.43146	0.975286119	NC_000012.12:52020832-52022832	1092	1102	+	TCCCCTCCCCC
MA0079.5.SP1	CHI3L1	14.750445	0.975201446	NC_000001.11:c203178931-203176931	1059	1067	+	GGGGAGGGG
MA0079.2.SP1	FBLN1	13.213753	0.964074552	NC_000022.11:45500883-45502883	1939	1948	+	CCCCGCCTCC
MA0079.3.SP1	FBLN1	15.706597	0.978747657	NC_000022.11:45500883-45502883	1938	1948	+	GCCCCGCCTCC
MA0079.5.SP1	FBLN1	13.402603	0.951780456	NC_000022.11:45500883-45502883	1732	1740	+	GGGGAGGAG
Total 8 putative site(s) on the positive strand were predicted with relative profile score threshold 90%								
MA0018.2.CREB1	FOXA1	9.00289	0.906041171	NC_000014.9:c37589552-37587552	349	356	+	TGACATCA
MA0079.1.SP1	EPOR	9.171796	0.906789836	NC_000019.10:c11377207-11375207	1670	1679	+	GAGGGTGGGT
MA0079.2.SP1	EPOR	10.835842	0.904188444	NC_000019.10:c11377207-11375207	1760	1769	+	CCCTGCCTCC
MA0079.5.SP1	LCAT	12.212311	0.931097155	NC_000016.10:c67939750-67937750	129	137	+	GGGGCGGTG
MA0079.5.SP1	LCAT	12.212311	0.931097155	NC_000016.10:c67939750-67937750	140	148	+	GGGGCGGTG
MA0079.3.SP1	LCAT	11.298021	0.923282724	NC_000016.10:c67939750-67937750	99	109	+	GCTCCACCCAC
MA0079.1.SP1	LCAT	9.226104	0.908684185	NC_000016.10:c67939750-67937750	140	149	+	GGGGCGGTGA
MA0079.1.SP1	LCAT	9.026768	0.90173102	NC_000016.10:c67939750-67937750	138	147	+	GGGGGGCGGT
Total 7 putative site(s) on the positive strand were predicted with relative profile score threshold 85%								
MA0114.2.HNF4A	ABCC6	8.896688	0.853294207	NC_000016.10:c16149565-16147565	753	767	+	GAGGACTTGGTTCTT
MA0114.4.HNF4A	ABCC6	11.323141	0.872754521	NC_000016.10:c16149565-16147565	1104	1116	+	ACCAAATTCCAGC
MA0114.2.HNF4A	SLC22A6	10.119499	0.869570966	NC_000011.10:c62976597-62974597	140	154	+	CTTGCCTTTGCCCCT
MA0114.4.HNF4A	MMP7	11.524467	0.876765433	NC_000011.10:c102520508-102518508	228	240	+	TGGAAAGTCCAAT
MA0102.3.CEBPA	PCK2	7.1550646	0.88370774	NC_000014.9:24092171-24094171	1191	1201	+	GTTTCCTCATT
MA0102.3.CEBPA	PCK2	6.1691127	0.871895949	NC_000014.9:24092171-24094171	1865	1875	+	GTTACATCATG
MA0476.1.FOS	FOXA1	5.975023	0.868628017	NC_000014.9:c37589552-37587552	3	13	+	GGAGACTCATG
Total 5 putative site(s) on the positive strand were predicted with relative profile score threshold 80%								
MA1106.1.HIF1A	ASS1	6.545462	0.846239267	NC_000009.12:130442707-130444707	1003	1012	+	CCACGTGGCT
MA1106.1.HIF1A	ASS1	5.385243	0.818920892	NC_000009.12:130442707-130444707	1367	1376	+	GGACTTGCTC
MA1106.1.HIF1A	ASS1	4.8551283	0.80643888	NC_000009.12:130442707-130444707	1604	1613	+	GCAGGTGCCA
MA1106.1.HIF1A	ASS1	4.7103024	0.803028827	NC_000009.12:130442707-130444707	32	41	+	CTAGGTGCTG
MA1106.1.HIF1A	ASS1	4.5892386	0.800178276	NC_000009.12:130442707-130444707	18	27	+	CCACCTGCTC

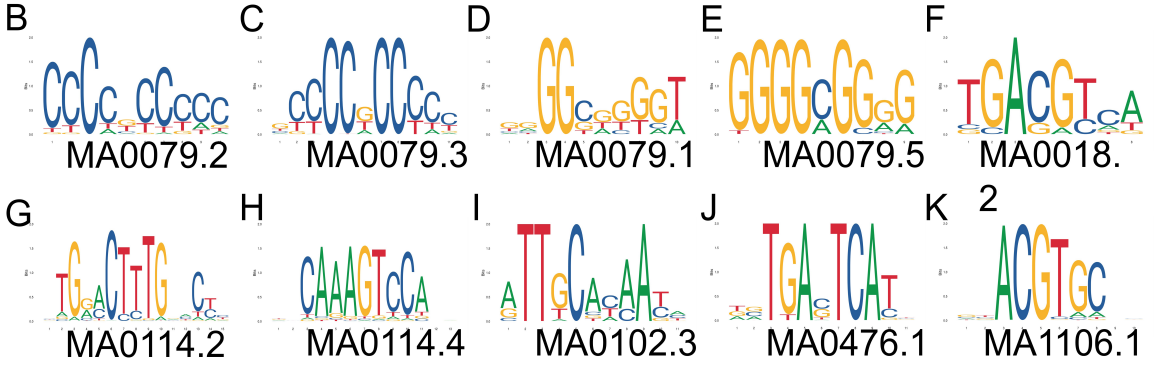

renal tubules (Figure 5B). CREB1 distributed in the nucleus of both glomerulus and renal tubules (Figure 5C). Interestingly, FOS was almost expressed in the whole kidney (Figure 5D). On the contrary, HIF1A was expressed at low protein levels in the glomerulus (Figure 5E). SP1 mainly distributed in the nucleus of glomerulus (Figure 5F).

Figure 5. Immunohistochemistry of the hub TFs based on the Human Protein Atlas database. A. The protein expression of HNF4A in the normal kidney tissue. **B.** The protein expression of CEBPA in the normal kidney tissue. **C.** The protein expression of CREB1 in the normal kidney tissue. **D.** The protein expression of FOS in the normal kidney tissue. **E.** The protein expression of HIF1A in the normal kidney tissue. **F.** The protein expression of SP1 in the normal kidney tissue.

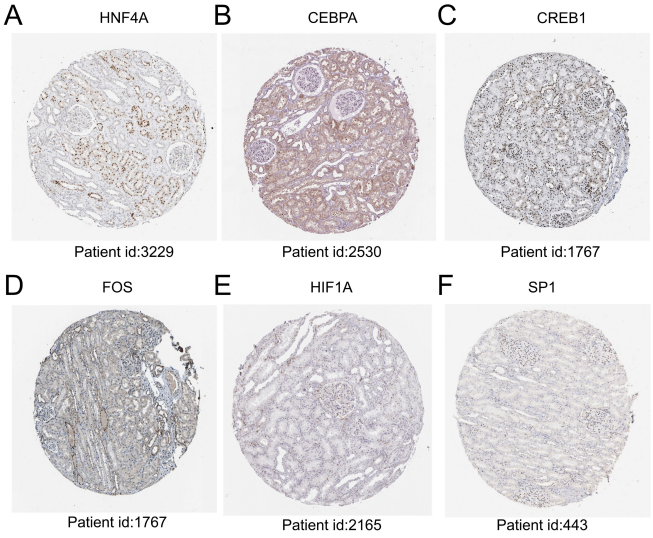

Predictive efficiency of core TFs in CKD patients

ROC analysis was employed to evaluate the predictive efficiency of the six genes mentioned. Four of their AUC values were greater than 0.9, including CREB1, FOS, HIF1A and SP1 (Figure 6C-F), while the AUC value of HNF4A and CEBPA were just 0.658 and 0.5802 (Figure 6A & B), and the summary result was shown in Figure 6G. The combined predictive efficiency of the above TFs was shown in Figure 6H, whose AUC is equal to 1.

Discussion

CKD is a kind of progressive disease whose clinical assessment is usually based on laboratory examination and pathological examination. Over the past years, proteinuria, eGFR, Scr, BUN and some other indexes have reflected the function of kidney. However, when these indexes show significant pathological changes, the kidney has progressed to the end stage. Therefore, a strategy for early diagnosis of CKD needs to be developed urgently.

With the rapid development of the technology of multi-omics, molecular diagnosis has been applied to clinical practice. Many researchers have found some key biomarkers highly related to CKD. Zhang et al identify that XDH is positively correlated with kidney damage [31]. MMP2 and MMP9, which are closely related to glomerulonephritis as we have identified before, are also important biomarkers for CKD [23, 32].

Different from the former diagnostic models, in this study, we focused on searching some diagnostic biomarkers for CKD from transcription factors because of their upstream regulatory effects. We used TRRUST database to predict the regulatory TFs for DEGs and got a series of TFs, among which some were also differentially expressed genes. Further analysis revealed that 6 of them had multiple regulatory relationships with DEGs including HNF4A, CEBPA, CREB1, FOS, HIF1A and SP1, which were supported by linear correlation analysis and evidence from JASPAR database. HNF4A, namely hepatocyte nuclear factor 4-alpha, is associated with the differentiation of proximal tubules, whose deletion or mutation will result in Fanconi renotubular syndrome [33-35]. HNF4A is also down-regulated in the unilateral ureteral obstruction model, which is a classic model used for researching CKD [36]. Additionally, liver-specific HNF4A-deficient mice progress to liver fibrosis, which can be rescued by applicability of HNF4A mRNA therapeutics [37-38]. CEBPA, namely CCAAT/enhancer-binding protein alpha, was down-regulated in our analysis. Interestingly, conversely, it is reported to be up-regulated in the UUO kidney [39]. However, another study supports that the expression of CEBPA is repressed by TGFβ, which contributed to the initiation of endothelial-to-mesenchymal transition in the endothelium [40]. Cyclic AMP-responsive element-binding protein 1 (CREB1) can be induced by TGFβ, which can result in matrix metalloproteinase and fibronectin accumulation [41-43]. FOS, also called protein c-FOS, is increased in the UUO model for 12 days [44]. FOS is a vital component of TGFβ/SMADs signaling, which mediates cell proliferation [45-46]. However, our analysis shows that FOS is down-regulated in human CKD renal tissues. These discrepant results could be attributed to differences in species or to biases arising from the unequal sample sizes between the control and disease groups in the clinical cohort. More samples may need to be included in order to test whether FOS can be a biomarker for CKD at the early stage. HIF1A, also named hypoxia-inducible factor 1-alpha, can promote renal fibrosis in some kidney diseases [47-48]. Therapeutic strategy targeting HIF-1α can protect the kidney from AKI to CKD progression [49]. SP1 is increased in glomerular or proximal tubular tissues in glomerulonephritis and obstructive nephropathy, whose expression is positively correlative with p-Smad2/3 [50]. In addition, the expression of SP1 is positively related to collagen I [51]. Interestingly, the TF SP1 has more binding sites than numerous other TFs as Figure 4 shows. Based on our earlier review [52], SP1 possesses a considerably long amino acid sequence, thereby enabling the potential for more extensive DNA binding. Furthermore, SP1 is evolutionarily an ancient gene, implying that it may have more diverse biological roles.

Furthermore, the above TFs separately have their own target genes. These target genes, including FOS, COL11A2, PRSS50, NR4A1, CHI3L1, FBLN1, FOXA1, EPOR, LCAT, ABCC6, SLC22A6, MMP7, PCK2 and ASS1, are also differentially expressed in human CKD kidney. Among these genes, some are reported to be related to renal fibrosis, such as MMP7, NR4A1, LCAT and so on [53-55]. Some correlations between TFs and downstream target genes reflect the intricate web of transcriptional regulation, characterized by its one-to-many architecture. The net influence of a TF on a given gene is frequently the result of a regulatory calculus involving the summation of multiple positive inputs or the antagonism between opposing regulatory signals. This complexity inherently defies a purely linear

representation (Figure 3H, Q, R). At the same time, ROC analysis reveals that transcription factor CREB1, FOS, HIF1A and SP1 have higher diagnostic efficacy than HNF4A and CEBPA. Based on the results from Figure 3 and 6, SP1, CREB1 and HIF1A seem to have stronger evidence for further clinical transformation.

However, the study has some limitations. First, as the TF-target regulatory network is based on the published literature, quite a few TFs are not reported in TRRUST. Therefore, there may be other TFs which are able to be used for early diagnosis of CKD. Second, our findings just come from numerous data analysis and documentary evidence, some experiments ought to be performed for validation. For instance, the binding affinity between TFs and corresponding DNA sequence should depend on electrophoretic mobility shift assay or chromatin immunoprecipitation. And also, dual-luciferase reporter assay is necessary for analyzing the gene expression regulated by TFs in the kidney cell model. Third, CKD patients have different

Figure 6. The diagnostic efficacy of 6 key TFs and their combined predictive efficiency in CKD. A. ROC analysis of HNF4A in CKD. **B.** ROC analysis of CEBPA in CKD. **C.** ROC analysis of CREB1 in CKD. **D.** ROC analysis of FOS in CKD. **E.** ROC analysis of HIF1A in CKD. **F.** ROC analysis of SP1 in CKD. **G.** The collected results of the above single result. **H.** The combined predictive efficiency for the above six TFs.

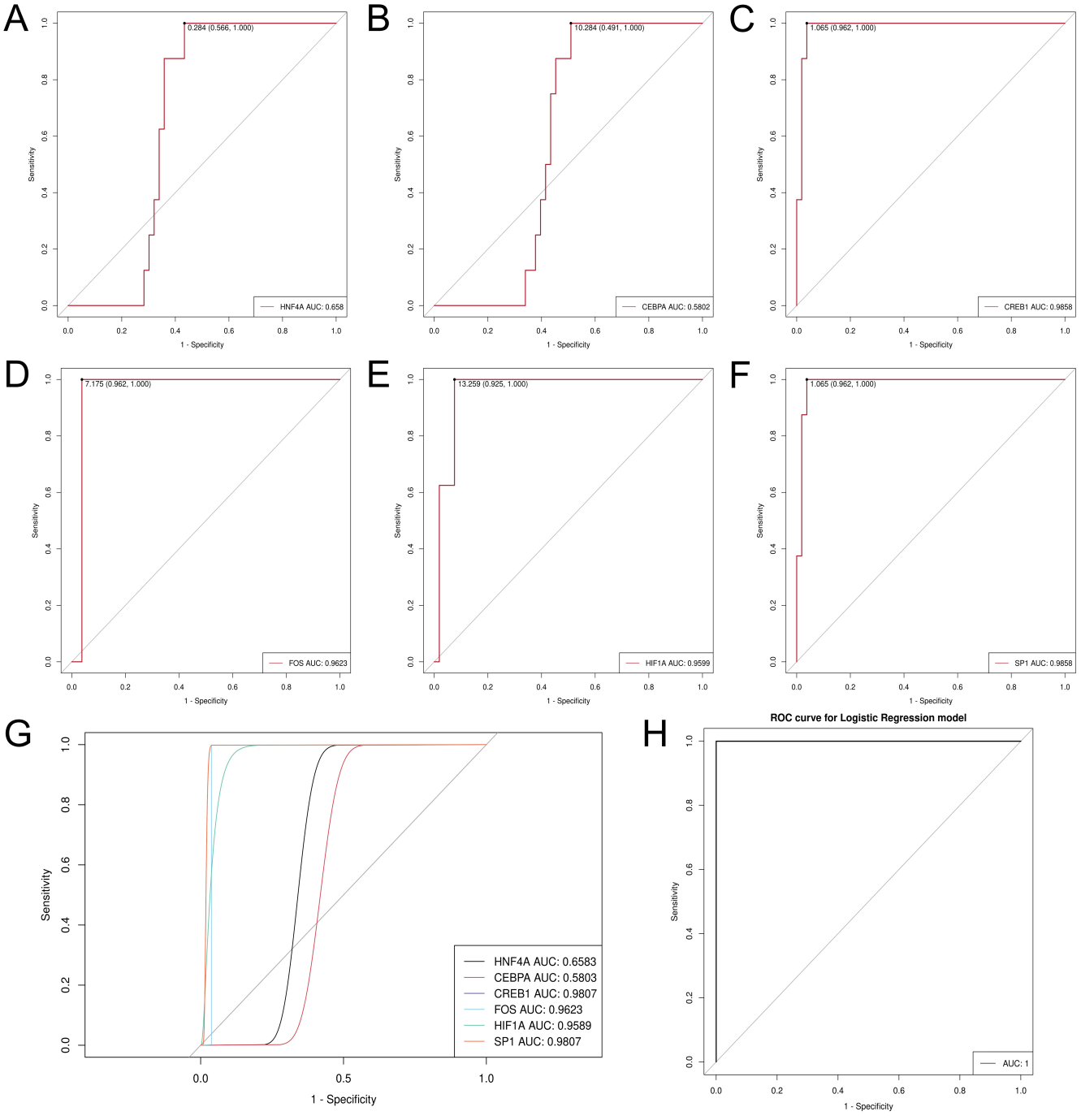

primary diseases. This research does not divide CKD patients into diverse subgroups. Fourth, Single-cell transcriptomics data may provide more comprehensive gene expression information than the microarray data used in this study [56-57]. We will overcome these shortcomings and make a deep exploration in the next work.

Conclusion

In summary, transcription factors play an important role in the pathophysiological process of chronic kidney disease. We have identified 6 TFs closely associated with CKD based on a comprehensive method containing HNF4A, CEBPA, CREB1, FOS, HIF1A and SP1. According to the literature evidence and deep data analysis, we conclude that SP1, CREB1 and HIF1A may have greater potential for clinical translation.

Abbreviations

AKI, acute kidney injury; AUC, area under the curve; BUN, blood urea nitrogen; CKD, chronic kidney disease; CREB1, cAMP-responsive element-binding protein 1; DEGs, differentially expressed genes; ECM, extracellular matrix; eGFR, estimated glomerular filtration rate; ESKD, end-stage kidney disease; GEO, Gene Expression Omnibus; GSEA, gene set enrichment analysis; HIF1A, hypoxia-inducible factor 1-alpha; KEGG, Kyoto Encyclopedia of Genes and Genomes; MMP, matrix metalloproteinase; ROC, receiver operating characteristic; Scr, serum creatinine; SP1, specificity protein 1; TF, transcription factor; TGFβ, transforming growth factor beta; TRRUST, Transcriptional Regulatory Relationships Unraveled by Sentence-based Text-mining; UUO, unilateral ureteral obstruction.

Author Contributions

Jianhua Mao designed the research. Wei Zhou, Qingqing Jia and Shujun Wu performed bioinformatic analysis and wrote the manuscript. Xinyu Wang, Mingzhu Jiang and Hanyan Meng helped to solve the clinical problems and contributed to data collection. All authors read and approved the final manuscript.

Acknowledgements

Not Applicable.

Funding Information

This work was supported by grants from the Fundamental Research Funds for the Central Universities (226-2023-00056), the Zhejiang Xinmiao Talents Program (2023R401208), the Scientific Research Fund of Zhejiang University (XY2023011) and Key Research and Development Plan of Zhejiang Province (2021C03079), National key research and development program (2021YFC2702002, 2022YFC2705103).

Ethics Approval and Consent to Participate

Not Applicable.

Competing Interests

All the authors declared that they have no competing interests.

Data Availability

The datasets analysed during the current study are available in the GEO Database (GSE66494, https://www.ncbi.nlm.nih.gov/geo/query/acc.cgi?acc=GSE66494). In addition, the datasets analyzed during the current study are available from the corresponding author on reasonable request.

Reference

[1] Webster AC, Nagler EV, Morton RL, & Masson P. (2017). Chronic Kidney Disease. Lancet, 389(10075), 1238-1252. https://doi.org/10.1016/S0140-6736(16)32064-5

[2] Jiang M, Bai M, Lei J, Xie Y, Xu S, Jia Z, et al. (2020). Mitochondrial dysfunction and the AKI-to-CKD transition. Am J Physiol Renal Physiol, 319(6), F1105-F1116. https://doi.org/10.1152/ajprenal.00285.2020

[3] Chen TK, Knicely DH, & Grams ME. (2019). Chronic Kidney Disease Diagnosis and Management: A Review. JAMA, 322(13), 1294-1304. https://doi.org/10.1001/jama.2019.14745

[4] Chawla LS, Eggers PW, Star RA, & Kimmel PL. (2014). Acute kidney injury and chronic kidney disease as interconnected syndromes. N Engl J Med, 371(1), 58-66. https://doi.org/10.1056/NEJMra1214243

[5] Tepus M, Tonoli E, & Verderio EAM. (2022). Molecular profiling of urinary extracellular vesicles in chronic kidney disease and renal fibrosis. Front Pharmacol, 13, 1041327. https://doi.org/10.3389/fphar.2022.1041327

[6] Humphreys BD. (2018). Mechanisms of Renal Fibrosis. Annu Rev Physiol, 80, 309-326. https://doi.org/10.1146/annurev-physiol-022516-034227

[7] Tang PM, Nikolic-Paterson DJ, & Lan HY. (2019). Macrophages: versatile players in renal inflammation and fibrosis. Nat Rev Nephrol, 15(3), 144-158. https://doi.org/10.1038/s41581-019-0110-2

[8] Li L, Fu H, & Liu Y. (2022). The fibrogenic niche in kidney fibrosis: components and mechanisms. Nat Rev Nephrol, 18(9), 545-557. https://doi.org/10.1038/s41581-022-00590-z

[9] Chen S, Liu YH, Dai DP, Zhu ZB, Dai Y, Wu ZM, et al. (2021). Using circulating O-sulfotyrosine in the differential diagnosis of acute kidney injury and chronic kidney disease. BMC Nephrol, 22(1), 66. https://doi.org/10.1186/s12882-021-02268-3

[10] Lambert SA, Jolma A, Campitelli LF, Das PK, Yin Y, Albu M, et al. (2018). The Human Transcription Factors. Cell, 172(4), 650-665. https://doi.org/10.1016/j.cell.2018.01.029

[11] Ruiz-Ortega M, Rayego-Mateos S, Lamas S, Ortiz A, & Rodrigues-Diez RR. (2020). Targeting the progression of chronic kidney disease. Nat Rev Nephrol, 16(5), 269-288. https://doi.org/10.1038/s41581-019-0248-y
[12] Hishikawa A, Hayashi K, & Itoh H. (2018). Transcription Factors as Therapeutic Targets in Chronic Kidney Disease. Molecules, 23(5). https://doi.org/10.3390/molecules23051123
[13] Ma TT, & Meng XM. (2019). TGF-beta/Smad and Renal Fibrosis. Adv Exp Med Biol, 1165, 347-364. https://doi.org/10.1007/978-981-13-8871-2_16
[14] Li W, Feng W, Su X, Luo D, Li Z, Zhou Y, et al. (2022). SIRT6 protects vascular smooth muscle cells from osteogenic transdifferentiation via Runx2 in chronic kidney disease. J Clin Invest, 132(1). https://doi.org/10.1172/JCI150051
[15] Yang Y, Yu X, Zhang Y, Ding G, Zhu C, Huang S, et al. (2018). Hypoxia-inducible factor prolyl hydroxylase inhibitor roxadustat (FG-4592) protects against cisplatin-induced acute kidney injury. Clin Sci (Lond), 132(7), 825-838. https://doi.org/10.1042/CS20171625
[16] Wen Y, Lu X, Ren J, Privratsky JR, Yang B, Rudemiller NP, et al. (2019). KLF4 in Macrophages Attenuates TNFalpha-Mediated Kidney Injury and Fibrosis. J Am Soc Nephrol, 30(10), 1925-1938. https://doi.org/10.1681/ASN.2019020111
[17] Huang Y, Wang S, Zhou J, Liu Y, Du C, Yang K, et al. (2020). IRF1-mediated downregulation of PGC1alpha contributes to cardiorenal syndrome type 4. Nat Commun, 11(1), 4664. https://doi.org/10.1038/s41467-020-18519-0
[18] Tang TT, Wang B, Li ZL, Wen Y, Feng ST, Wu M, et al. (2021). Kim-1 Targeted Extracellular Vesicles: A New Therapeutic Platform for RNAi to Treat AKI. J Am Soc Nephrol, 32(10), 2467-2483. https://doi.org/10.1681/ASN.2020111561
[19] Wang J, Ge S, Wang Y, Liu Y, Qiu L, Li J, et al. (2021). Puerarin Alleviates UUO-Induced Inflammation and Fibrosis by Regulating the NF-kappaB P65/STAT3 and TGFbeta1/Smads Signaling Pathways. Drug Des Devel Ther, 15, 3697-3708. https://doi.org/10.2147/DDDT.S321879
[20] Nakagawa S, Nishihara K, Miyata H, Shinke H, Tomita E, Kajiwara M, et al. (2015). Molecular Markers of Tubulointerstitial Fibrosis and Tubular Cell Damage in Patients with Chronic Kidney Disease. PLoS One, 10(8), e0136994. https://doi.org/10.1371/journal.pone.0136994
[21] Lyu F, Han F, Ge C, Mao W, Chen L, Hu H, et al. (2023). OmicStudio: A composable bioinformatics cloud platform with real-time feedback that can generate high-quality graphs for publication. Imeta, 2(1), e85. https://doi.org/10.1002/imt2.85
[22] Han H, Cho JW, Lee S, Yun A, Kim H, Bae D, et al. (2018). TRRUST v2: an expanded reference database of human and mouse transcriptional regulatory interactions. Nucleic Acids Res, 46(D1), D380-D386. https://doi.org/10.1093/nar/gkx1013
[23] Zhou W, Sha Y, Zeng J, Zhang X, Zhang A, & Ge X. (2021). Computational Systems Pharmacology, Molecular Docking and Experiments Reveal the Protective Mechanism of Li-Da-Qian Mixture in the Treatment of Glomerulonephritis. J Inflamm Res, 14, 6939-6958. https://doi.org/10.2147/JIR.S338055
[24] Castro-Mondragon JA, Riudavets-Puig R, Rauluseviciute I, Lemma RB, Turchi L, Blanc-Mathieu R, et al. (2022). JASPAR 2022: the 9th release of the open-access database of transcription factor binding profiles. Nucleic Acids Res, 50(D1), D165-D173. https://doi.org/10.1093/nar/gkab1113
[25] Yu X, Xu M, Meng X, Li S, Liu Q, Bai M, et al. (2020). Nuclear receptor PXR targets AKR1B7 to protect mitochondrial metabolism and renal function in AKI. Sci Transl Med, 12(543). https://doi.org/10.1126/scitranslmed.aay7591
[26] Ming WH, Luan ZL, Yao Y, Liu HC, Hu SY, Du CX, et al. (2023). Pregnane X receptor activation alleviates renal fibrosis in mice via interacting with p53 and inhibiting the Wnt7a/beta-catenin signaling. Acta Pharmacol Sin, 44(10), 2075-2090. https://doi.org/10.1038/s41401-023-01113-7
[27] You R, Zhou W, Li Y, Zhang Y, Huang S, Jia Z, et al. (2020). Inhibition of ROCK2 alleviates renal fibrosis and the metabolic disorders in the proximal tubular epithelial cells. Clin Sci (Lond), 134(12), 1357-1376. https://doi.org/10.1042/CS20200030
[28] Romagnani P, Remuzzi G, Glassock R, Levin A, Jager KJ, Tonelli M, et al. (2017). Chronic kidney disease. Nat Rev Dis Primers, 3, 17088. https://doi.org/10.1038/nrdp.2017.88
[29] Edeling M, Ragi G, Huang S, Pavenstadt H, & Susztak K. (2016). Developmental signalling pathways in renal fibrosis: the roles of Notch, Wnt and Hedgehog. Nat Rev Nephrol, 12(7), 426-439. https://doi.org/10.1038/nrneph.2016.54
[30] Schunk SJ, Floege J, Fliser D, & Speer T. (2021). WNT-beta-catenin signalling - a versatile player in kidney injury and repair. Nat Rev Nephrol, 17(3), 172-184. https://doi.org/10.1038/s41581-020-00343-w
[31] Zhang Y, Ding X, Guo L, Zhong Y, Xie J, Xu Y, et al. (2023). Comprehensive analysis of the relationship between xanthine oxidoreductase activity and chronic kidney disease. iScience, 26(11), 107332. https://doi.org/10.1016/j.isci.2023.107332
[32] Saucedo AL, Perales-Quintana MM, Paniagua-Vega D, Sanchez-Martinez C, Cordero-Perez P, & Minsky NW. (2018). Chronic Kidney Disease and the Search for New Biomarkers for Early Diagnosis. Curr Med Chem, 25(31), 3719-3747. https://doi.org/10.2174/09298673256661803071109 08
[33] Muto Y, Wilson PC, Ledru N, Wu H, Dimke H, Waikar SS, et al. (2021). Single cell transcriptional and chromatin accessibility profiling redefine cellular heterogeneity in the adult human kidney. Nat Commun, 12(1), 2190. https://doi.org/10.1038/s41467-021-22368-w
[34] Marable SS, Chung E, Adam M, Potter SS, & Park JS. (2018). Hnf4a deletion in the mouse kidney phenocopies Fanconi renotubular syndrome. JCI Insight, 3(14). https://doi.org/10.1172/jci.insight.97497
[35] Hamilton AJ, Bingham C, McDonald TJ, Cook PR, Caswell RC, Weedon MN, et al. (2014). The HNF4A R76W mutation causes atypical dominant Fanconi syndrome in addition to a beta cell phenotype. J Med Genet, 51(3), 165-169. https://doi.org/10.1136/jmedgenet-2013-102066
[36] Wu B, & Brooks JD. (2012). Gene expression changes induced by unilateral ureteral obstruction in mice. J Urol, 188(3), 1033-1041. https://doi.org/10.1016/j.juro.2012.05.004
[37] Kasano-Camones CI, Takizawa M, Ohshima N, Saito C,

Iwasaki W, Nakagawa Y, et al. (2023). PPARalpha activation partially drives NAFLD development in liver-specific Hnf4a-null mice. J Biochem, 173(5), 393-411. https://doi.org/10.1093/jb/mvad005

[38] Yang T, Poenisch M, Khanal R, Hu Q, Dai Z, Li R, et al. (2021). Therapeutic HNF4A mRNA attenuates liver fibrosis in a preclinical model. J Hepatol, 75(6), 1420-1433. https://doi.org/10.1016/j.jhep.2021.08.011

[39] Fujiu K, Manabe I, & Nagai R. (2011). Renal collecting duct epithelial cells regulate inflammation in tubulointerstitial damage in mice. J Clin Invest, 121(9), 3425-3441. https://doi.org/10.1172/JCI57582

[40] Gao R, Wu Y, Yang Q, Chen L, Chen J, Wang B, et al. (2023). The Interaction of Apelin and FGFR1 Ameliorated the Kidney Fibrosis through Suppression of TGF-beta-Induced Endothelial-to-Mesenchymal Transition. Oxid Med Cell Longev, 2023, 5012474. https://doi.org/10.1155/2023/5012474

[41] Liu G, Ding W, Neiman J, & Mulder KM. (2006). Requirement of Smad3 and CREB-1 in mediating transforming growth factor-beta (TGF beta) induction of TGF beta 3 secretion. J Biol Chem, 281(40), 29479-29490. https://doi.org/10.1074/jbc.M600579200

[42] Yano N, Suzuki D, Endoh M, Zhang W, Xu YC, Padbury JF, et al. (2012). In vitro silencing of the insulin receptor attenuates cellular accumulation of fibronectin in renal mesangial cells. Cell Commun Signal, 10(1), 29. https://doi.org/10.1186/1478-811X-10-29

[43] Shan Q, Zheng G, Zhu A, Cao L, Lu J, Wu D, et al. (2016). Epigenetic modification of miR-10a regulates renal damage by targeting CREB1 in type 2 diabetes mellitus. Toxicol Appl Pharmacol, 306, 134-143. https://doi.org/10.1016/j.taap.2016.06.010

[44] Silverstein DM, Travis BR, Thornhill BA, Schurr JS, Kolls JK, Leung JC, et al. (2003). Altered expression of immune modulator and structural genes in neonatal unilateral ureteral obstruction. Kidney Int, 64(1), 25-35. https://doi.org/10.1046/j.1523-1755.2003.00067.x

[45] Zhang Y, Feng XH, & Derynck R. (1998). Smad3 and Smad4 cooperate with c-Jun/c-Fos to mediate TGF-beta-induced transcription. Nature, 394(6696), 909-913. https://doi.org/10.1038/29814

[46] Singhal PC, Sharma P, Sanwal V, Prasad A, Kapasi A, Ranjan R, et al. (1998). Morphine modulates proliferation of kidney fibroblasts. Kidney Int, 53(2), 350-357. https://doi.org/10.1046/j.1523-1755.1998.00758.x

[47] Zhao H, Han Y, Jiang N, Li C, Yang M, Xiao Y, et al. (2021). Effects of HIF-1alpha on renal fibrosis in cisplatin-induced chronic kidney disease. Clin Sci (Lond), 135(10), 1273-1288. https://doi.org/10.1042/CS20210061

[48] Li X, Yang S, Yan M, Guan N, Li J, Xie Q, et al. (2020). Interstitial HIF1A induces an estimated glomerular filtration rate decline through potentiating renal fibrosis in diabetic nephropathy. Life Sci, 241, 117109. https://doi.org/10.1016/j.lfs.2019.117109

[49] Li ZL, Wang B, Lv LL, Tang TT, Wen Y, Cao JY, et al. (2021). FIH-1-modulated HIF-1alpha C-TAD promotes acute kidney injury to chronic kidney disease progression via regulating KLF5 signaling. Acta Pharmacol Sin, 42(12), 2106-2119. https://doi.org/10.1038/s41401-021-00617-4

[50] Kassimatis TI, Nomikos A, Giannopoulou I, Lymperopoulos A, Moutzouris DA, Varakis I, et al. (2010). Transcription factor Sp1 expression is upregulated in human glomerulonephritis: correlation with pSmad2/3 and p300 expression and renal injury. Ren Fail, 32(2), 243-253. https://doi.org/10.3109/08860220903411164

[51] Jiang L, Zhou Y, Xiong M, Fang L, Wen P, Cao H, et al. (2013). Sp1 mediates microRNA-29c-regulated type I collagen production in renal tubular epithelial cells. Exp Cell Res, 319(14), 2254-2265. https://doi.org/10.1016/j.yexcr.2013.06.007

[52] Zhou W, Fang J, Jia Q, Meng H, Liu F, & Mao J. (2025). Transcription factor specificity protein (SP) family in renal physiology and diseases. PeerJ, 13, e18820. https://doi.org/10.7717/peerj.18820

[53] Hirohama D, Abedini A, Moon S, Surapaneni A, Dillon ST, Vassalotti A, et al. (2023). Unbiased Human Kidney Tissue Proteomics Identifies Matrix Metalloproteinase 7 as a Kidney Disease Biomarker. J Am Soc Nephrol, 34(7), 1279-1291. https://doi.org/10.1681/ASN.0000000000000141

[54] Tveitaras MK, Skogstrand T, Leh S, Helle F, Iversen BM, Chatziantoniou C, et al. (2015). Matrix Metalloproteinase-2 Knockout and Heterozygote Mice Are Protected from Hydronephrosis and Kidney Fibrosis after Unilateral Ureteral Obstruction. PLoS One, 10(12), e0143390. https://doi.org/10.1371/journal.pone.0143390

[55] Tao Y, Tang C, Wei J, Shan Y, Fang X, & Li Y. (2023). Nr4a1 promotes renal interstitial fibrosis by regulating the p38 MAPK phosphorylation. Mol Med, 29(1), 63. https://doi.org/10.1186/s10020-023-00657-y

[56] Long X, Yan B, & Mo Z. (2023). Uncovering the heterogeneity and cell fate decisions of endothelial cells after myocardial infarction by single-cell sequencing. Medicine Advances, 1(3), 234-245. https://doi.org/10.1002/med4.34

[57] Dong Z, & Liang X. (2023). A glimpse of recent advances in the research of acute kidney injury. Medicine Advances, 1(2), 158-162. https://doi.org/10.1002/med4.26

Artificial Intelligence–Enabled Dissection of Regulatory T Cells in the Tumor Immune Microenvironment: From Mechanistic Insight to Population-Scale Inference

Authors

Xuexue Hao, Muwei Li, Tao Xiong, Xiaoqiang Liu

Correspondence

xiaoqiangliu1@163.com (X. Liu)

Graphical Abstract

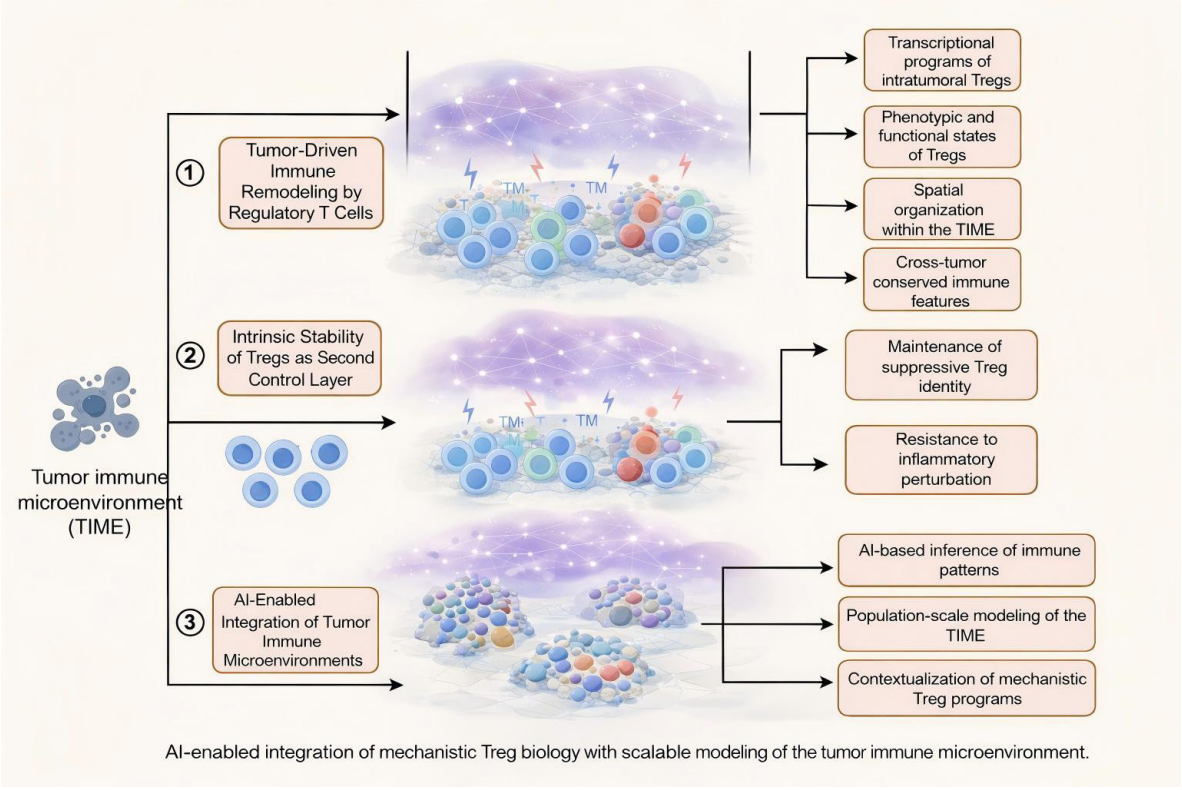

AI-enabled integration of mechanistic Treg biology with scalable modeling of the tumor immune microenvironment.

https://doi.org/10.71321/s2yhxp11

Artificial Intelligence–Enabled Dissection of Regulatory T Cells in the Tumor Immune Microenvironment: From Mechanistic Insight to Population-Scale Inference

Xuexue Hao [1†], Muwei Li [1†], Tao Xiong [1†], Xiaoqiang Liu [1*]

Received: 2025-12-24 | Accepted: 2026-01-25 | Published online: 2026-02-08

Abstract

Background: Regulatory T cells (Tregs) are central regulators of immune tolerance in the tumor immune microenvironment (TIME) and are increasingly implicated in tumor immune evasion and immunotherapy resistance. While mechanistic studies have delineated pathways governing Treg recruitment and functional stability, extending these insights to spatial organization and population-level heterogeneity remains a major challenge.

Methods: In this correspondence, we integrate recent advances in tumor immunology with emerging artificial intelligence (AI)–based analytical frameworks to highlight how Treg-driven immune programs can be interrogated at scale. We draw on representative experimental mechanisms and AI-enabled multimodal modeling approaches, including virtual tumor microenvironment reconstruction and vision–language foundation models, to illustrate a mechanism-informed computational perspective.

Results: Evidence supports a layered model of tumor-driven Treg regulation, combining chemokine-mediated recruitment with intrinsic transcriptional stabilization within the TIME. AI-enabled approaches enable population-scale inference of Treg abundance, spatial distribution, and functional states, revealing clinically relevant heterogeneity and associations with differential immunotherapy responses that are difficult to capture using conventional experimental strategies alone.

Conclusion: The convergence of mechanistic Treg biology and AI-driven TIME modeling offers a conceptual framework for bridging experimental insight with real-world tumor heterogeneity. Mechanism-informed AI has the potential to refine immune stratification and guide Treg-targeted therapeutic strategies, highlighting a translational path forward for precision immuno-oncology.

Keywords: Artificial intelligence; Regulatory T cells; Tumor immune microenvironment; Immunotherapy; Precision oncology

Introduction

The study of regulatory T cells (Tregs) has garnered significant attention due to their pivotal role in modulating the tumor immune microenvironment (TIME). This year, the Nobel Prize in Physiology or Medicine recognized fundamental discoveries in peripheral immune tolerance, centered on Tregs, a lineage now widely implicated in tumor immune evasion. In parallel, last year's Nobel Prize in Physics honored advancements in artificial intelligence (AI) and machine learning, technologies now increasingly integral to understanding cancer biology. As AI begins to unravel the complexities of immune systems, it offers unprecedented tools for analyzing immune interactions at a population scale, which is particularly beneficial for exploring the spatial and functional dynamics of Tregs in cancer.

The convergence of these two fields—the Nobel-winning discoveries of Tregs in cancer immunotherapy and AI's expanding role in precision oncology—lays the foundation for a transformative shift in how we approach cancer research. By leveraging AI, we can begin to address longstanding challenges in oncology, including the intricate mechanisms of immune cell behavior, such as Treg recruitment and function in the tumor context.

Recent advances in artificial intelligence have shifted biomedical research from purely data-driven analysis toward integrated biological intelligence, emphasizing multimodal learning and cross-scale data fusion for complex biological systems [1]. This evolution provides a general methodological foundation for studying tumor immune regulation in a scalable and biologically informed manner.

Within oncology, such integrative strategies are increasingly necessary to contextualize immune mechanisms across heterogeneous tumors. Evidence from molecularly stratified clinical studies demonstrates that tumor-intrinsic alterations, such as FGFR pathway changes, can influence immune checkpoint inhibitor efficacy [2], while multi-omics and machine-learning–based integration of imaging, molecular, and pathological data has emerged as a generalizable approach to resolve biological heterogeneity and support clinically relevant inference [3-4].

1 Department of Urology, Tianjin Medical University General Hospital, Tianjin, China

† These authors contributed equally to this work.

* Corresponding Author.

Tregs as Active Targets of Tumor-Driven Immune Remodeling

Rather than passive bystanders, regulatory T cells (Tregs) are increasingly recognized as central executors of tumor-driven immune remodeling. In clear cell renal cell carcinoma (ccRCC), our recent study identified a TGFBI–CCL22–Treg axis, illustrating how tumor- and stroma-derived signals can promote the selective accumulation of $FOXP3^+$ Tregs within the tumor immune microenvironment (TIME) [5]. Importantly, this observation serves primarily as a mechanistic entry point, highlighting the broader concept that tumors actively shape immune tolerance by recruiting and sustaining Tregs.

Accumulating high-impact evidence supports the notion that Tregs are deliberately co-opted by tumors to establish immune privilege. A landmark study in *Nature Medicine* first demonstrated that tumors selectively recruit Tregs through the CCL22–CCR4 chemokine axis, leading to suppressed antitumor immunity and poor clinical outcomes, thereby establishing chemokine-guided Treg trafficking as a conserved immune evasion strategy [6]. Beyond recruitment, Tregs have been shown to critically determine therapeutic responses. Seminal work published in *The Journal of Experimental Medicine* revealed that the efficacy of anti–CTLA-4 therapy depends on Fc-mediated depletion of intratumoral Tregs, redefining immune checkpoint blockade as a Treg-modulating intervention rather than solely an effector T cell–activating strategy [7].

At the cellular and transcriptional levels, recent high-dimensional profiling studies further reinforce the central role of Tregs in the TIME. Comprehensive analyses reported in *Nature Immunology* demonstrated that intratumoral Tregs share conserved gene regulatory and transcriptional programs across diverse cancer types, enabling the maintenance of their suppressive phenotype irrespective of tissue origin [8]. Consistently, distinct but functionally specialized Treg populations have been characterized in human breast cancer, highlighting tumor-specific adaptation of Tregs while preserving core suppressive functions [9].

Collectively, these findings support a unifying framework in which tumors do not merely evade immune surveillance but actively co-opt Tregs as functional mediators of immune suppression. Within this conceptual landscape, the TGFBI–CCL22–Treg axis observed in ccRCC exemplifies one of multiple mechanisms through which tumors orchestrate Treg biology, underscoring the broader relevance of targeting Tregs to disrupt tumor-driven immune remodeling across cancers.

Beyond Recruitment: Intrinsic Stability of Tregs as a Second Control Layer

Recruitment alone, however, does not fully explain the persistence and suppressive potency of Tregs within the TIME. Their functional dominance also depends on intrinsic transcriptional and epigenetic stability, which safeguards Treg identity under inflammatory pressure. Elegant mechanistic studies have revealed that Foxp3, the master regulator of Treg lineage commitment, forms a repressive complex with the transcription factor Ikzf1 to silence effector genes such as *IFNG*, thereby stabilizing the suppressive phenotype of Tregs [10].

Disruption of the Foxp3–Ikzf1 interaction destabilizes Tregs, leading to IFN-γ overproduction, loss of suppressive function, and paradoxically enhanced antitumor immunity. These findings suggest that tumors benefit not only from attracting Tregs into the TIME but also from maintaining their transcriptional integrity once established. Conceptually, Treg regulation in cancer can therefore be viewed as a two-tiered system: tumor-mediated recruitment followed by intrinsic transcriptional reinforcement.

This layered mode of control creates therapeutic opportunities but also introduces substantial analytical challenges. Dissecting where, when, and to what extent recruitment-dependent versus stability-dependent mechanisms dominate across heterogeneous patient populations exceeds the capacity of traditional experimental approaches. This motivates scalable, population-level approaches capable of resolving TIME heterogeneity.

AI and the Emergence of Virtual Tumor Immune Microenvironments

Artificial intelligence has begun to address this scalability problem. Multimodal frameworks such as GigaTIME leverage deep learning to infer spatial proteomic patterns from routine hematoxylin and eosin (H&E) slides, generating virtual multiplex immunofluorescence (mIF) data at population scale [11]. Specifically, such models take whole-slide histopathology images as primary inputs, employ convolutional and transformer-based architectures to learn spatially resolved feature representations, and are trained against matched molecular or imaging-derived ground truth to enable cross-modality inference.

By translating morphological features into immune activation maps, GigaTIME enables the construction of "virtual populations" comprising tens of thousands of tumors across cancer types. This approach fundamentally changes how the TIME can be studied: rare immune configurations, spatial arrangements, and combinatorial protein signatures—previously inaccessible due to cost and throughput limitations—become analyzable at scale. Model robustness is typically assessed through cross-cohort validation and comparison with orthogonal experimental measurements, ensuring that inferred immune patterns are reproducible and biologically meaningful.

For Treg-focused research, such platforms provide a powerful means to contextualize mechanistic immune programs across diverse clinical settings. Rather than asking whether a pathway exists, AI-enabled modeling allows investigators to ask how frequently, in which spatial niches, and in which patient subsets a given immunosuppressive program predominates. Importantly, alignment with biological mechanisms can be achieved by anchoring model interpretation to experimentally validated pathways—such as chemokine-driven Treg recruitment or transcriptional stability programs—thereby enabling AI-derived predictions to inform, and be iteratively refined by, mechanistic immunology.

Vision–Language Foundation Models and Mechanism-Aware Oncology

Beyond spatial inference, vision–language foundation models such as MUSK represent a further evolution in AI-driven oncology [12]. By jointly learning from pathology images and clinical text, these models demonstrate strong zero-shot performance in prognostic prediction and immunotherapy response assessment. Importantly, they move AI from pattern recognition toward integrative reasoning across modalities.

The next conceptual step is to align such models with bio-

logical mechanisms. Mechanistic discoveries—such as tumor-derived chemokine gradients driving Treg recruitment or transcriptional circuits stabilizing Treg identity—can serve as interpretive anchors for AI outputs. In turn, AI can highlight unexpected contexts in which these mechanisms are amplified, suppressed, or overridden.

In this sense, AI should not be viewed as a replacement for mechanistic immunology, but as a force multiplier that extends mechanistic insight into real-world complexity.

Toward a Convergent Framework

The convergence of molecular immunology and AI-driven TIME modeling marks a turning point in cancer research. Mechanistic dissection of tumor-driven Treg programs illustrates how focused experimental studies can reveal actionable immune vulnerabilities, while AI frameworks provide the scale and spatial resolution required to translate these insights into population-level relevance. At the same time, the effective application of such AI frameworks remains contingent on the availability of large, well-curated, and standardized datasets, as well as rigorous cross-cohort validation to mitigate bias and ensure biological interpretability.

Future progress will depend on mechanism-informed AI, in which experimentally validated pathways guide model interpretation, validation, and clinical deployment. Conversely, AI-derived hypotheses should inform experimental prioritization, focusing attention on the most clinically impactful immune circuits. Bridging this vision to implementation will require coordinated advances in data harmonization, model transparency, and close integration between computational predictions and experimental validation.

Ultimately, integrating biological depth with computational breadth may redefine how immune evasion is understood and overcome across immunologically complex solid tumors. A clear recognition of current technical and translational constraints will be essential for ensuring that AI-driven insights move beyond conceptual promise toward robust and clinically actionable applications.

Translational and Therapeutic Perspectives

AI-driven analysis of the tumor immune microenvironment offers practical opportunities to translate Treg biology into therapeutic decision-making. By integrating histopathology, molecular profiling, and clinical data at population scale, AI frameworks can enable patient stratification based on Treg abundance, spatial localization, and functional states, thereby identifying tumor subsets more likely to benefit from Treg-modulating strategies. Such stratification may inform the selection of patients for therapies targeting Treg recruitment, stability, or suppressive function, beyond conventional biomarkers that rely solely on tumor genetics or bulk immune signatures.

In addition, AI-enabled approaches can facilitate biomarker discovery and rational combination strategies by linking Treg-associated immune programs with treatment outcomes across large cohorts. For example, population-scale modeling may reveal contexts in which Treg enrichment predicts resistance to immune checkpoint blockade, supporting combination approaches that pair immunotherapy with agents targeting chemokine pathways, stromal cues, or transcriptional programs sustaining Treg stability. Importantly, a mechanism-informed AI framework allows these hypotheses to be grounded in experimentally validated pathways, enabling iterative refinement through focused preclinical and clinical studies. Together, such integrative strategies position AI not only as an analytical tool, but as a translational bridge connecting Treg-centered immunology with precision immunotherapy.

Abbreviations

AI, artificial intelligence; CCR4, C-C motif chemokine receptor 4; ccRCC, clear cell renal cell carcinoma; CTLA-4, cytotoxic T-lymphocyte–associated protein 4; FGFR, fibroblast growth factor receptor; FOXP3, forkhead box P3; Foxp3, forkhead box P3; H&E, hematoxylin and eosin; ICI, immune checkpoint inhibitor; IFNG, interferon gamma; Ikzf1, Ikaros family zinc finger 1; mIF, multiplex immunofluorescence; TIME, tumor immune microenvironment; TGFBI, transforming growth factor beta–induced; Treg(s), regulatory T cell(s).

Author Contributions

Xuexue Hao, Muwei Li and Tao Xiong contributed equally to this work. Xuexue Hao and Muwei Li conceived the central concept and wrote the initial manuscript. Tao Xiong contributed to the integration of immunological mechanisms and AI-related frameworks and participated in critical revisions of the manuscript. Xiaoqiang Liu supervised the overall project, provided conceptual guidance, and critically revised the manuscript for important intellectual content. All authors read and approved the final manuscript.

Acknowledgements

Not Applicable.

Funding Information

The author(s) declare that no financial support was received for the research and/or publication of this article.

Ethics Approval and Consent to Participate

Not Applicable.

Competing Interests

The authors declare that they have no existing or potential commercial or financial relationships that could create a conflict of interest at the time of conducting this study.

Data Availability

Not Applicable.

References

[1] Li Z-C, Qin W, Liang D, & Zheng H. (2025). Biomedical AI: Evolving from digital to physical and biological intelligence. The Innovation Informatics, 1(1), 100010. https://doi.org/10.59717/j.xinn-inform.2025.100010

[2] Song Y, Jiang S, Peng Y, Qin C, Du Y, & Xu T. (2024). Effect of FGFR alteration on prognosis in 1963 urothelial carcinoma patients with immune checkpoint inhibitors: Implying combination of FGFR inhibitor and immunotherapy for FGFR-altered urothelial carcinoma. Pharmacol Res, 205, 107230. https://doi.org/10.1016/j.phrs.2024.107230

[3] Chen H, Li W, Hu W, Liu J, Zhang C, Wang Y, et al. (2025). Discovery of a novel tetrapeptide as glucose homeostasis modulator with bifunctionalities of targeting DPP-IV and microbiota. Imeta, 4(5), e70072. https://doi.org/10.1002/imt2.70072

[4] Luo Y, Li Y, Fang M, Wang S, Shao L, Zou R, et al. (2025). Multi-omics synergy in oncology: Unraveling the complex interplay of radiomic, genoproteomic, and pathological data. Intelligent Oncology, 1(1), 17-30. https://doi.org/https://doi.org/10.1016/j.intonc.2024.10.003

[5] Hao X, Liu L, Li S, Wang Q, Xu Z, & Liu X. (2025). The regulatory role and mechanism of TGFBI on Tregs in the immune microenvironment of clear cell renal cell carcinoma. Int J Surg, 111(12), 9134-9146. https://doi.org/10.1097/js9.0000000000003225

[6] Curiel TJ, Coukos G, Zou L, Alvarez X, Cheng P, Mottram P, et al. (2004). Specific recruitment of regulatory T cells in ovarian carcinoma fosters immune privilege and predicts reduced survival. Nat Med, 10(9), 942-949. https://doi.org/10.1038/nm1093

[7] Simpson TR, Li F, Montalvo-Ortiz W, Sepulveda MA, Bergerhoff K, Arce F, et al. (2013). Fc-dependent depletion of tumor-infiltrating regulatory T cells co-defines the efficacy of anti-CTLA-4 therapy against melanoma. J Exp Med, 210(9), 1695-1710. https://doi.org/10.1084/jem.20130579

[8] Glasner A, Rose SA, Sharma R, Gudjonson H, Chu T, Green JA, et al. (2023). Conserved transcriptional connectivity of regulatory T cells in the tumor microenvironment informs new combination cancer therapy strategies. Nat Immunol, 24(6), 1020-1035. https://doi.org/10.1038/s41590-023-01504-2

[9] Plitas G, Konopacki C, Wu K, Bos PD, Morrow M, Putintseva EV, et al. (2016). Regulatory T Cells Exhibit Distinct Features in Human Breast Cancer. Immunity, 45(5), 1122-1134. https://doi.org/10.1016/j.immuni.2016.10.032

[10] Ichiyama K, Long J, Kobayashi Y, Horita Y, Kinoshita T, Nakamura Y, et al. (2024). Transcription factor Ikzf1 associates with Foxp3 to repress gene expression in Treg cells and limit autoimmunity and anti-tumor immunity. Immunity, 57(9), 2043-2060.e2010. https://doi.org/10.1016/j.immuni.2024.07.010

[11] Valanarasu JMJ, Xu H, Usuyama N, Kim C, Wong C, Argaw P, et al. (2025). Multimodal AI generates virtual population for tumor microenvironment modeling. Cell, 10.1016/j.cell.2025.11.016. https://doi.org/10.1016/j.cell.2025.11.016

[12] Xiang J, Wang X, Zhang X, Xi Y, Eweje F, Chen Y, et al. (2025). A vision-language foundation model for precision oncology. Nature, 638(8051), 769-778. https://doi.org/10.1038/s41586-024-08378-w

Research Article Life Conflux

Puerarin Inhibits Gastric Cancer Cell Proliferation by Blocking the G2/M Phase Transition

Authors

Jianye Han, Weiwei Yuan

Correspondence

yww15391960716@163.com (W. Yuan)

Graphical Abstract

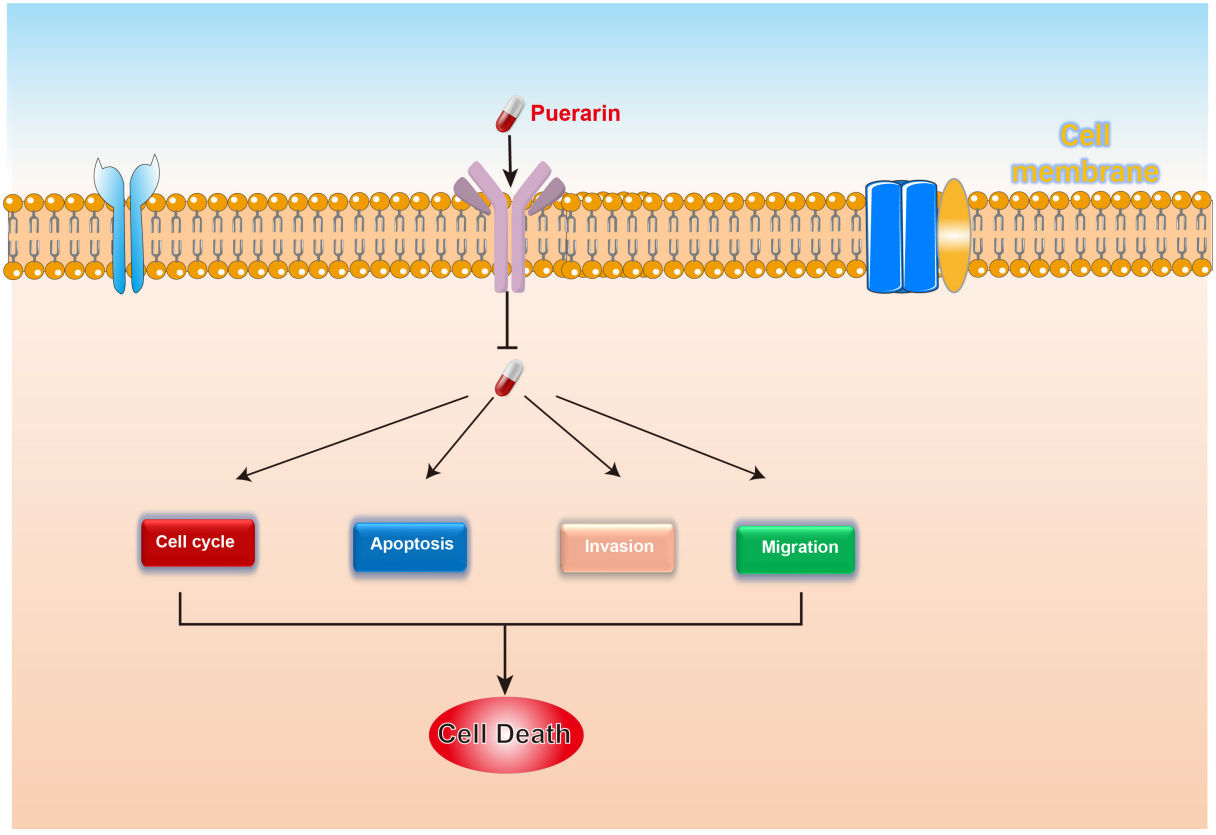

https://doi.org/10.71321/zf32x172
 L. Conflux. Vol. 2, No. 2 (2026)

Puerarin Inhibits Gastric Cancer Cell Proliferation by Blocking the G2/M Phase Transition

Jianye Han [1] , Weiwei Yuan [2*]

Received: 2025-10-11 | Accepted: 2025-12-23 | Published online: 2026-02-10

Abstract

Background: Gastric cancer is a tumor with high morbidity and mortality with in the world, and according to the statistics of the World Health Organization (WHO), the incidence of gastric cancer is predominant in Asia, especially in East Asia, China and Japan are high-incidence areas, which is related to the special dietary habits of East Asians.

Methods: In this study, we first investigated the effects of puerarin on the biological behaviors of two gastric cancer cell lines, HGC27 and AGS. To further explore the underlying mechanisms, we performed transcriptome sequencing, which revealed that puerarin primarily influences gastric cancer progression by regulating cell cycle transitions. To validate these findings, we examined the expression levels of cell cycle-related proteins and analyzed cell cycle distribution using flow cytometry.

Results: This study demonstrated that puerarin significantly inhibits the proliferation, migration, and invasion of gastric cancer cells (HGC27 and AGS) while promoting their apoptosis. Transcriptome sequencing analysis revealed that puerarin primarily affects the biological behaviors of gastric cancer cells by regulating the G2-to-M phase transition. To validate this mechanism, we further employed flow cytometry to assess cell cycle distribution and analyzed the expression levels of cell cycle-related proteins, providing protein-level evidence that supports the G2/M phase transition regulation identified in the transcriptomic data.

Conclusion: Puerarin effectively inhibits the proliferation and invasion of gastric cancer cells. Its mechanism is closely related to the regulation of the G2-to-M phase transition, thereby affecting cell cycle progression and proliferative capacity.

Keywords: Puerarin; Gastric cancer; Cell cycle

Introduction

Cancer is the second leading cause of death in the world, and gastric cancer has become an important health problem worldwide due to its high mortality rate [1]. Gastric cancer has a complex pathological mechanism, with a high degree of cellular heterogeneity [2] and a lack of specific clinical symptoms in the early stages of the disease, which leads to the majority of patients being in the middle and late stages when diagnosed and missing the best time for treatment. This is one of the main reasons for the high mortality rate [3]. The pathogenesis of gastric cancer involves the interaction of multiple factors, mainly including infectious factors and dietary factors. Among the infectious factors, Helicobacter pylori infection is considered to be the most important risk factor for gastric cancer, which may ultimately lead to gastric cancer by triggering chronic gastritis, gastric mucosal atrophy, and intestinal epithelial metaplasia [4]. In addition, Epstein-Barr virus (EBV) infection is also closely related to some gastric cancers (especially lymphoepithelioma-like gastric cancer). Among dietary factors, high salt diet and excessive intake of red meat and processed meat are important triggers of gastric cancer [5]. High salt diet not only directly damages the gastric mucosa, but also promotes the conversion of nitrite into the potent carcinogen nitrosamine in the stomach, and certain ingredients in red meat and processed meat may also increase the risk of gastric cancer [6]. Currently, the treatment of gastric cancer is relatively homogeneous, relying mainly on surgical resection, chemotherapy, and radiotherapy. For early gastric cancer, surgical resection is the main method of eradication, but for patients with intermediate and advanced stages, the therapeutic effect is often limited [7]. In addition, with the emergence of drug-resistant strains, the efficacy of chemotherapy and radiotherapy gradually decrease, which has become a major

1 Department of General Surgery, The First Affiliated Hospital of Anhui Medical University, Hefei 230022, China.

2 Department of Thyroid Surgery, Baoshan Hospital Affiliated to Shanghai University of Traditional Chinese Medicine, Shanghai 201999, China.

* Corresponding Author.

problem in gastric cancer treatment. In recent years, the rise of targeted therapy and immunotherapy has provided a new direction for the treatment of gastric cancer [8-9]. For example, for patients with HER2-positive gastric cancer, targeted drugs such as trastuzumab have shown certain efficacy.

The cell cycle is the entire process that a cell undergoes from the end of one division to the end of the next, and is the central biological mechanism of cell proliferation [10].The cell cycle is divided into four main phases: G1 phase (preparation for cell growth and metabolism), S phase (DNA replication), G2 phase (preparation for mitosis) and M phase (mitosis). Normally, the cell cycle is tightly regulated to ensure that cell proliferation matches the needs of the organism and maintains tissue homeostasis. However, in tumour cells, the regulatory mechanisms of the cell cycle are disrupted, leading to uncontrolled cell proliferation, which is one of the key features of tumourigenesis and progression [11-12]. The normal transformation of the cell cycle is largely dependent on the co-regulation between cytosolic proteins and cytosolic protein-dependent kinases [13]. Cyclins form complexes with CDKs and phosphorylate downstream target proteins to drive cell cycle progression. In addition, cell cycle protein-dependent kinase inhibitors (e.g., p21, p27) and tumour suppressor proteins (e.g., p53, Rb) play key roles in cell cycle checkpoints to ensure that cells move to the next phase with DNA integrity and replication complete [14-15]. In the cell cycle, the G1/S checkpoint and the G2/M checkpoint are two important regulatory nodes [16]. At the G1/S checkpoint, the cell detects whether DNA is intact and growth signals are appropriate to decide whether to enter S phase. p53 and Rb proteins play key roles in this checkpoint. At the G2/M checkpoint, the cell detects whether DNA replication is complete and ensures that it is suitable for mitosis [17]. If this checkpoint is out of control, the cell may enter division with incompletely replicated DNA, further exacerbating genomic instability. In most tumours, abnormalities in cell cycle regulatory mechanisms are central to the excessive proliferation of tumour cells. For example, overexpression of molecules such as Cyclin D1, Cyclin E, and CDK4/6, as well as inactivation of CDKIs (e.g., p21, p27), leads to accelerated cell cycle progression. With the in-depth study of cell cycle regulatory mechanisms, studies have found that the cell cycle is closely related to tumour therapy. For example, CDK4/6 inhibitors (e.g., pabocinib, repocinib) have been approved for the treatment of tumours such as breast cancer and inhibit the proliferation of tumour cells by inhibiting the activity of the Cyclin D-CDK4/6 complex, which prevents the cell cycle from moving from the G1 phase to the S phase [18]. In addition, in the process of radiotherapy and chemotherapy, ionising radiation and chemotherapeutic drugs (e.g., cisplatin, paclitaxel) are effective in the treatment of tumours by inducing DNA damage and activating cell cycle checkpoints, leading to cell cycle arrest or apoptosis, thus inhibiting the proliferation of tumour cells [11].

Puerarin is an isoflavonoid compound extracted from the traditional Chinese medicine pueraria lobata with a wide range of biological activities and pharmacological effects [19-20]. Puerarin has a wide range of pharmacological effects, including cardiovascular protection (e.g., vasodilation, improved microcirculation, lowered blood pressure, anti-myocardial ischemia, and anti-arrhythmia), antioxidant effects (e.g., scavenging free radicals...), anti-inflammatory effects (e.g., inhibiting the release of inflammatory mediators, reducing inflammatory response); neuroprotection (e.g., improving cerebral ischemia and brain damage, protecting neurons, and slowing down the progress of neurodegenerative diseases (e.g., Alzheimer's disease, Parkinson's disease)) [21-22]. It also exhibits anti-tumour effects by inhibiting proliferation of tumour cells, inducing apoptosis of tumour cells, and inhibiting tumour angiogenesis. In breast cancer, puerarin inhibits the proliferation and metastasis of breast cancer cells by inhibiting the estrogen receptor (ER) signalling pathway [23]. In hepatocellular carcinoma, it significantly inhibits the growth of hepatocellular carcinoma by inducing apoptosis and inhibiting angiogenesis [24]. In lung cancer, puerarin inhibits the proliferation and invasion of lung cancer cells through the modulation of the PI3K/Akt and MAPK signalling pathways [25]. The present study mainly explored the effect of puerarin on gastric cancer cells, and it was found that puerarin affects the proliferation of gastric cancer cells mainly by influencing the cell cycle progression.

In this study, we first systematically investigated the effects of puerarin on the biological functions of gastric cancer cells. The experimental results showed that puerarin markedly suppressed the proliferation and invasion ability of gastric cancer cells, and at the same time induced tumour cell apoptosis. In order to further reveal the mechanism of action of puerarin against gastric cancer, we carried out an in-depth analysis of its molecular mechanism by using transcriptome sequencing technology. The results showed that puerarin inhibited the proliferation of gastric cancer cells mainly by regulating the expression of cell cycle-related genes and blocking the cell cycle process. To verify the anti-tumour effect of puerarin in vivo, we constructed a subcutaneous transplantation tumour model of gastric cancer to simulate the tumour microenvironment in vivo. The results of animal experiments showed that puerarin was able to significantly inhibit the subcutaneous tumour-forming ability of gastric cancer cells and reduced the tumour volume and weight, with no obvious toxic side effects observed. This finding not only confirmed the anti-tumour activity of puerarin in vivo, but also provided an important experimental basis for its potential use as a drug for gastric cancer treatment.

Materials and methods

Western blot

Proteins in tissues or cells were extracted with RIPA lysate (Beyotime, Shanghai, China) with the addition of PMSF and phosphatase inhibitors. Then proteins were separated by SDS-PAG, transferred using PVDF membranes, and blotted with suitable primary antibodies. The primary antibodies used were: GAPDH (Proteintech Group, Wuhan, China; dilution 1:5000), CDK1, CDK4, Cyclin A, Cyclin B, BAX, and BCL2 (all from Cell Signaling Technology, Shanghai, China; dilution 1:1000).

Transwell and wound-healing assays

Transwell inserts (Corning, NY, USA), either coated or uncoated with BD Matrigel, were used to assess the invasive or migratory capacity of the cells. A total of 5×10^4 cells were resuspended in 200 µl of serum-free medium and loaded into the upper chamber. After cells that had successfully invaded through the Matrigel (for invasion assays) or migrated through the membrane (for migration assays) reached the lower sur-

face of the membrane, they were fixed with methanol and stained with crystal violet. Images were captured using an inverted phase-contrast microscope (Olympus, Tokyo, Japan), and the number of stained cells was quantified by counting them with ImageJ software.

Flow cytometry for apoptosis analysis

Apoptosis was assessed in the DMSO and dosing groups using an apoptosis kit (Annexin V-AF647/PI Apoptosis Kit, GOONOE) and data were collected using BD FACScelesta 3 (NJ, USA). The final results were analysed using Flowjo.

Flow cytometry for cell cycle analysis

Cell cycle was assessed in the DMSO and dosing groups using the Cell Cycle Assay Kit GOONOE) and data were collected using BD FACScelesta 3 (NJ, USA). Final results were analysed using Flowjo.

Animal studies

Twelve 3-4 weeks old female BALB/c thymus-free nude mice (strain: BALB/c-nu/nu) weighing 18-22 g were purchased from Jiangsu Jicui Pharmacology Co., Ltd. They were housed in SPF-grade barriers with a temperature of 22±2°C, a relative humidity of 50±10%, a 12-h light/dark cycle, and an ad libitum intake of irradiated sterilized chow and autoclaved water. The mice were domesticated for 7 days after purchase, and the experiments were started after daily observation of their health condition and confirmation of no abnormality. Inoculation method: Mice were injected with 100 μL of cell suspension subcutaneously in the right axilla (the skin was sterilized with 75% ethanol before injection).

Experimental groups (n=6/group):

Control group (DMSO): 100 μL saline + 0.1% DMSO (solvent control);

Low dose group: puerarin 20 μg (dissolved in saline);

High dose group: puerarin 40 μg (dissolved in saline).

Euthanasia and sample collection (21 days after inoculation):

Anesthesia: Intraperitoneal injection of 5% isoflurane (dosage: 0.1 mL/10 g) to confirm the absence of nociceptive reflexes in the mice. Cervical dislocation was performed: the head and tail were quickly immobilized and the cervical vertebrae were pulled back to ensure instantaneous death.

Sample processing: complete excision of the tumor, weighing and portioning. Portions were placed in 4% paraformaldehyde for fixation (stained with HE and TUNEL). This study was approved by the Animal Ethics Committee of Anhui Medical University (Protocol No. 2024123)

RNA sequencing

RNA sequencing was performed by Genedenovo Biotechnology Ltd (Guangzhou, China) using libraries sequenced on the Illumina sequencing platform. The samples were divided into two groups. After treating cells with DMSO or the IC50 concentration of puerarin, we extracted RNA and sent it for sequencing.

Results

Chemical structure of puerarin and its effect on gastric cancer cell activity

The chemical structure and three-dimensional molecular structure of puerarin are shown in Figure 1A and B. To investigate the toxic effects of puerarin on gastric cancer cells, two commonly used gastric cancer cell lines, AGS and HGC27, were selected as the experimental models in this study. By setting up different concentration gradients of puerarin treatment, we determined that its optimal administration concentration for both cell lines was 1 mM (Figure 1C and D). To further investigate the effects of puerarin on gastric cancer cells, the inhibitory effects of different concentrations of puerarin on cell proliferation over time were systematically detected using the CCK-8 (Cell Counting Kit-8) method (Figure 1E). This experiment was designed to comprehensively evaluate the toxic effects of puerarin on gastric cancer cells and its concentration dependence.

Figure 1. Spatial structure of Puerarin and toxic effects of two gastric cancer cells

(**A**) Two-dimensional chemical structure of puerarin. (**B**) Three-dimensional molecular structure of puerarin. (**C**) The effect of different concentration gradients of puerarin treatment on the viability of HGC27 cells over 24 h was detected by CCK-8 method. (**D**) The effect of different concentration gradients of puerarin treatment on the viability of AGS cells over 24 h was detected by CCK-8 method. (**E**) The concentrations of DMSO (control), 1 mM, and 2 mM were used to treat HGC27 gastric cancer cells, respectively. of Puerarin were treated with HGC27 gastric cancer cells and cell viability was determined by CCK-8 assay at 0, 12, 24, 36 and 48 h time points. (**F**) AGS gastric cancer cells were treated with DMSO (control), 1 mM and 2 mM concentrations of Puerarin, respectively, and cell viability was determined by CCK-8 assay at 0, 12, 24, 36 and 48 h time points.

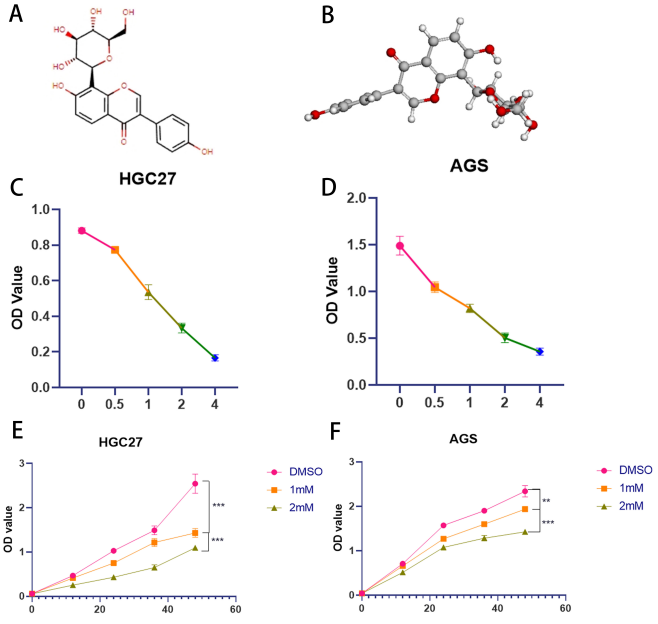

Puerarin inhibited the proliferation and invasion of gastric cancer cells.

To investigate the effect of puerarin on the proliferation function of gastric cancer cells, The EdU and colony formation assays were performed in this study. The results of EdU assay showed that the fluorescence positivity rate of 1 mM and 2 mM puerarin-treated groups was significantly reduced com-

pared with that of the DMSO control group, which indicated that puerarin could inhibit the DNA replication activity of gastric cancer cells effectively (Figure 2A and B). The results of colony formation assay further showed that the number of clone-forming clusters in the 1 mM and 2 mM puerarin-treated groups was significantly reduced, which confirmed the inhibitory effect of puerarin on cell proliferation (Figure 2C). Taken together, the above results indicated that puerarin was able to significantly inhibit the proliferative ability of gastric cancer cells. In addition, to assess the effect of puerarin on the invasive ability of gastric cancer cells, we used the Transwell assay. The results showed that the number of cells passing through the lower chamber was significantly reduced in the 1 mM and 2 mM puerarin treatment groups, indicating that puerarin was able to effectively inhibit the invasive ability of gastric cancer cells (Figure 2D).

Figure 2. Puerarin inhibited the proliferation and invasion of gastric cancer

(**A**) The fluorescence positivity rate of AGS cells in DMSO (control group), 1 mM and 2 mM Puerarin-treated groups was detected by EdU assay to evaluate the effect of the drug on the proliferative viability of the cells. (**B**) The fluorescence positivity rate of HGC27 cells in DMSO (control group), 1 mM and 2 mM Puerarin-treated groups was detected by EdU assay to further evaluate the effect of Puerarin on the proliferative ability of the cells. (**C**) The monoclonal formation ability of AGS and HGC27 cells under different concentrations of puerarin treatment was analysed by colony formation assay to clarify the dose-dependent effect of the drug on the cell proliferation function. (**D**) The effects of different concentrations of puerarin treatment on the invasion ability of AGS and HGC27 cells were investigated by using Transwell assay to reveal the potential mechanism of the drug's action in inhibiting cell migration and invasion. (**E**) The effects of different concentrations of puerarin treatment on the invasion ability of AGS and HGC27 cells were investigated by using Transwell assay. potential mechanism of action in inhibiting cell migration and invasion.

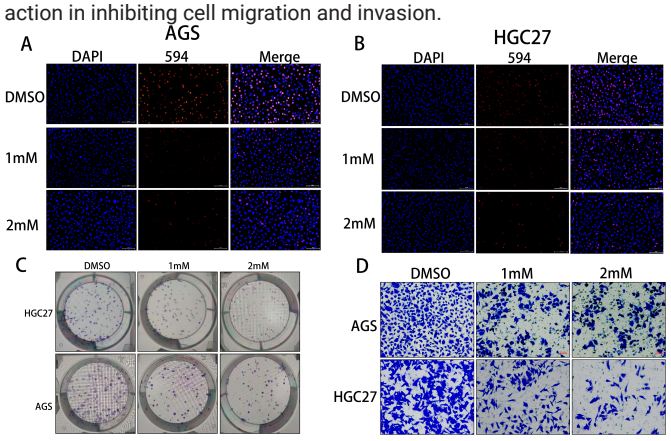

Transcriptome sequencing showed that puerarin affects tumour cell cycle progression.

In order to deeply investigate the mechanism of the effect of puerarin on the biological behaviour of gastric cancer cells, we performed transcriptome sequencing analysis on the DMSO control group and the 1 mM puerarin-treated group, respectively. The sequencing results showed that there were significantly differentially expressed genes between the two groups of samples, and a total of more than 3,000 differentially expressed genes were screened (Figure 3A). To further elucidate the functions of these differential genes, we performed bioinformatics analyses, including KEGG pathway enrichment analysis and GO functional annotation. The results of the analyses indicated that puerarin affected the biological behaviours of gastric cancer cells mainly by regulating cell cycle-related pathways and DNA replication processes (Figure 3B-D). Specifically, puerarin significantly interfered with the normal progression of the cell cycle, leading to cell cycle arrest. In addition, puerarin was found to induce apoptosis in gastric cancer cells, thereby effectively inhibiting the proliferation of tumour cells (Figure 3E). These findings provide a basis for the molecular mechanism for the potential application of puerarin in gastric cancer treatment.

Puerarin promotes apoptosis

Sequencing results indicated that Puerarin may induce cells to undergo apoptosis. To verify this result, we first treated AGS and HGC27 cells with different concentrations of puerarin and detected the apoptosis rate by flow cytometry (Figure 4A and B). The results showed that the apoptosis rate was significantly increased in the drug-treated group compared with the DMSO control group, which initially confirmed the pro-apoptotic effect of puerarin. To further validate this phenomenon, we examined the expression levels of apoptosis-related proteins (BAX, BCL2, Caspase3) using the Western blot technique (Figure 4C and D). The experimental results showed that puerarin treatment significantly up-regulated the expression of pro-apoptotic proteins BAX and Caspase3, while down-regulated the expression of the anti-apoptotic protein BCL2, a finding that was highly consistent with those detected by flow cytometry. In summary, the above experimental data together confirmed that puerarin is able to promote apoptosis in gastric cancer cells by regulating the expression of apoptosis-related proteins.

Puerarin inhibits the transition from G2 to M phase in cells.

Sequencing results indicated that puerarin may affect the cell cycle progression of gastric cancer cells. To verify this result, we firstly treated different concentrations of puerarin in AGS and HGC27 cells respectively and detected the cell cycle distribution by flow cytometry (Figure 5A and B). The results showed that the proportion of cells in G2 phase was significantly increased in the puerarin-treated group compared with the DMSO control group, indicating that puerarin was able to induce cells to arrest in G2 phase. To further verify this phenomenon, we examined the expression levels of cell cycle-related proteins (CDK1, CDK4, CyclinA and CyclinB) in the DMSO group, the 1 mM group and the 2 mM group by using the Western blot technique (Figure 5C and D). The results showed that puerarin treatment significantly down-regulated the expression of CDK1 and CyclinB, while affecting the expression pattern of CDK4 and CyclinA. In addition, the effect of puerarin on cell cycle regulation was further confirmed by detecting the content of CDK4 in HGC27 cells by cellular immunofluorescence assay (Figure 5E). In summary, the above experimental results collectively indicated that puerarin promotes cell arrest in G2 phase by regulating the expression of cell cycle-related proteins, thus inhibiting the transformation of cells to M phase.

Effect of puerarin on tumours in vivo

To investigate the effect of puerarin on tumour growth in vivo,

we performed subcutaneous transplantation tumour experiments. First, 1 × 10^7 HGC27 cells were injected into the axillary region of mice, and one week later, the mice were randomly divided into three groups: the DMSO control group (injected with saline), the 1 mM group (injected with 20 μg of puerarin), and the 2 mM group (injected with 40 μg of puerarin). The experimental results showed that puerarin treatment significantly inhibited the growth of tumours in vivo, indicating its significant anti-tumour activity (Figure 6A and B). To further assess the effect of puerarin on the proliferation and apoptosis of tumour cells, we sectioned the tumour tissues and detected the proliferation and apoptosis levels of tumour cells using KI-67 staining and TUNEL staining respectively (Figure 6C). The results showed that the proportion of KI-67-positive cells was significantly reduced in the puerarin-treated group, whereas the proportion of TUNEL-positive cells was significantly increased, in-

Figure 3. Analysis of the transcriptome sequencing results revealed the significant effects of Puerarin on the gene expression profiles of gastric cancer cells.

(**A**) RNA sequencing results showed that more than 2,000 significantly up-regulated genes and more than 1,000 significantly down-regulated genes existed in the Puerarin-treated group compared with the control group. (**B**) KEGG dot plot enrichment analysis further demonstrated that the differentially expressed genes were significantly enriched in the DNA replication and cell-cycle related pathways. (**C**) KEGG histogram enrichment analysis results were consistent with the dot plot, which further verified that DNA replication and cell cycle pathways in the mechanism of action of puerarin. (**D**) GO functional annotation histogram showed that the differentially expressed genes were significantly enriched in cell cycle-related functional categories, which further supported the regulatory effect of puerarin on cell cycle progression. (**E**) In addition, the sequencing results also showed that puerarin significantly affected the apoptosis-related pathway, suggesting that it may inhibit the growth of gastric cancer cells by inducing cell apoptosis. growth of gastric cancer cells by inducing apoptosis.

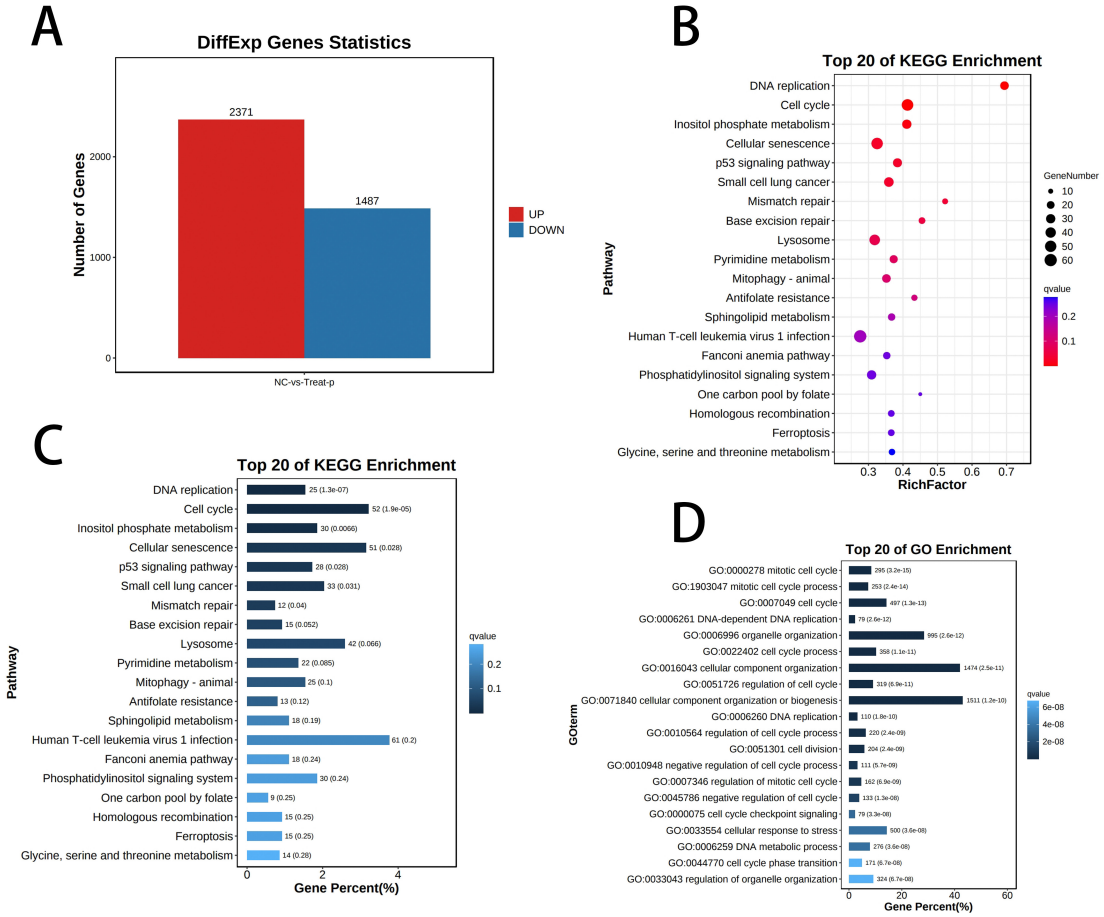

E

#	Pathway	DEGs with pathway annotation (2085)	All genes with pathway annotation (8986)	Pvalue	Qvalue	Pathway ID
1	Metabolic pathways	307 (14.72%)	1081 (12.03%)	1.354119e-05	0.002911356	ko01100
2	Proteasome	23 (1.1%)	48 (0.53%)	0.000182570	0.01593762	ko03050
3	B cell receptor signaling pathway	29 (1.39%)	70 (0.78%)	0.000508534	0.03644494	ko04662
4	Apoptosis	34 (1.63%)	89 (0.99%)	0.001018471	0.04573788	ko04210
5	Hematopoietic cell lineage	31 (1.49%)	80 (0.89%)	0.001271905	0.04573788	ko04640
6	Primary immunodeficiency	16 (0.77%)	33 (0.37%)	0.001276406	0.04573788	ko05340
7	Glycosylphosphatidylinositol(GPI)-anchor biosynthesis	13 (0.62%)	25 (0.28%)	0.001618825	0.04972105	ko00563
8	N-Glycan biosynthesis	18 (0.86%)	40 (0.45%)	0.001901140	0.05109313	ko00510
9	Huntington's disease	60 (2.88%)	187 (2.08%)	0.003132988	0.07484360	ko05016
10	Other glycan degradation	9 (0.43%)	16 (0.18%)	0.004361382	0.09376971	ko00511
11	Alzheimer's disease	56 (2.69%)	176 (1.96%)	0.005133783	0.10034212	ko05010
12	Biosynthesis of steroids	13 (0.62%)	28 (0.31%)	0.005747707	0.10297975	ko00100
13	Chronic myeloid leukemia	27 (1.29%)	74 (0.82%)	0.006681019	0.11049377	ko05220
14	Epithelial cell signaling in Helicobacter pylori infection	25 (1.2%)	68 (0.76%)	0.007943713	0.12199273	ko05120

dicating that puerarin was able to inhibit the proliferation of tumour cells and induce their apoptosis (Figure 6D). In addition, to assess the potential toxicity of puerarin on the major organs of mice, we performed HE staining analysis on the heart, liver, kidney, lung and spleen of mice in the normal and treated groups (Figure 6E). The results showed that no significant pathological changes were observed in the major organs of mice in all groups, indicating that puerarin had no significant organ toxicity at the experimental dose. In conclusion, this study confirmed that puerarin could effectively inhibit the growth of tumours in vivo without showing obvious organ toxicity, which provides an important experimental basis for its further development as an anti-tumour drug.

Discussion

Puerarin is a natural isoflavonoid, one of the main active components in Pueraria lobata. It has a variety of pharmacological effects, including antioxidant, anti-inflammatory, cardiovascular protection, neuroprotection, etc. [19] In recent years, it has been found that puerarin is closely related to cancer, and that it affects the proliferation, apoptosis, invasion, and metastasis of tumour cells through a variety of mechanisms, possesses both antioxidant and anti-inflammatory effects and may indirectly inhibit tumourigenesis and progression. For example, in breast cancer puerarin inhibits the proliferation and invasion of breast cancer cells by inhibiting the PI3K/AKT and MAPK signalling pathways [19, 21]. In hepatocellular carcinoma, Puerarin inhibits the proliferation and metastasis of hepatocellular carcinoma cells by modulating the Wnt/β-catenin and PI3K/AKT signalling pathways. In animal models, puerarin significantly inhibited the growth of hepatocellular carcinoma. Meanwhile, Puerarin is also closely related to cancer treatment. Experimental studies have shown that Puerarin can enhance the sensitivity of tumour cells to chemotherapeutic drugs (e.g., cisplatin, 5-fluorouracil), and reduce the dosage and side effects of chemotherapeutic drugs. For example, in lung and gastric cancer studies, puerarin showed synergistic anti-tumour effects in combination with chemotherapeutic drugs. Through its antioxidant and anti-inflammatory effects, puerarin reduces oxidative stress and inflammation in tumour patients, thereby improving their quality of life. Recent studies highlight that dysregulation of the cell cycle plays a central role in gastric cancer, closely linked to multi omics molecular subtypes. A G2/M phase related PDEGs signature can predict survival and immunotherapy response, with key genes such as *F2R* associated with oxaliplatin resistance, while natural products and epigenetic modulation (e.g., p21 upregulation) induce G2/M arrest, while axes involving *UBE2C* and *Hip2* regulate proliferation and metastasis, offering novel targets for precision therapy [26].

The aim of this experiment was to investigate the effect of puerarin on gastric cancer and its potential mechanism. Firstly, we selected two common gastric cancer cell lines (HGC27 and AGS) and determined the optimal administration concentration of puerarin within 24 hours by a CCK-8 assay, and found that puerarin had a significant inhibitory effect on the

Figure 4. Detection of apoptosis by flow and WB experiments
(**A**) Detection of apoptosis of AGS gastric cancer cells in DMSO (control group), 1 mM and 2 mM Puerarin-treated groups by flow cytometry. (**B**) Detection of apoptosis of HGC27 gastric cancer cells in DMSO (control group), 1 mM and 2 mM Puerarin-treated groups by flow cytometry. (**C**) Detection of apoptosis in DMSO (control group), 1 mM and 2 mM expression levels of AGS apoptosis-related proteins (BAX, BCL2, Caspase3) and the internal reference protein GAPDH in the Puerarin-treated groups. (**D**) The expression levels of apoptosis-related proteins (BAX, BCL2, Caspase3) and the internal reference protein GAPDH in HGC27 cells in the DMSO (control group), the 1 mM and the 2 mM Puerarin-treated groups were examined by Western blotting technique. protein GAPDH in the DMSO (control) and 2 mM Puerarin-treated groups.

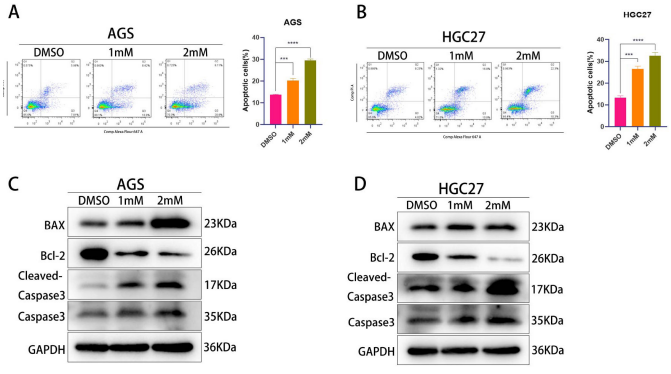

Figure 5. Effects of Puerarin on the cell cycle of gastric cancer
(**A**) The cell cycle distribution of AGS gastric cancer cells in DMSO (control group), 1 mM and 2 mM Puerarin-treated groups was examined by flow cytometry to analyse the changes in the proportions of cells in the G1, S and G2 phases. (**B**) The cell cycle distribution of HGC27 gastric cancer cells in DMSO (control group), 1 mM and 2 mM Puerarin-treated groups was examined by flow cytometry to analyse the changes in the proportions of cells in the G1, S and G2 phases. and G2 phases. (**C**) The expression levels of AGS cell cycle-related proteins (CDK1, CDK4, CyclinA and CyclinB) and the endogenous protein GAPDH were detected in DMSO (control group), 1 mM and 2 mM Pueraria Mirifica-treated groups using Western blot. (**D**) The expression level of expression levels of HGC27 cell cycle-related proteins (CDK1, CDK4, CyclinA and CyclinB) and the endogenous reference protein GAPDH in the DMSO (control), 1 mM and 2 mM geraniol-treated groups. (**E**) Cellular immunofluorescence was used to detect the expression of CDK4 in HGC27 gastric cancer cells.

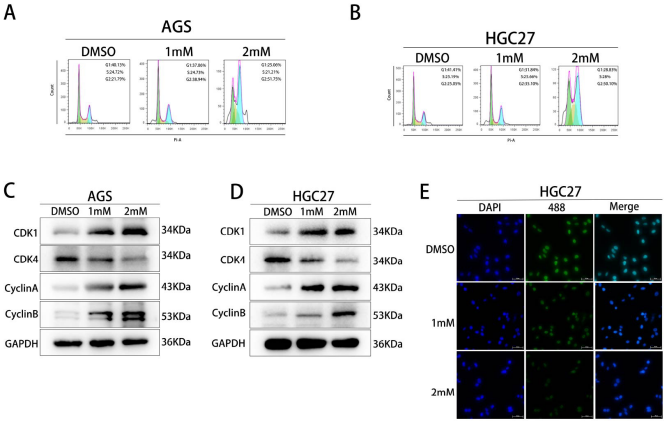

proliferation of gastric cancer cells. To further validate this result, we used EdU staining and plate cloning experiments, both of which confirmed that puerarin could effectively inhibit the proliferation ability of gastric cancer cells. Given the high metastatic characteristics of gastric cancer, we explored the effect of puerarin on the invasive ability of gastric cancer cells by transwell assay. The results showed that puerarin significantly inhibited cell invasion. In order to further investigate the mechanism of puerarin, we performed transcriptome sequencing on the blank and puerarin-treated groups. Transcriptome sequencing analysis revealed that puerarin inhibited cell proliferation primarily by affecting the expression of cell cycle-related genes. Therefore, we further detected the changes in cell cycle by flow cytometry and found that, compared with the control group, the additive group showed a significantly increased proportion of cells in G2 phase and a significantly decreased proportion in G1 phase. This suggests that puerarin may inhibit tumour cell proliferation by blocking the cell cycle. In addition, the transcriptome sequencing results also showed that puerarin was able to induce apoptosis. To verify this, we detected key proteins of apoptosis (e.g., Bax, Bcl-2 and Caspase-3) by flow cytometry and Western blotting, and the results further confirmed that puerarin could promote apoptosis of gastric cancer cells. Taking the above experimental results together, we systematically elucidated the inhibitory effect of puerarin on gastric cancer cells and its potential mechanism in terms of cell proliferation, invasion, cycle arrest, and apoptosis. Although we performed multiple experiments to investigate the

Figure 6. Effects of Puerarin in rats

(**A**) At the end of the experiment, nude mice in the DMSO control group, 1 mM group and 2 mM group were executed to collect tumour tissues and major organs for subsequent analysis. (**B**) The inhibitory effect of puerarin on tumour growth was assessed by measuring the volume of tumours in nude mice in the DMSO control group, 1 mM group and 2 mM group. (**C**) Sections of tumour tissues in the DMSO control, 1 mM and 2 mM groups were subjected to KI67 staining for the detection of tumour growth. KI67 staining was performed to detect the proliferation level of tumour cells to clarify the effect of puerarin on tumour cell proliferation. (**D**) TUNEL staining was performed on tumour tissue sections from DMSO control, 1 mM and 2 mM groups to detect the apoptosis level of tumour cells, to further validate the apoptosis-inducing effect of puerarin on tumour cells. (**E**) Hepatitis B and Hepatitis C staining was performed on hearts, livers, kidneys, lungs, and spleens of nude mice in DMSO control and 2 mM groups to assess the inhibitory effect of puerarin on tumour growth. , lungs and spleens were subjected to HE staining to assess the potential toxicity of gerberellin to major organs and ensure its safety.

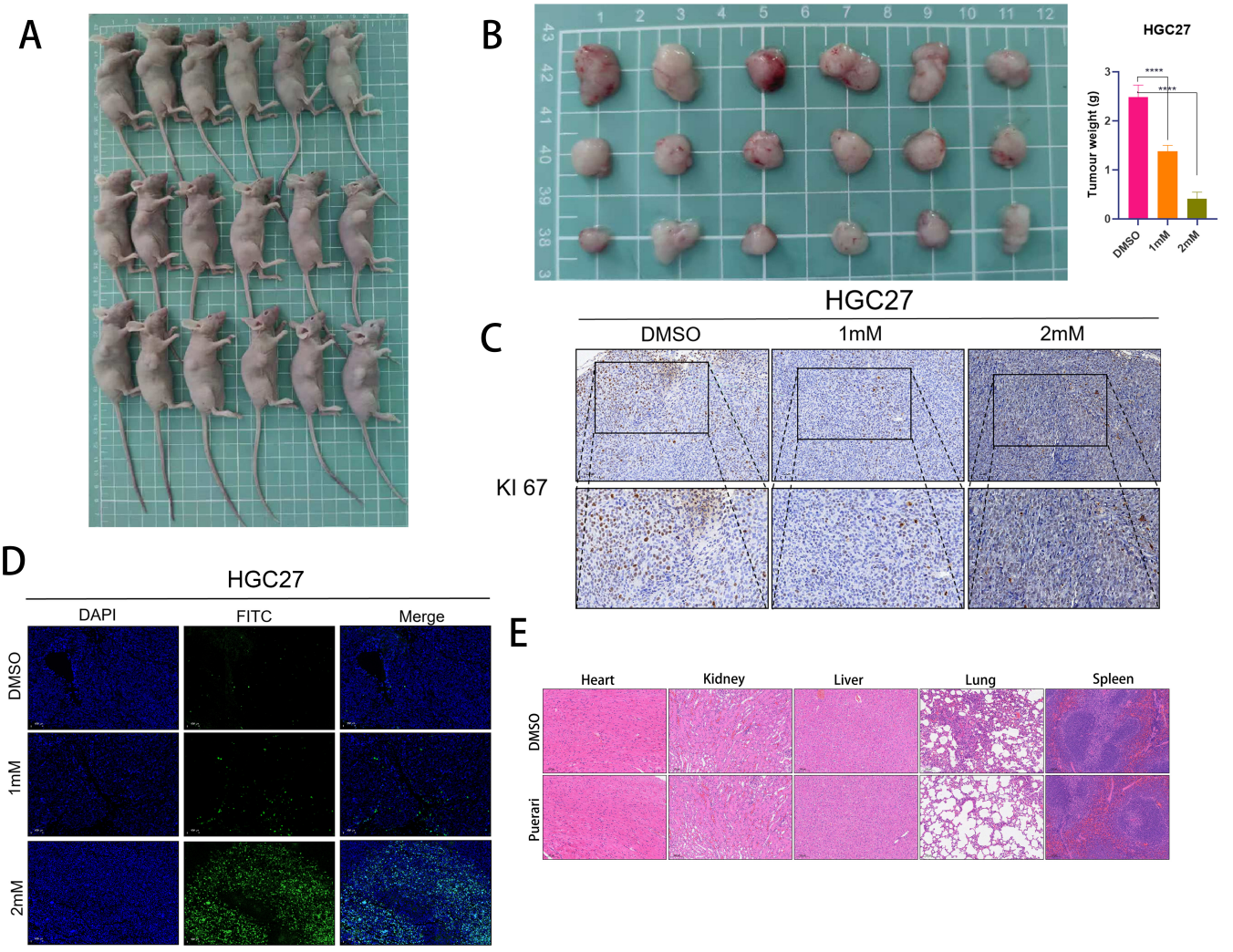

cell cycle and apoptosis, further investigation is still needed as to the way in which puerarin leads to cell cycle changes.

In order to further investigate the anti-tumour effects of puerarin in vivo, we carried out animal experiments in which the experimental animals were divided into the treatment group and control groups, and the effects of puerarin on tumour growth were investigated by constructing a subcutaneous tumour-forming model in nude mice. The experimental results showed that the tumour volume of the drug-added group was significantly smaller than that of the control group, suggesting that puerarin has an obvious tumour-suppressing effect in vivo. To further verify this result, we sectioned the tumour tissues of nude mice and analysed the proliferative activity of tumour cells by KI-67 immunohistochemical staining, and found that the proportion of KI67-positive cells in the drug-added group was significantly reduced, which further confirmed the inhibitory effect of puerarin on tumour proliferation. Although we preliminarily verified the in vivo anti-tumour effect of puerarin through the nude mice tumour-forming assay, this study has not yet been subjected to clinical trials, and therefore the actual efficacy and safety of puerarin in humans cannot be assessed. In addition, future studies could further explore the combined effects of puerarin and chemotherapeutic agents (e.g., cisplatin) to assess whether it can enhance the effects of chemotherapy or reduce the side effects of chemotherapeutic agents, thus providing new strategies for the combination therapy of gastric cancer.

In summary, the present study demonstrated that puerarin inhibited the proliferation of tumour cells by regulating the cell cycle, providing an experimental basis for its use as a potential anticancer drug. However, further clinical studies are needed to assess the efficacy and safety of puerarin in humans, as well as to explore its synergistic effects with other chemotherapeutic agents. In addition, more in-depth studies on the mechanism of action of puerarin in gastric cancer are also needed to reveal the molecular mechanisms behind it and to provide a new theoretical basis and a direction for drug development in gastric cancer treatment.

Conclusion

Our findings demonstrate that puerarin significantly suppresses malignant biological behaviors in gastric cancer cells. Transcriptome sequencing analysis revealed that puerarin inhibits cell proliferation by blocking cell cycle progression. Furthermore, in vivo experiments confirmed that puerarin effectively reduces the tumorigenic capacity of gastric cancer cells in a nude mouse subcutaneous xenograft model.

Abbreviations

EdU: 5-Ethynyl-2'-deoxyuridine; WB:Western Blot; DMSO: dimethylsulfoxide; GAPDH: glyceraldehyde-3-phosphate; CCK8: Cell Counting Kit-8; IC50: Half maximal inhibitory concentration; Rpm: Revolutions per minute; DAPI: 4', 6-diamidino-2-phenylindole; 594: Fluorescein 594.

Author Contributions

Jianye Han: Experimental design and execution, Writing original draft. Weiwei Yuan: Data management. All authors read and approved the final manuscript.

Acknowledgements

Not Applicable.

Funding Information

Not Applicable.

Ethics Approval and Consent to Participate

This study was approved by the Animal Ethics Committee of Anhui Medical University (Protocol No. 2024123). All procedures were conducted in strict compliance with the Guidelines for Ethical Review of Laboratory Animal Welfare in China (GB/T 35892-2018) and the ARRIVE 2.0 guidelines to ensure the ethical treatment of animals. No human tissues were used.

Competing Interests

The authors declare that they have no existing or potential commercial or financial relationships that could create a conflict of interest at the time of conducting this study.

Data Availability

All data needed to evaluate the conclusions in the paper are present in the paper or the Supplementary Materials. Additional data related to this paper may be requested from the authors.

Reference

[1] Smyth EC, Nilsson M, Grabsch HI, van Grieken NC, & Et. A. (2020). Gastric cancer. The Lancet. https://doi.org/10.1016/S0140-6736(20)31288-5

[2] Chia N-Y, & Tan P. (2016). Molecular classification of gastric cancer. Annals of Oncology. https://doi.org/10.1093/annonc/mdw040

[3] Sexton RE, Al Hallak MN, Diab M, & Azmi AS. (2020). Gastric Cancer: A Comprehensive Review of Current and Future Treatment Strategies. Cancer Metastasis Rev, 39(4), 1179–1203. https://doi.org/10.1007/s10555-020-09925-3

[4] Rha SY, Oh D-Y, Yañez P, Bai Y, Ryu M-H, Lee J, et al. (2023). Pembrolizumab plus chemotherapy versus placebo plus chemotherapy for HER2-negative advanced gastric cancer (KEYNOTE-859): a multicentre, randomised, double-blind, phase 3 trial. Lancet Oncol, 24(11), 1181–1195. https://

doi.org/10.1016/S1470-2045(23)00515-6
[5] Zheng X, Wang R, Zhang X, Sun Y, Zhang H, Zhao Z, et al. (2022). A deep learning model and human-machine fusion for prediction of EBV-associated gastric cancer from histopathology. Nat Commun, 13, 2790. https://doi.org/10.1038/s41467-022-30459-5
[6] Li W-Q, Zhang J-Y, Ma J-L, Li Z-X, Zhang L, Zhang Y, et al. (2019). Effects of Helicobacter pylori treatment and vitamin and garlic supplementation on gastric cancer incidence and mortality: follow-up of a randomized intervention trial. BMJ, 366, l5016. https://doi.org/10.1136/bmj.l5016
[7] Zeng Y, & Jin RU. (2022). Molecular pathogenesis, targeted therapies, and future perspectives for gastric cancer. Seminars in Cancer Biology, 86, 566–582. https://doi.org/10.1016/j.semcancer.2021.12.004
[8] Ma S, Zhou M, Xu Y, Gu X, Zou M, Abudushalamu G, et al. (2023). Clinical application and detection techniques of liquid biopsy in gastric cancer. Mol Cancer, 22, 7. https://doi.org/10.1186/s12943-023-01715-z
[9] Wang X, Zhang J, Cao G, Hua J, Shan G, & Lin W. (2022). Emerging roles of circular RNAs in gastric cancer metastasis and drug resistance. J Exp Clin Cancer Res, 41, 218. https://doi.org/10.1186/s13046-022-02432-z
[10] Suski JM, Braun M, Strmiska V, & Sicinski P. (2021). Targeting Cell-cycle Machinery in Cancer. Cancer Cell, 39(6), 759–778. https://doi.org/10.1016/j.ccell.2021.03.010
[11] Liu J, Peng Y, & Wei W. (2022). Cell cycle on the crossroad of tumorigenesis and cancer therapy. Trends Cell Biol, 32(1), 30–44. https://doi.org/10.1016/j.tcb.2021.07.001
[12] Evan GI, & Vousden KH. (2001). Proliferation, cell cycle and apoptosis in cancer. Nature, 411(6835), 342–348. https://doi.org/10.1038/35077213
[13] Engeland K. (2022). Cell cycle regulation: p53-p21-RB signaling. Cell Death Differ, 29(5), 946–960. https://doi.org/10.1038/s41418-022-00988-z
[14] Wang H, Guo M, Wei H, & Chen Y. (2023). Targeting p53 pathways: mechanisms, structures and advances in therapy. Signal Transduct Target Ther, 8, 92. https://doi.org/10.1038/s41392-023-01347-1
[15] Engeland K. (2018). Cell cycle arrest through indirect transcriptional repression by p53: I have a DREAM. Cell Death Differ, 25(1), 114–132. https://doi.org/10.1038/cdd.2017.172
[16] Bertoli C, Skotheim JM, & de Bruin RAM. (2013). Control of cell cycle transcription during G1 and S phases. Nat Rev Mol Cell Biol, 14(8), 518–528. https://doi.org/10.1038/nrm3629
[17] Icard P, Fournel L, Wu Z, Alifano M, & Lincet H. (2019). Interconnection between Metabolism and Cell Cycle in Cancer. Trends Biochem Sci, 44(6), 490–501. https://doi.org/10.1016/j.tibs.2018.12.007
[18] Targeting Cell-cycle Machinery in Cancer - PMC. https://pmc.ncbi.nlm.nih.gov/articles/PMC8206013/. Accessed 19 Jan 2026
[19] Zhou Y-X, Zhang H, & Peng C. (2013). Puerarin: A Review of Pharmacological Effects. Phytotherapy Research. https://doi.org/10.1002/ptr.5083
[20] Liu X, Huang R, & Wan J. (2023). Puerarin: a potential natural neuroprotective agent for neurological disorders. Biomedicine & Pharmacotherapy, 162, 114581. https://doi.org/10.1016/j.biopha.2023.114581
[21] Meng F, Guo B, Ma Y, Li K, & Niu F. (2022). Puerarin: A review of its mechanisms of action and clinical studies in ophthalmology. Phytomedicine, 107, 154465. https://doi.org/10.1016/j.phymed.2022.154465
[22] Lv J, Shi S, Zhang B, Xu X, Zheng H, Li Y, et al. (2022). Role of puerarin in pathological cardiac remodeling: A review. Pharmacological Research, 178, 106152. https://doi.org/10.1016/j.phrs.2022.106152
[23] Ye Y, Gao Y, Fang Y, Xu L, & He F. (2022). Anticancer Effect of Puerarin on Ovarian Cancer Progression Contributes to the Tumor Suppressor Gene Expression and Gut Microbiota Modulation. J Immunol Res, 2022, 4472509. https://doi.org/10.1155/2022/4472509
[24] ZENG Y-P, YANG Z-R, GUO X-F, JUN W, & DONG W-G. (2014). Synergistic effect of puerarin and 5-fluorouracil on hepatocellular carcinoma. Oncol Lett, 8(6), 2436–2442. https://doi.org/10.3892/ol.2014.2534
[25] Lang J, Guo Z, Xing S, Sun J, Qiu B, Shu Y, et al. (2022). Inhibitory role of puerarin on the A549 lung cancer cell line. Transl Cancer Res, 11(11), 4117–4125. https://doi.org/10.21037/tcr-22-2246
[26] Wang H, Wang Z, Zhang Z, Liu J, & Hong L. (2023). β-Sitosterol as a Promising Anticancer Agent for Chemoprevention and Chemotherapy: Mechanisms of Action and Future Prospects. Adv Nutr, 14(5), 1085–1110. https://doi.org/10.1016/j.advnut.2023.05.013

Risk Factors of Reactive Cutaneous Capillary Endothelial Proliferation in Advanced Non-small Cell Lung Cancer Treated with Camrelizumab

Authors

Liuning Wang, Shuxing Chen, Siyu Sun,Wenyi Li, Congjun Zhang

Correspondence

yfy137907@fy.ahmu.edu.cn (C. Zhang)

Graphical Abstract

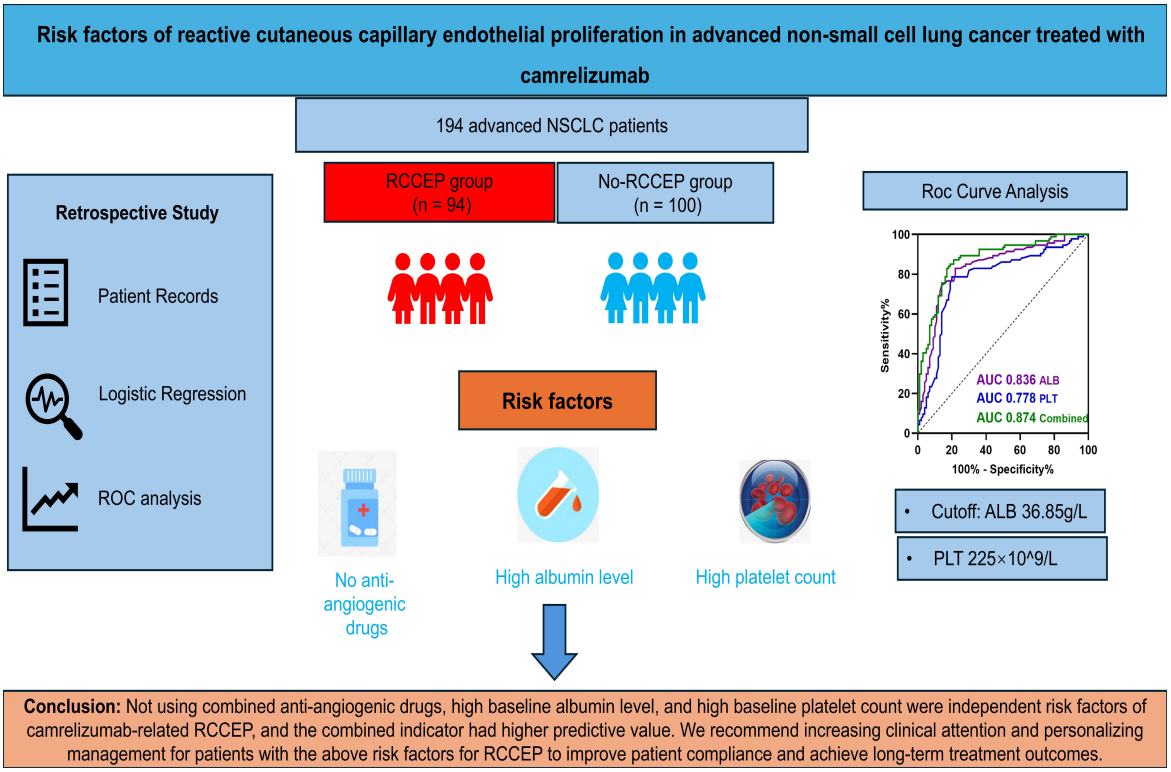

https://doi.org/10.71321/ncbcdv45

Research Article

Life Conflux

Risk Factors of Reactive Cutaneous Capillary Endothelial Proliferation in Advanced Non-small Cell Lung Cancer Treated with Camrelizumab

Liuning Wang [1†], Shuxing Chen [1†], Siyu Sun [2†], Wenyi Li [1], Congjun Zhang [1*]

Received: 2026-01-08 | Accepted: 2026-02-24 | Published online: 2026-03-06

Abstract

Background: Reactive cutaneous capillary endothelial proliferation (RCCEP) is the most common cutaneous immune-related adverse event (irAE) of camrelizumab. The purpose of our research was to explore the risk factors associated with RCCEP and their predictive values.

Methods: We conducted a retrospective investigation examining clinical records of advanced non-small cell lung cancer (NSCLC) patients treated with camrelizumab at our hospital between June 2022 and December 2024. Study participants were grouped based on whether they developed RCCEP. To pinpoint potential risk factors associated with RCCEP, we employed logistic regression analysis, while receiver operating characteristic (ROC) curve analysis helped determine the predictive values of our identified variables.

Results: Among 194 patients, 94 (48.5%) developed RCCEP, of whom 92 cases developed grade 1-2 RCCEP, only 2 cases developed grade 3 RCCEP, with no grade 4-5 cases. Multivariate logistic regression analysis suggested that not using combined anti-angiogenic drugs (OR: 2.962, 95% CI 1.042-8.422, P = 0.042), high baseline albumin level (OR: 1.422, 95% CI 1.264-1.599, P < 0.001), and high baseline platelet count (OR: 1.018, 95% CI 1.010-1.026, P < 0.001) were significantly associated with RCCEP. ROC curve analysis showed that baseline albumin level, baseline platelet count, and their combination predicted RCCEP occurrence in advanced NSCLC patients receiving camrelizumab, with areas under the curve (AUCs) of 0.836 (95% CI 0.777-0.895), 0.778 (95% CI 0.709-0.847), and 0.874 (95% CI 0.823-0.924), respectively. The cutoff values for albumin and platelet were calculated using the maximum Youden index from the ROC curve, which were 36.85 g/L and 225×10^9/L, respectively.

Conclusion: Not using combined anti-angiogenic drugs, high baseline albumin level, and high baseline platelet count were independent risk factors of camrelizumab-related RCCEP, and the combined indicator had higher predictive value. We recommend increasing clinical attention and personalizing management for patients with the above risk factors for RCCEP to improve patient compliance and achieve long-term treatment outcomes.

Keywords: Camrelizumab; advanced non-small cell lung cancer (NSCLC); reactive cutaneous capillary endothelial proliferation (RCCEP); albumin; platelet; anti-angiogenic drugs

Introduction

Lung cancer stands as one of the most prevalent malignant tumors globally, and is a leading cause of cancer-related death. Non-small cell lung cancer (NSCLC) is the main type of lung cancer, and by the time most patients are diagnosed, the disease is already at an advanced stage. As a result, the overall prognosis is not ideal, with a 5-year survival rate of only 10% to 20% [1]. In recent years, immunotherapy, as an emerging treatment strategy, has significantly improved the prognosis of patients with advanced NSCLC, opening a new chapter in lung cancer immunotherapy. The immune checkpoint inhibitors (ICIs) used in tumor immunotherapy are mainly divided into two categories: one is monoclonal antibodies targeting cytotoxic T-lymphocyte antigen 4 (CTLA-4), and the other acts on the programmed cell death protein 1 (PD-1) and its ligand programmed cell death protein ligand 1 (PD-L1) signaling pathway. PD-1 and PD-L1 inhibitors, as new anti-tumor drugs, can block the inhibitory pathway between T lymphocytes and tumor cells or antigen-presenting cells [2], relieve immune suppression, stimulate T cells to attack tumor cells, and strengthen anti-tumor immunity. However, while ICIs activate the patient's immune system to fight cancer, they also enhance the body's immune response, leading to various immune-related adverse events (irAEs). Cancer immunotherapy has different toxic characteristics and management approaches compared to traditional chemotherapy [3-4]. IrAEs are essentially autoimmune in nature and can affect almost any organ system [4].

1 Department of Oncology, The First Affiliated Hospital of Anhui Medical University, Hefei, China

2 Department of Geriatric Pulmonology, The First Affiliated Hospital of Anhui Medical University, Hefei, China

† These authors contributed equally to this work.

* Corresponding Author.

Common irAEs involve the skin, gastrointestinal tract, endocrine organs, liver, and lungs [5]. Severe irAEs may force the discontinuation of ICI treatment, interfering with the patient's cancer treatment process. Therefore, early identification and timely intervention of irAEs are necessary.

Camrelizumab is a high-affinity, humanized monoclonal antibody of the IgG4 kappa subclass that targets PD-1, which is now applied in the treatment of various malignant tumors, such as classical Hodgkin lymphoma, hepatocellular carcinoma, non-small cell lung cancer, small cell lung cancer, melanoma, and esophageal squamous cell carcinoma. It is currently the most widely approved ICI with the most indications in China. However, in a series of clinical studies and practices, it has been found that camrelizumab treatment can lead to a common skin irAE— reactive cutaneous capillary endothelial proliferation (RCCEP) [6-8]. RCCEP has unique clinical manifestations and pathological features. Its occurrence may be due to the disruption of the skin immune microenvironment, leading to an imbalance in the expression of angiogenesis-related factors. RCCEP exhibits five distinct morphological patterns that can be classified as follows: "red-nevus-like", "pearl-like", "mulberry-like", "patch-like" and "tumor-like". It most commonly occurs on the facial and trunk skin, and less frequently on the eyelids, oral mucosa, and nasal mucosa. Previous data from a multicenter phase II trial showed an RCCEP incidence rate of 66.8% [7], while another large-scale pooled analysis covering 10 clinical trials in China further suggested the rate could reach 77.0% [9]. Together, these results indicate that RCCEP has a relatively high incidence rate. However, RCCEP is not unique to camrelizumab. Studies have shown that other ICIs, such as nivolumab or pembrolizumab, can also cause RCCEP, with an incidence rate of about 2.4% [10]. This suggests that while RCCEP may not be specific to camrelizumab, it appears to occur more frequently and present differently with this particular medication [7]. Although RCCEP is usually self-limiting and can be relieved by laser therapy, surgical excision, hemostatic treatment, local steroid treatment, or cryotherapy, for some patients with multiple or widely distributed lesions, local treatments may be limited in effectiveness. This can affect the patient's appearance, impair their quality of life, and reduce patient compliance, leading to delays or interruptions in immunotherapy. Additionally, some tumor patients may have low coagulation function, which could lead to the lesions rupturing and bleeding, increasing the risk of infection, and in severe cases, even life-threatening complications [11]. Given the high incidence rate of RCCEP, identifying patients at high risk of RCCEP before starting treatment with camrelizumab in clinical practice has important clinical value for optimizing the management of camrelizumab therapy. In recent years, the field of international oncology has seen a continuously increasing focus on irAEs. Existing studies suggested that peripheral blood cells, such as eosinophil [12] and lymphocyte [13], and patient clinical characteristics, such as age [14] and sex [15], may have some reference value in predicting irAEs. However, research on predictive factors for specific skin irAEs like RCCEP was still relatively limited, with only a few retrospective studies exploring this to date. A retrospective study in patients with NSCLC, using multivariate logistic regression analysis, found that a baseline peripheral blood eosinophil percentage > 1.75% and not using anti-angiogenic drugs in combination were independent risk factors for developing RCCEP after treatment with camrelizumab [16]. This study was one of the few reports directly exploring predictive factors for the risk of RCCEP, suggesting the potential value of peripheral blood test results in predicting RCCEP. Our study aimed to analyze baseline clinical characteristics and laboratory indicators that may be linked to the occurrence of RCCEP. The findings will help clinicians to early identify populations at high risk for RCCEP, allowing for personalized management.

Subjects and Methods

Study Subjects

This study was a single-center retrospective cohort study. The subjects were patients with advanced NSCLC who received camrelizumab treatment at our hospital from June 2022 to December 2024, with follow-up ending on June 30, 2025. Inclusion criteria: (1) underwent a minimum of two cycles of treatment of camrelizumab; (2) Age ≥ 18 years; (3) Histologically confirmed advanced NSCLC; (4) Eastern Cooperative Oncology Group Performance Status (ECOG-PS) score of 0-3. Exclusion criteria: (1) Previous immunotherapy prior to using camrelizumab; (2) History of autoimmune diseases; (3) Coexisting with other malignant tumors; (4) Severe organ diseases such as heart, brain, and kidney disorders, intolerant to immunotherapy; (5) Death within 24 hours of admission; (6) Had medical records that were incomplete or missing. (7) Patients who could not be evaluated for adverse reactions due to loss to follow-up. This research was carried out in strict accordance with the Declaration of Helsinki and its later revisions.

Clinical Data Collection

We extracted baseline patient data from medical records, capturing information such as age, sex, smoking history, histological type, TNM stage, ECOG-PS score at admission, camrelizumab-containing treatment regimens, line of immunotherapy, along with the grading and initial identification date of RCCEP. Laboratory data obtained within one week before camrelizumab treatment were collected, including neutrophil count (Neu), lymphocyte count (L), eosinophil count (EOS), white blood cell count (WBC), platelet count (PLT), lymphocyte percentage (L%), neutrophil percentage (Neu%), eosinophil percentage (EOS%), lactate dehydrogenase (LDH), albumin level (ALB), C-reactive protein (CRP), and D-dimer (D-D).

Diagnosis and Assessment of RCCEP

The diagnostic and grading criteria for RCCEP were the following [7]:grade 1, nodule(s) with a maximum diameter of ≤ 10 mm, with or without rupture and bleeding; grade 2, nodule(s) with a maximum diameter of > 10 mm, with or without rupture and bleeding; grade 3, generalized nodules throughout the body, potentially complicated by skin infections; grade 4, multiple and generalized nodules accompanied by a life-threatening condition; and grade 5, death.

Statistical Methods

Data analysis was processed using SPSS 27.0 software (New York, USA) and GraphPad Prism (version 10.0, USA). Metric data following a normal distribution were presented as mean ± standard deviation, with independent samples t-tests employed for intergroup comparisons. Metric data not following

a normal distribution were presented as median (M) and interquartile range (Q1, Q3), with non-parametric tests used for intergroup comparisons. Count data were presented as frequency (n) and proportion (%), and compared using the chi-squared test. Univariate and multivariate logistic regression analyses were employed for factor analysis. Factors with P < 0.1 in univariate logistic regression were incorporated into multivariate logistic regression analysis. Receiver operating characteristic (ROC) curves and area under the curve (AUC) were used to evaluate the predictive ability of peripheral blood markers and their combinations for RCCEP. The cut-off values for peripheral blood markers at baseline were set based on the maximum Youden index on the ROC curve. P < 0.05 was considered statistically significant.

Results

Characteristics of the patients

This research enrolled 194 patients with advanced NSCLC who received camrelizumab therapy. Among them, 109 patients (56.2%) were aged ≥ 65 years, 166 patients (85.6%) were male, 122 patients (62.9%) had a smoking history, and 140 patients (72.2%) were in stage IV. There were 44 patients (22.7%) with squamous carcinoma and 150 patients (77.3%) with non-squamous carcinoma. The ECOG-PS score was 0-1 in 180 patients (92.8%). Camrelizumab was used as first-line treatment in 144 patients (74.2%). A total of 158 patients (81.4%) did not receive combined anti-angiogenic therapy, while 36 patients (18.6%) received combined anti-angiogenic therapy. (Table 1). Among 194 patients, 94 cases of RCCEP at different levels were reported, of which 92 cases developed grade 1-2 RCCEP, only 2 cases developed grade 3 RCCEP, with no grade 4-5 cases. No significant differences were found between the RCCEP group and non-RCCEP group regarding age, sex, histological type, smoking history, TNM stage, and ECOG PS score (P ≥ 0.05). However, baseline albumin level, baseline platelet count, and treatment regimen were associated with the development of RCCEP (P < 0.05), as indicated in Table 1. Among patients who received combined anti-angiogenic therapy, 1 received bevacizumab, 15 received anlotinib, 11 received Apatinib and 9 received recombinant human endostatin. (Table 2).

Risk factors for RCCEP

Table 3 presented the results of the univariate logistic regression analysis. Based on these results, we selected variables with P<0.10, including smoking history, treatment regimen, baseline albumin level and baseline platelet count, and incorporated them into the multivariate logistic regression model for further analysis. The findings indicated that not using combined anti-angiogenic drugs (OR: 2.962, 95% CI 1.042-8.422, P = 0.042), high baseline albumin level (OR: 1.422, 95% CI 1.264-1.599, P < 0.001), and high baseline platelet count (OR: 1.018, 95% CI 1.010-1.026, P < 0.001) were independent risk factors for the occurrence of RCCEP.

Predictive Value

(1) The AUC of ALB was 0.836, with an optimal cutoff value of 36.85, sensitivity of 0.830, and specificity of 0.780 (95% CI 0.777-0.895, P < 0.001); (2) The AUC of PLT was 0.778, with an optimal cutoff value of 225, sensitivity of 0.787, and specificity of 0.800 (95% CI 0.709-0.847, P < 0.001); (3) The AUC of the combination of both was 0.874, with sensitivity of 0.872 and specificity of 0.790 (95% CI 0.823-0.924, P < 0.001). Based on the maximum Youden index from the ROC curves, the cutoff values for ALB and PLT were 36.85 g/L and 225×10^9/L, respectively (Table 4). The ROC curves for ALB, PLT, and the combination of both were shown in Figure 1.

Figure 1. The ROC curves of risk factors for RCCEP in advanced NSCLC. Notes: ROC, receiver operating characteristics; RCCEP, reactive cutaneous capillary endothelial proliferation; ALB, albumin level; PLT, low density lipoprotein; NSCLC, non-small cell lung cancer.

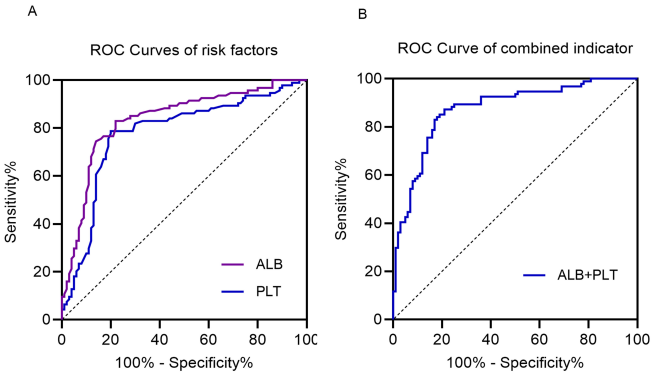

Discussion

Lung cancer ranks among the top malignant tumors worldwide in terms of incidence and mortality, seriously threatening public health. The emergence of ICIs has significantly improved the prognosis of patients with advanced NSCLC. Camrelizumab, as the first domestically approved PD-1 inhibitor, is widely used in the treatment of lung cancer and other solid tumors, marking a new chapter in domestic immunotherapy. In recent years, several clinical studies on camrelizumab have revealed that, in addition to the common irAEs associated with ICIs, there is a relatively special irAE known as RCCEP. RCCEP is an irAE that mainly occurs in the skin, characterized by increased capillaries in the dermis and endothelial cell proliferation in capillaries. The exact mechanism remains unclear. Furthermore, more and more studies suggest that RCCEP is associated with the efficacy of immunotherapy. Recently, Lou et al. conducted a pooled analysis of two phase III registration studies on carelizumab in treating advanced esophageal squamous cell carcinoma(ESCC). The results indicated that patients who experienced RCCEP during carelizumab treatment had better objective response rates (ORR), longer median progression-free survival (mPFS), and longer median overall survival (mOS) compared to those who did not experience RCCEP [17]. This result further supports the possibility that the development of RCCEP is linked to better treatment response and survival benefits, suggesting it could serve as a potential biomarker for anti-tumor immunotherapy. This study retrospectively enrolled patients with advanced NSCLC who received camrelizumab treatment at our center from June 2022 to December 2024. It investigated the real-world incidence rate of RCCEP, studied its clinical characteristics and potential predictive factors. The study results showed that 94 patients (48.5%) with advanced NSCLC treated with camrelizumab developed RCCEP. Most cases were grade 1-2. The RCCEP

lesions were mainly distributed on the skin of the head, face, and trunk, and were predominantly red nevus-like (47.9%) and pearl-like (38.3%). Most cases of RCCEP did not require special management. In a small number of patients, symptoms improved significantly after symptomatic treatment. Only 2 patients with grade 3 RCCEP (4.2%) temporarily discontinued camrelizumab treatment to avoid further functional impairment. No life-threatening serious adverse events occurred in any patient. Multivariate logistic regression analysis indicated that not using anti-angiogenic drugs in combination, high baseline albumin level, and high baseline platelet count were independent risk factors for RCCEP occurrence.

Camrelizumab may activate CD4+ T lymphocytes, increase the release of the inflammatory factor interleukin-4 (IL-4), and subsequently induce the differentiation of CD163+ M2 macrophages, which release vascular endothelial growth factor A (VEGF-A) to promote angiogenesis [7]. Additionally, camrelizumab acts on PD-1-expressing cells in the skin and may trigger the release of chemokines, leading to VEGF synthesis [18]. The enhanced immune response induced by camrelizumab may lead to an imbalance in the expression of angiogenesis-related factors, thereby causing RCCEP. Therefore, the activation of the VEGF-A/VEGF receptor-2(VEGFR-2) signaling pathway and increased VEGF-A expression can partially explain the pathogenesis of RCCEP. Anti-angiogenic drugs may block the VEGF/VEGFR signaling pathway, inhibiting the occurrence of RCCEP. Several previous research have consistently demonstrated that combining camrelizumab with anti-angio-

Table 1. Baseline characteristics of patients.

Characteristics	Total (n=194)	Non-RCCEP (n=100)	RCCEP (n=94)	Statistic	P value
Age (years), n (%)					
≥65	109(56.2%)	57(57.0%)	52(55.3%)	0.056	0.814
<65	85(43.8%)	43(43.0%)	42(44.7%)		
Sex, n (%)					
Female	28(14.4%)	16(16.0%)	12(12.8%)	0.410	0.522
Male	166(85.6%)	84(84.0%)	82(87.2%)		
Smoking history, n (%)					
Current or former	122(62.9%)	57(57.0%)	65(69.1%)	3.064	0.080
None	72(37.1%)	43(43.0%)	29(30.9%)		
Histology, n (%)					
Squamous	44(22.7%)	22(22.0%)	22(23.4%)	0.054	0.815
Non-squamous	150(77.3%)	78(78.0%)	72(76.6%)		
Tumor staging, n (%)					
IIIB/IIIC	54(27.8%)	24(24.0%)	30(31.9%)	1.511	0.219
IV	140(72.2%)	76(76.0%)	64(68.1%)		
ECOG PS, n (%)					
<2	180(92.8%)	92(92.0%)	88(93.6%)	0.189	0.664
≥2	14(7.2%)	8(8.0%)	6(6.4%)		
Treatment regimen (Whether to combine with anti-angiogenic drugs), n (%)					
No	158(81.4%)	73(73.0%)	85(90.4%)	9.735	0.002*
Yes	36(18.6%)	27(27.0%)	9(9.6%)		
Treatment line, n (%)					
First-line	144(74.2%)	73(73.0%)	71(75.5%)	0.162	0.687
Second-line and above	50(25. 8%)	27(27.0%)	23(24.5%)		
Peripheral blood biomarkers					
WBC (×10 ^{9} /L)	—	6.71(5.29,8.06)	6.37(5.04,7.71)	1.030	0.303
Neu (×10 ^{9} /L)	—	4.39(3.23,5.86)	4.34(3.19,5.37)	0.578	0.563
L (×10 ^{9} /L)	—	1.44(1.10,1.88)	1.26(1.00,1.62)	1.888	0.059
EOS (×10 ^{9} /L)	—	0.13(0.04,0.26)	0.14(0.07,0.29)	1.133	0.257
PLT (×10 ^{9} /L)	—	197.00(160.75,216.25)	243.50(227.75,267.00)	6.677	<0.001*
L%	—	21.95(16.78,26.90)	20.95(14.85,26.93)	0.604	0.546
Neu% (mean ± SD)	—	66.66±9.92	66.73±9.59	0.051	0.959
EOS%	—	1.80(0.73,3.98)	2.15(1.10,3.73)	0.915	0.360
ALB (mean ± SD, g/L)	—	34.46±3.85	39.32±3.70	8.964	<0.001*
LDH(U/L)	—	205.00(169.25,240.65)	190.40(166.53,235.85)	1.189	0.235
CRP (mg/L)	—	3.55(1.29,11.57)	5.15(1.39,21.79)	0.873	0.383
D-D(μg/mL)	—	0.70(0.53,1.15)	0.62(0.40,1.27)	1.231	0.218

Notes: Student's t-test or Mann-Whitney U test was used for continuous variables; Chi-square test was used for categorical variables. *: P-values < 0.05 represented statistical significant.

genic drugs significantly cuts down on RCCEP occurrences. In a Phase II clinical trial of camrelizumab monotherapy for hepatocellular carcinoma, the incidence of RCCEP was 66.8% [7], while in another trial of camrelizumab combined with apatinib for hepatocellular carcinoma, the RCCEP incidence was only 29.5% [19]. Furthermore, a large-scale pooled analyses encompassing ten clinical trials also indicated that RCCEP occurrence rates were substantially higher among patients receiving camrelizumab alone (77%) or camrelizumab alongside chemotherapy (67.8%) compared to those treated with the combination of camrelizumab and anti-angiogenic drugs (23.6%) [20]. Based on these results, it seems that combining anti-angiogenic drugs may help mitigate the incidence of RCCEP.

Earlier research indicated that elevated serum albumin may increase the risk of immune-related disorders [21-23]. Patients with high serum albumin level and good ECOG scores are more likely to experience irAEs due to better nutritional status and overall condition [24], and this may be associated with a better prognosis [21, 25-26]. It is speculated that good nutritional status may make the immune system more active, and compared to patients with poor nutritional status, these patients are more likely to develop irAEs. No study has yet analyzed the relationship between RCCEP, a specific adverse reaction, and serum albumin level. In this study, multivariate logistic regression analysis found that higher baseline albumin level is an independent risk factor for RCCEP. The level of serum albumin typically serves as an indicator of a patient's nutritional condition and overall immune activation potential, and elevated level may indicate that the immune system is relatively active, potentially leading to multi-organ irAEs, including RCCEP. In addition, serum albumin can also influence the activation of inflammatory cytokines. Studies have shown that when albumin levels increase, prostaglandin

Table 2. The treatment regimen containing camrelizumab.

Variables	Total	Non-RCCEP(n=100)	RCCEP(n=94)
Combination with anti-angiogenic drugs			
Bevacizumab	1	1(100%)	0
Anlotinib	15	13(86.7%)	2(13.3%)
Apatinib	11	8(72.7%)	3(27.3%)
Recombinant human endostatin	9	5(55.6%)	4(44.4%)
Monotherapy or combination with chemotherapy	158	73(46.2%)	85(53.8%)

Table 3. Logistic regression analysis for risk factors of RCCEP.

Variables	Univariate logistic		Multivariate logistic	
	OR(95%CI)	P value	OR(95%CI)	P value
Age	0.934(0.530-1.647)	0.814		
Sex	0.768(0.342-1.724)	0.523		
Smoking history	1.691(0.937-3.051)	0.081*	1.814(0.800-4.113)	0.154
Histology	0.923(0.471-1.808)	0.815		
Stage	0.674(0.358-1.267)	0.220		
ECOG PS	0.784(0.261-2.351)	0.664		
Treatment regimen	3.493(1.544-7.905)	0.003*	2.962(1.042-8.422)	0.042*
Treatment line	0.876(0.460-1.669)	0.687		
Peripheral blood biomarkers				
WBC (×10 ^{9} /L)	0.931(0.828-1.047)	0.232		
Neu (×10 ^{9} /L)	0.941(0.825-1.073)	0.364		
L (×10 ^{9} /L)	0.667(0.386-1.153)	0.147		
EOS (×10 ^{9} /L)	0.935(0.335-2.609)	0.898		
PLT (×10 ^{9} /L)	1.017(1.011-1.024)	<0.001*	1.018(1.010-1.026)	<0.001*
L%	0.986(0.954-1.019)	0.392		
Neu%	1.001(0.972-1.030)	0.959		
EOS%	1.002(0.917-1.096)	0.961		
ALB (g/L)	1.431(1.282-1.598)	<0.001*	1.422(1.264-1.599)	<0.001*
LDH(U/L)	0.997(0.993-1.001)	0.111		
CRP (mg/L)	1.002(0.993-1.011)	0.712		
D-D(μg/mL)	0.877(0.718-1.070)	0.195		

Notes: *: P-values < 0.05 represented statistical significant.

Table 4. The predictive value of ALB, PLT, and their combined indicator for RCCEP.

Factors	AUC	Cut-off value	95%CI	Sensitivity	Specificity	P value
ALB (g/L)	0.836	36.85	0.777-0.895	0.830	0.780	<0.001
PLT (×10 ^{9} /L)	0.778	225	0.709-0.847	0.787	0.800	<0.001
combined indicator	0.874	0.425	0.823-0.924	0.872	0.790	<0.001

E2 levels decrease, which may induce the release of inflammatory cytokines, including tumor necrosis factor-α (TNFα) [27]. TNFα is a major mediator of cancer-related inflammation and has been found to have an indirect pro-angiogenic effect in recent years [28-29]. This may explain the association between elevated baseline albumin level and an increased risk of developing RCCEP. Therefore, the relationship between baseline albumin and RCCEP is worth further investigation.

In addition, the results of the multivariate logistic regression analysis revealed that a high platelet count at baseline independently increased the risk of RCCEP occurrence. Studies conducted in recent years suggest that platelets are key players in thrombosis and hemostasis, and they also contribute to a wide range of other physiological and pathological events, such as immunity, inflammation, tissue remodeling, and angiogenesis [30]. Abnormal activation of these processes may be an important basis for promoting RCCEP. Platelets serve as the main reservoir of VEGF and have been confirmed to have a direct pro-angiogenic effect. VEGF binds specifically to VEGFR2 on the surface of endothelial cells and activates intracellular signaling pathways, which is the key signal driving endothelial cell proliferation, migration, and new vessel formation. At the same time, after VEGF is released, it can also bind to various growth factor receptors, further strengthening the pro-angiogenic effect [30]. In addition to VEGF, platelets can release other types of pro-angiogenic factors, such as epidermal growth factor (EGF), transforming growth factor-β (TGF-β), platelet-derived growth factor (PDGF), and basic fibroblast growth factor (bFGF) [31]. These factors work together and may provide the conditions for the abnormal blood vessel environment needed for RCCEP to occur. Importantly, there is a complex interaction between platelets and cancer cells. On one hand, cancer cells can activate platelets by releasing platelet-activating mediators such as adenosine diphosphate(ADP) and thromboxane A2(TXA2) or through direct cell contact [32]. On the other hand, activated platelets can further promote tumor cells to express pro-angiogenic factors [33], further driving abnormal angiogenesis. In addition, the role of platelets in immune regulation and inflammation may also promote the occurrence of RCCEP. In the bloodstream, platelets can directly interact with immune cells or activate immune cells by releasing mediators, and they can also affect endothelial cells, amplifying local inflammatory responses [34], which may further induce the occurrence of RCCEP. Further ROC curve analysis suggested that baseline albumin and platelet count at admission had some predictive values for the occurrence of RCCEP in immunotherapy, and their combined predictive value was higher. We also calculated the optimal cutoff values for albumin and platelet using the maximum Youden index from the ROC curve, which were 36.85 g/L and 225 × 10^9 / L, respectively. When the values exceeded these cutoff points, the risk of RCCEP increased. When using camrelizumab treatment, close attention should be paid to blood test indicators such as albumin level and platelet count.

The above study suggested that the choice of treatment regimen, as well as albumin level and platelet count at admission, could serve as important reference indicators for clinicians to predict RCCEP risk. For high-risk patients, health education should be strengthened before medication, focusing on the clinical characteristics and potential clinical significance of RCCEP. This can help patients set reasonable expectations, enhance treatment confidence, and prevent reduced medication adherence due to changes in appearance. During medication treatment, the frequency of skin monitoring should be increased, and relevant adverse reactions should be closely observed, with timely interventions taken. This study, based on baseline peripheral blood biomarkers and treatment regimens, predicted the occurrence of RCCEP, helping provide scientific medication guidance for advanced NSCLC patients receiving camrelizumab and enhancing patient confidence in treatment, ultimately achieving long-term treatment outcomes. At the same time, the results of this study also provided important clues for further exploration of the pathogenesis of RCCEP in the future.

Conclusion

In conclusion, not using combined anti-angiogenic drugs, high baseline albumin level and high baseline platelet count were independent risk factors for the occurrence of RCCEP in advanced NSCLC patients treated with camrelizumab. These factors had certain predictive values for RCCEP, with higher predictive value when combined. However, some limitations existed in this study, including its retrospective design and single-center nature, as well as the relatively small sample size. Future studies could address these issues by using a larger sample, conducting multi-center studies, and considering more potential factors to further validate the conclusions of this study.

Abbreviations

Adenosine diphosphate: ADP; Albumin level: ALB; Area under the curve: AUC; Basic fibroblast growth factor: bFGF; Confidence interval: CI; C-reactive protein: CRP; Cytotoxic T-lymphocyte antigen 4: CTLA-4; D-dimer: D-D; Eastern Cooperative Oncology Group performance status: ECOG PS; Epidermal growth factor: EGF; Eosinophil count: EOS; Eosinophil percentage: EOS%; Esophageal squamous cell carcinoma: ESCC; Immune checkpoint inhibitors: ICIs; Interleukin-4: IL-4; Immune-related adverse events: irAEs; Lymphocyte: L; Lymphocyte percentage: L%; Lactate dehydrogenase: LDH; Median overall survival: mOS; Median progression-free survival: mPFS; Neutrophil: Neu; Neutrophil percentage: Neu%; Non-small cell lung cancer: NSCLC; Objective response rates: ORR; Programmed cell death protein 1: PD-1; Programmed cell death protein ligand 1: PD-L1; Platelet-derived growth factor: PDGF; Platelet count: PLT; Reactive cutaneous capillary endothelial proliferation: RCCEP; Transforming growth factor-β: TGF-β; Tumor necrosis factor-α: TNFα; Thromboxane A2: TXA2; Vascular endothelial growth factor A: VEGF-A; White blood cell: WBC.

Author Contributions

Liuning Wang, Shuxing Chen and Siyu Sun contributed equally to this work. All authors contributed to the research design and conceptualization. Siyu Sun and Wenyi Li were responsible for data collection and analysis, while Liuning Wang, Shuxing Chen, and Congjun Zhang, were involved in writing the article.

All authors reviewed theearlier versions of the manuscript and approved the final manuscript.

Acknowledgements

Not Applicable.

Funding Information

This study was supported by the Heng Rui Special - General Project Medical Research Fund for the prospective phase II clinical study of Adebepilumab combined with chemotherapy as second-line treatment for advanced gastric or gastroesophageal junction adenocarcinoma (2024Bac20029).

Ethics Approval and Consent to Participate

The study was reviewed and approved by the Medical Ethics Committee of the First Clinical Medical College (First Affiliated Hospital) (PJ2023-08–35). The written informed consent was obtained from patients in accordance with the Declaration of Helsinki.

Competing Interests

The authors declare that they have no existing or potential commercial or financial relationships that could create a conflict of interest at the time of conducting this study.

Data Availability

All data needed to evaluate the conclusions in the paper are present in the paper or the Supplementary Materials. Additional data related to this paper may be requested from the authors.

References

[1] Bray F, Laversanne M, Sung H, Ferlay J, Siegel RL, Soerjomataram I, et al. Global cancer statistics 2022: GLOBOCAN estimates of incidence and mortality worldwide for 36 cancers in 185 countries. CA A Cancer J Clinicians. 2024 May;74(3):229–63. https://doi.org/10.3322/caac.21834

[2] Zhou X, Yao Z, Yang H, Liang N, Zhang X, Zhang F. Are immune-related adverse events associated with the efficacy of immune checkpoint inhibitors in patients with cancer? A systematic review and meta-analysis. BMC Med. 2020 Dec;18(1):87. https://doi.org/10.1186/s12916-020-01549-2

[3] Johnson DB, Nebhan CA, Moslehi JJ, Balko JM. Immune-checkpoint inhibitors: long-term implications of toxicity. Nat Rev Clin Oncol. 2022 Apr;19(4):254–67. https://doi.org/10.1038/s41571-022-00600-w

[4] Ramos-Casals M, Brahmer JR, Callahan MK, Flores-Chávez A, Keegan N, Khamashta MA, et al. Immune-related adverse events of checkpoint inhibitors. Nat Rev Dis Primers. 2020 May 7;6(1):38. https://doi.org/10.1038/s41572-020-0160-6

[5] Naidoo J, Page DB, Li BT, Connell LC, Schindler K, Lacouture ME, et al. Toxicities of the anti-PD-1 and anti-PD-L1 immune checkpoint antibodies. Annals of Oncology. 2015 Dec;26(12):2375–91. https://doi.org/10.1093/annonc/mdv383

[6] Chen X, Ma L, Wang X, Mo H, Wu D, Lan B, et al. Reactive capillary hemangiomas: a novel dermatologic toxicity following anti-PD-1 treatment with SHR-1210. Cancer Biol Med. 2019;16(1):173–81. https://doi.org/10.20892/j.issn.2095-3941.2018.0172

[7] Wang F, Qin S, Sun X, Ren Z, Meng Z, Chen Z, et al. Reactive cutaneous capillary endothelial proliferation in advanced hepatocellular carcinoma patients treated with camrelizumab: data derived from a multicenter phase 2 trial. J Hematol Oncol. 2020;13(1). https://doi.org/10.1186/s13045-020-00886-2

[8] Wang H, Xia J, Cao M, Zhao Y, Yu A, Qin X, et al. Observation on the Therapeutic Efficacy of Camrelizumab Combined with Chemotherapy in Non-small Cell Lung Cancer and the Cutaneous Immune-related Adverse Events: A Retrospective Study. ACAMC. 2025 May;25(8):574–87. https://doi.org/10.2174/0118715206350978241105080452

[9] Qu W, Wang F, Qin S, Sun Y, Huang C. Reactive cutaneous capillary endothelial proliferation following camrelizumab monotherapy or combination therapy for multi-cancers: a large-scale pooled analysis of 10 studies in China. Ther Adv Med Oncol. 2024 Jan;16:17588359241242607. https://doi.org/10.1177/17588359241242607

[10] Hwang SJE, Carlos G, Wakade D, Byth K, Kong BY, Chou S, et al. Cutaneous adverse events (AEs) of anti-programmed cell death (PD)-1 therapy in patients with metastatic melanoma: A single-institution cohort. Journal of the American Academy of Dermatology. 2016 Mar;74(3):455-461.e1. https://doi.org/10.1016/j.jaad.2015.10.029

[11] Song G, Zhang F, Cheng H. Thalidomide for prevention of camrelizumab-induced reactive cutaneous capillary endothelial proliferation. Aust J Dermatology. 2022 May;63(2):217–21. https://doi.org/10.1111/ajd.13812

[12] Hu WT, Zhang Q, Zhang Z, He X, Zhou M, Guo Y, et al. Eosinophil and IFN-γ associated with immune-related adverse events as prognostic markers in patients with non-small cell lung cancer treated with immunotherapy. Front Immunol. 2023 Mar 6;14:1112409. https://doi.org/10.3389/fimmu.2023.1112409

[13] Zhang X, Zhang B, Li D, Yang Y, Lin S, Zhao R, et al. Peripheral blood cell counts as predictors of immune-related adverse events in cancer patients receiving immune checkpoint inhibitors: a systematic review and meta-analysis. Front Immunol. 2025 Jan 30;16:1528084. https://doi.org/10.3389/fimmu.2025.1528084

[14] Kondo T, Okamoto I, Sato H, Koyama N, Fushimi C, Okada T, et al. Age-based efficacy and safety of nivolumab for recurrent or metastatic head and neck squamous cell carcinoma: A multicenter retrospective study. Asia-Pac J Clncl Oncology. 2020 Dec;16(6):340–7. https://doi.org/10.1111/ajco.13374

[15] Duma N, Abdel-Ghani A, Yadav S, Hoversten KP, Reed CT, Sitek AN, et al. Sex Differences in Tolerability to Anti-Programmed Cell Death Protein 1 Therapy in Patients with Metastatic Melanoma and Non-Small Cell Lung Cancer: Are We All Equal? The Oncologist. 2019 Nov 1;24(11):e1148–55. https://doi.org/10.1634/theoncologist.2019-0094
[16] He X, Fang J, Yu P, Hu W, Zhang Q, Zhang Z, et al. Risk of reactive cutaneous capillary endothelial proliferation induced by camrelizumab in patients with non-small cell lung cancer: a retrospective study. J Thorac Dis. 2023 Dec;15(12):6687–96. https://doi.org/10.21037/jtd-23-1144
[17] Luo HY, Hou ZG, Ma C, Chen Y, Zheng Z, Xu RH. 394P Reactive cutaneous capillary endothelial proliferation in esophageal squamous cell carcinoma patients treated with camrelizumab-based therapy: A pooled analysis of two phase III trials. Annals of Oncology. 2025 Jul;36:S154. https://doi.org/10.1016/j.annonc.2025.05.410
[18] Lickliter JD, Gan HK, Voskoboynik M, Arulananda S, Gao B, Nagrial A, et al. A First-in-Human Dose Finding Study of Camrelizumab in Patients with Advanced or Metastatic Cancer in Australia. DDDT. 2020 Mar;Volume 14:1177–89. https://doi.org/10.2147/DDDT.S243787
[19] Xu J, Shen J, Gu S, Zhang Y, Wu L, Wu J, et al. Camrelizumab in Combination with Apatinib in Patients with Advanced Hepatocellular Carcinoma (RESCUE): A Nonrandomized, Open-label, Phase II Trial. Clinical Cancer Research. 2021 Feb 15;27(4):1003–11. https://doi.org/10.1158/1078-0432.CCR-20-2571
[20] Qu W, Wang F, Qin S, Sun Y, Huang C. Reactive cutaneous capillary endothelial proliferation following camrelizumab monotherapy or combination therapy for multi-cancers: a large-scale pooled analysis of 10 studies in China. Ther Adv Med Oncol. 2024 Jan;16:17588359241242607. https://doi.org/10.1177/17588359241242607
[21] Hata H, Matsumura C, Chisaki Y, Nishioka K, Tokuda M, Miyagi K, et al. A Retrospective Cohort Study of Multiple Immune-Related Adverse Events and Clinical Outcomes Among Patients With Cancer Receiving Immune Checkpoint Inhibitors. Cancer Control. 2022 Nov;29:10732748221130576. https://doi.org/10.1177/10732748221130576
[22] Shimozaki K, Sukawa Y, Sato Y, Horie S, Chida A, Tsugaru K, et al. Analysis of Risk Factors for Immune-Related Adverse Events in Various Solid Tumors Using Real-World Data. Future Oncol. 2021 Jul;17(20):2593–603. https://doi.org/10.2217/fon-2020-0861
[23] Ozawa R, Sonehara K, Hachiya T, Nozawa S, Agatsuma T, Yamamoto H, et al. Evaluation of the association between predictive factors and the development of immune-related adverse events and prognostic factors for chemoimmunotherapy in patients with non-small cell lung cancer: A multicenter retrospective study. Cancer Medicine. 2024 Aug;13(15):e70080. https://doi.org/10.1002/cam4.70080
[24] Hara Y, Baba Y, Toihata T, Harada K, Ogawa K, Iwatsuki M, et al. Immune-related adverse events and prognosis in patients with upper gastrointestinal cancer treated with nivolumab. J Gastrointest Oncol. 2022 Dec;13(6):2779–88. https://doi.org/10.21037/jgo-22-281
[25] Greally M, Chou JF, Chatila WK, Margolis M, Capanu M, Hechtman JF, et al. Clinical and Molecular Predictors of Response to Immune Checkpoint Inhibitors in Patients with Advanced Esophagogastric Cancer. Clinical Cancer Research. 2019 Oct 15;25(20):6160–9. https://doi.org/10.1158/1078-0432.CCR-18-3603
[26] Sato S, Oshima Y, Matsumoto Y, Seto Y, Yamashita H, Hayano K, et al. The new prognostic score for unresectable or recurrent gastric cancer treated with nivolumab: A multi-institutional cohort study. Annals of Gastroent Surgery. 2021 Nov;5(6):794–803. https://doi.org/10.1002/ags3.12489
[27] Choe WH, Baik SK. Prostaglandin E2-mediated immunosuppression and the role of albumin as its modulator. Hepatology. 2015 Mar;61(3):1080–2. https://doi.org/10.1002/hep.27644
[28] Ren W, Liang H, Sun J, Cheng Z, Liu W, Wu Y, et al. TNFAIP2 promotes HIF1α transcription and breast cancer angiogenesis by activating the Rac1-ERK-AP1 signaling axis. Cell Death Dis. 2024 Nov 13;15(11):821. https://doi.org/10.1038/s41419-024-07223-2
[29] Wang J, Al-Lamki RS. Tumor Necrosis Factor Receptor 2: Its Contribution to Acute Cellular Rejection and Clear Cell Renal Carcinoma. BioMed Research International. 2013;2013:1–11. https://doi.org/10.1155/2013/821310
[30] Langer HF. Platelets and Immune Responses During Thromboinflammation. Frontiers in Immunology 2019;10. https://doi.org/10.3389/fimmu.2019.0173
[31] Wojtukiewicz MZ, Sierko E, Hempel D, Tucker SC, Honn KV. Platelets and cancer angiogenesis nexus. Cancer Metastasis Rev. 2017 Jun;36(2):249–62. https://doi.org/10.1007/s10555-017-9673-1
[32] Jiang L, Luan Y, Miao X, Sun C, Li K, Huang Z, et al. Platelet releasate promotes breast cancer growth and angiogenesis via VEGF–integrin cooperative signalling. Br J Cancer. 2017 Aug;117(5):695–703. https://doi.org/10.1038/bjc.2017.214
[33] Haemmerle M, Stone RL, Menter DG, Afshar-Kharghan V, Sood AK. The Platelet Lifeline to Cancer: Challenges and Opportunities. Cancer Cell. 2018 Jun;33(6):965–83. https://doi.org/10.1016/j.ccell.2018.03.002
[34] Koupenova M, Clancy L, Corkrey HA, Freedman JE. Circulating Platelets as Mediators of Immunity, Inflammation, and Thrombosis. Circulation Research. 2018 Jan 19;122(2):337–51. https://doi.org/10.1161/CIRCRESAHA.117.310795

Review Article

Life Conflux

Gut Microbiota and Hypertension: From Pathogenesis to Therapeutic Potential

Authors

Haitao Yang, Jingkun Liu

Correspondence

10787149@qq.com (J. Liu)

Graphical Abstract

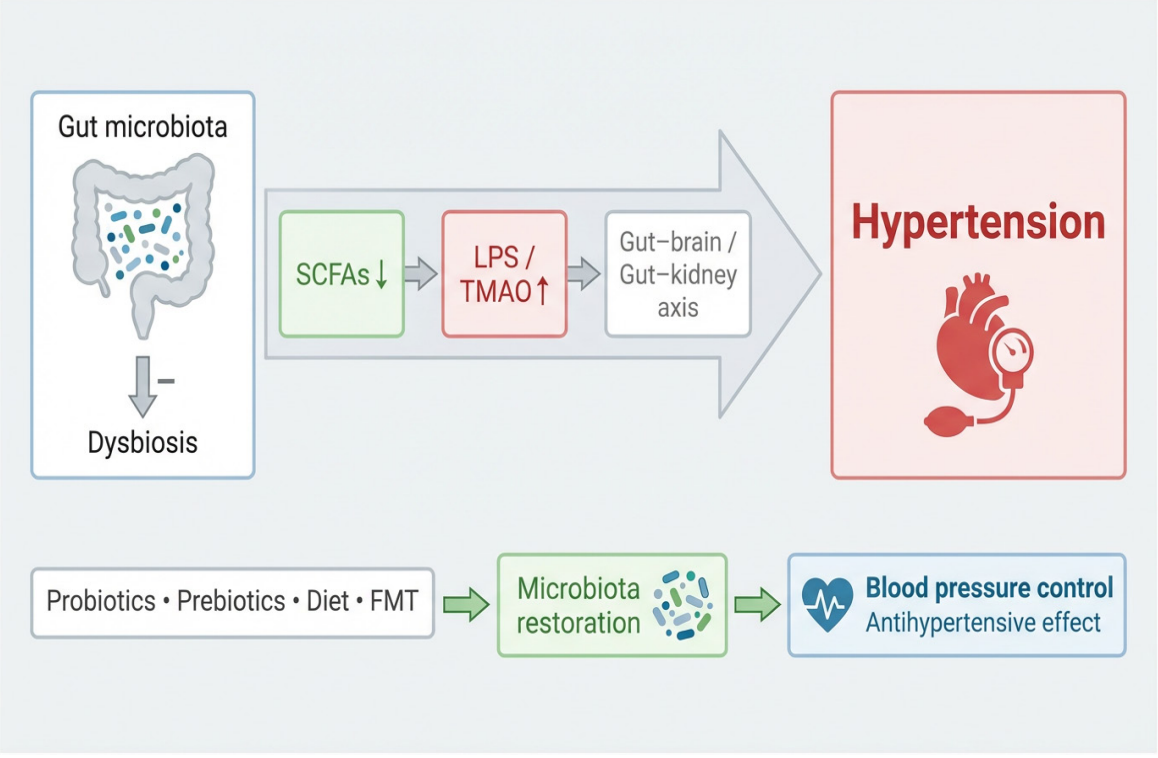

https://doi.org/10.71321/w9jjqk66

 L. Conflux. Vol. 2, No. 2 (2026)

Review Article Life Conflux

Gut Microbiota and Hypertension: From Pathogenesis to Therapeutic Potential

Haitao Yang[1,2], Jingkun Liu[3*]

Received: 2025-10-13 | Accepted: 2026-01-22 | Published online: 2026-03-07

Abstract

Hypertension is a major global health burden with high morbidity. Beyond traditional genetic and metabolic factors, increasing evidence shows that gut microbiota dysbiosis plays an important role in the development and progression of hypertension. Clinical studies have revealed that hypertensive patients display reduced microbial diversity, decreased abundance of short-chain fatty acid (SCFA)–producing bacteria, and enrichment of pro-inflammatory taxa such as Prevotella and Klebsiella. These microbial alterations are associated with endothelial dysfunction, chronic inflammation, and activation of the sympathetic nervous system through the gut–brain and gut–kidney axis. Mechanistically, microbial metabolites such as SCFAs, lipopolysaccharide (LPS), and trimethylamine-N-oxide (TMAO) participate in blood pressure regulation by influencing vascular tone, immune responses, and renal sodium handling. Loss of SCFA-producing bacteria decreases nitric oxide bioavailability and impairs vasodilation, while accumulation of LPS and TMAO promotes vascular inflammation and oxidative stress. Disruption of intestinal barrier integrity further exacerbates systemic inflammation, creating a feedback loop that sustains elevated blood pressure. Therapeutically, modulation of gut microbiota through probiotics, prebiotics, dietary interventions, and fecal microbiota transplantation (FMT) has shown promising antihypertensive effects in both animal and human studies. In addition, some antihypertensive drugs can remodel gut microbiota composition, suggesting potential synergistic benefits of combined treatment. In conclusion, the gut microbiota serves as a key and modifiable factor in hypertension pathogenesis. Understanding its mechanisms and therapeutic potential provides novel perspectives for developing microbiota-based and personalized strategies to improve blood pressure control and reduce cardiovascular risk.

Keywords: Gut microbiota; Hypertension; Microbiota-targeted therapy

Introduction

Hypertension is one of the most prevalent cardiovascular disorders worldwide, characterized by high morbidity. Hypertension is one of the most prevalent cardiovascular disorders worldwide, characterized by high morbidity, disability, and mortality. According to the World Health Organization (WHO), approximately one-third of adults globally suffer from hypertension, and this proportion continues to rise [1]. Hypertension is not only a major risk factor for myocardial infarction, stroke, and renal failure but also one of the leading causes of global disease burden. The pathogenesis of hypertension is complex and multifactorial, involving genetic predisposition, dietary habits, metabolic disturbances, and neurohumoral dysregulation. In recent years, accumulating evidence has revealed that the interaction between the host and the gut microbiota plays a crucial role in the development and progression of hypertension [2].

A growing body of basic and clinical studies demonstrate a close association between hypertension and gut microbiota dysbiosis. Alterations in gut microbial composition may serve as an important causative factor for hypertension, while the hypertensive state and its related metabolic disturbances can in turn further modify gut microbial communities, forming a bidirectional and self-perpetuating cycle. Mechanistically, gut microbiota participate in blood pressure regulation through multiple pathways, including the production of short-chain fatty acids (SCFAs), immune modulation, and the gut–brain and gut–kidney axis [3]. Conversely, hypertension-induced chronic inflammation, endothelial dysfunction, and disruption of the intestinal barrier exacerbate microbial imbalance, promoting the accumulation of pro-inflammatory metabolites such as

1 Department of Cardiology, The first Affiliated Hospital of Xinjiang Medical University, Urumqi 830011, China.

2 State Key Laboratory of Cardiovascular Disease, Fuwai Hospital, National Center for Cardiovascular Diseases, Chinese Academy of Medical Sciences and Peking Union Medical College, Beijing 100037, China

3 Department of Thoracic and Abdominal Radiotherapy, The Affiliated Tumor Hospital of Xinjiang Medical University, Urumqi 830011, China.

* Corresponding Author.

lipopolysaccharide (LPS) and trimethylamine-N-oxide (TMAO), which contribute to vascular injury and systemic inflammation [4-5].

Given the pivotal role of the gut microbiota in hypertension pathogenesis, targeting gut microbial homeostasis has emerged as a novel therapeutic strategy. In recent years, interventions such as probiotics, prebiotics, dietary modulation, and fecal microbiota transplantation (FMT) have shown promising antihypertensive effects and good safety profiles in both animal models and early clinical trials [6]. Compared with conventional pharmacological treatments, microbiota-targeted approaches offer multi-target regulation, metabolic and immune modulation, and the potential for long-term restoration of host homeostasis [7]. Therefore, this review systematically summarizes the relationship between gut microbiota and hypertension from three major perspectives—clinical evidence, pathogenic mechanisms, and therapeutic interventions—to provide new insights and theoretical support for future precision prevention and treatment strategies.

Clinical Studies on Gut Microbiota and Hypertension

Accumulating clinical evidence supports a strong association between gut microbiota composition and blood pressure regulation in human populations. Large-scale cohort studies and cross-sectional analyses have consistently demonstrated that patients with hypertension exhibit reduced gut microbial diversity, characterized by depletion of SCFAs–producing bacteria such as Faecalibacterium prausnitzii, Roseburia, and Akkermansia muciniphila, along with an enrichment of pro-inflammatory taxa including Prevotella, Klebsiella, and Enterobacter species [8]. These microbial alterations are associated with decreased circulating levels of SCFAs—key metabolites that exert vasodilatory, anti-inflammatory, and renoprotective effects—while pro-hypertensive metabolites such as TMAO and LPS are elevated, promoting endothelial dysfunction and systemic inflammation. However, it is important to note that while SCFAs are generally associated with blood pressure reduction, certain SCFAs, especially acetate, may increase blood pressure under specific conditions, such as through the activation of the renin-angiotensin system or sympathetic nervous system [9]. This complexity in SCFA actions reflects the nuanced role of microbial metabolites in regulating blood pressure.

Notably, emerging longitudinal evidence suggests that gut microbiota dysbiosis may precede the development of hypertension rather than merely result from it. For instance, a longitudinal study on hypertensive disorders in pregnancy conducted in a Chinese cohort analyzed gut microbiota at early, mid, and late gestational stages, revealing dynamic microbial shifts associated with blood pressure changes. The study found that alterations in specific genera, including Methanobrevibacter, correlated with the progression of gestational hypertension, suggesting a possible causal link between microbial imbalance and hypertension onset [10]. Although this investigation focused on pregnancy-related hypertension—a distinct subtype from essential hypertension—its longitudinal design provides valuable evidence that microbiota alterations may precede the clinical onset of elevated blood pressure. Moreover, functional analyses indicated that changes in microbial metabolic activity may appear earlier than compositional shifts, supporting the hypothesis that microbial metabolism may be a more sensitive indicator of early hypertensive changes. Furthermore, FMT from normotensive donors to hypertensive patients has provided direct clinical evidence for microbiota-mediated blood pressure regulation. In a recent multicenter, randomized controlled trial, oral capsule-based FMT led to a transient reduction of approximately 4 mmHg in systolic blood pressure after one week, accompanied by increased microbial richness and the restoration of beneficial taxa such as Akkermansia and Adlercreutzia [6]. While these results highlight the potential therapeutic benefits of microbiota-targeted interventions, the antihypertensive effect was not maintained over time, and the long-term sustainability and efficacy of such interventions remain uncertain. These findings underscore the safety, feasibility, and therapeutic potential of microbiota-targeted interventions, yet challenges remain regarding their consistency and long-term outcomes.

In addition to FMT, dietary and probiotic interventions targeting gut microbial composition have also demonstrated blood pressure–lowering potential. Controlled clinical trials using Lactobacillus plantarum, Bifidobacterium breve, and dietary fiber supplementation have reported modest but significant reductions in both systolic and diastolic blood pressure, particularly in patients with metabolic syndrome or mild hypertension [11-12]. However, the effects of probiotics are often strain-specific, and their colonization in the gut tends to be transient, which limits their long-term impact. Collectively, these findings underscore the clinical relevance of gut microbial dysbiosis in hypertension and highlight the potential of microbiota-targeted strategies as adjunctive or alternative therapeutic options. However, current microbiota interventions typically yield more modest blood pressure reductions compared to conventional medications, and their long-term safety, efficacy, and ethical considerations, especially in FMT, require further exploration. Future large-scale, longitudinal, and mechanistic studies are needed to establish causality, identify microbial biomarkers predictive of treatment response, and optimize personalized microbiota-based interventions for long-term blood pressure control.

Mechanistic Insights

The gut microbiota contributes to blood pressure regulation through multiple interconnected mechanisms that involve metabolic, immunological, and neurohumoral pathways. Among these, SCFAs metabolism, immune and inflammatory modulation, the gut–brain axis, and the gut–kidney axis represent the four major mechanistic routes linking intestinal microbes to hypertension pathogenesis (Figure 1).

SCFAs and Vascular Regulation

SCFAs—primarily acetate, propionate, and butyrate—are key metabolites produced by bacterial fermentation of dietary fibers. These molecules exert antihypertensive effects through several mechanisms, including activation of G-protein–coupled receptors (GPR41, GPR43, and Olfr78), enhancement of endothelial nitric oxide synthase (eNOS) activity, and suppression of systemic inflammation. SCFAs can induce vasodilation by stimulating endothelial nitric oxide (NO) production and reducing oxidative stress [13]. Clinical and experimental studies have shown that hypertensive individuals and animal models exhibit reduced fecal and plasma SCFAs levels, mainly due to decreased abundance of SCFAs-producing genera such as Roseburia, Coprococcus, and Faecalibacterium [14]. Resto-

Figure 1. Gut microbiota and hypertension. Hypertension is associated with gut microbiota dysbiosis, characterized by reduced microbial diversity, depletion of short-chain fatty acid (SCFA)–producing bacteria (e.g., Faecalibacterium prausnitzii, Roseburia, Akkermansia muciniphila), and enrichment of pro-inflammatory taxa (e.g., Prevotella, Klebsiella). These alterations promote elevated levels of lipopolysaccharide (LPS) and trimethylamine-N-oxide (TMAO) and decreased SCFAs, leading to endothelial dysfunction, chronic inflammation, and sympathetic activation via the gut–brain and gut–kidney axis, thereby sustaining elevated blood pressure. Restoring microbial homeostasis through probiotics, prebiotics, dietary interventions, and fecal microbiota transplantation, alone or in combination with antihypertensive drugs, represents a promising therapeutic strategy for blood pressure control.

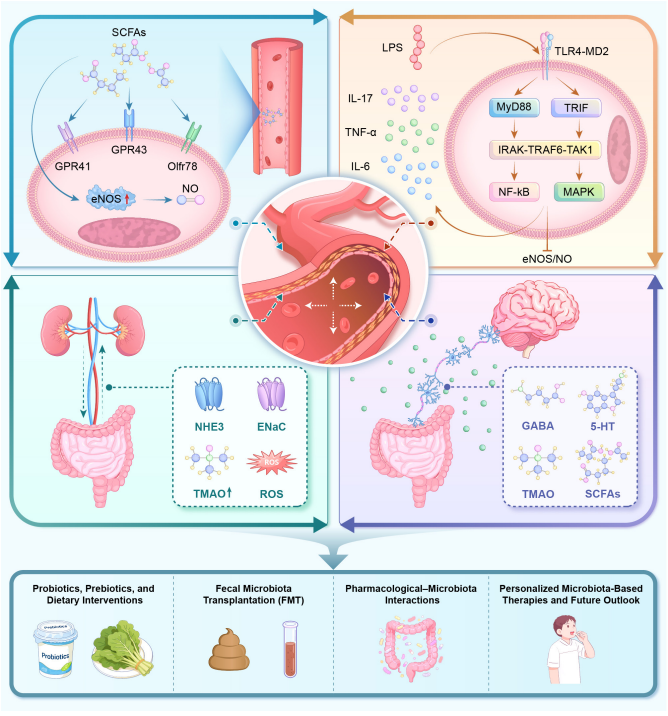

ration of SCFAs levels through dietary fiber supplementation or probiotic intervention has been demonstrated to lower blood pressure, underscoring the central role of microbial-derived metabolites in vascular homeostasis. However, the effects of SCFAs are context dependent and receptor specific. Although many studies report antihypertensive effects of short chain fatty acids, particularly propionate and butyrate, other evidence suggests that certain SCFAs may raise blood pressure under specific conditions. For example, acetate can activate the olfactory receptor Olfr78, promoting renin release and potentially increasing blood pressure via the renin–angiotensin system and sympathetic stimulation. This dual action highlights the nuanced regulatory role of SCFAs in cardiovascular physiology.

Immune and Inflammatory Modulation

Gut microbiota profoundly influence systemic immune tone and inflammatory status, both of which are closely associated with hypertension. Dysbiosis can promote intestinal barrier disruption and translocation of microbial components such as LPS into the circulation, activating toll-like receptor 4 (TLR4) signaling and inducing chronic low-grade inflammation. This process leads to increased production of pro-inflammatory cytokines including IL-6, TNF-α, and IL-17, which contribute to endothelial dysfunction, vascular remodeling, and elevated peripheral resistance [5]. Experimental studies in germ-free and antibiotic-treated hypertensive mice have shown that restoration of commensal bacteria attenuates inflammation and normalizes blood pressure, indicating that microbial-driven immune dysregulation is a key pathogenic mechanism in hypertension [15].

The Gut–Brain Axis

The gut–brain axis represents a bidirectional communication system between the gastrointestinal tract and central nervous system that modulates autonomic control of blood pressure. Microbial metabolites such as SCFAs, TMAO, and neurotransmitter-like molecules (e.g., γ-aminobutyric acid, serotonin) can cross the intestinal barrier and influence neuronal signaling. These signals interact with both the central and peripheral nervous systems, including pathways such as the vagus nerve, enteric nervous system, and hypothalamic-pituitary-adrenal (HPA) axis, which together regulate autonomic tone and vascular function. Dysbiosis enhances sympathetic nervous system activity via vagal afferents and hypothalamic inflammation, particularly within the paraventricular nucleus, thereby increasing vascular tone and sustaining hypertension [16]. However, the effects of microbial metabolites on blood pressure regulation are complex and receptor-specific. For instance, while some microbial metabolites such as butyrate exert antihypertensive effects, others like acetate, through activation of Olfr78, may increase blood pressure by promoting renin release and sympathetic activation. This dual action highlights the nuanced regulatory role of the gut microbiota in cardiovascular physiology. Studies have shown that antibiotic-induced modulation of gut microbiota reduces sympathetic output and lowers blood pressure, further supporting the contribution of gut–brain communication to hypertension pathophysiology [17]. Thus, while interventions targeting the gut–brain axis show potential, their long-term effectiveness and safety in humans remain unclear, and further studies are needed to elucidate the exact mechanisms and identify personalized therapeutic strategies.

The Gut–Kidney Axis and Sodium Homeostasis

The gut–kidney axis has emerged as another important pathway linking microbiota to hypertension, primarily through regulation of sodium balance, renal inflammation, and oxidative stress. Microbial metabolites can influence renal expression of sodium transporters such as NHE3 and ENaC, affecting sodium reabsorption and blood pressure. Moreover, elevated TMAO levels, commonly observed in hypertensive individuals, promote renal fibrosis and impair pressure natriuresis [18-19]. Conversely, SCFAs such as acetate and propionate enhance renal vasodilation and natriuresis via activation of GPR41/43, contributing to blood pressure reduction. These findings highlight that gut microbiota act as a metabolic–endocrine interface that modulates renal function and systemic hemodynamics.

However, evidence from human studies is still limited, and the relative contribution of gut derived metabolites to chronic kidney changes in hypertension requires further mechanistic and longitudinal investigation. In summary, the gut microbiota exerts multifaceted effects on blood pressure regulation through

metabolic, immune, neurogenic, and renal pathways. Dysbiosis can disrupt this homeostatic network, leading to increased vascular resistance, inflammation, sympathetic activation, and altered sodium handling. Understanding these mechanisms provides a theoretical foundation for microbiota-targeted therapies aimed at restoring host–microbe equilibrium and achieving long-term blood pressure control, but the translation of preclinical findings to consistent clinical outcomes remains a major challenge.

Interactions Between Mechanisms

The mechanisms through which gut microbiota regulate blood pressure are highly interconnected, creating a complex network that influences cardiovascular homeostasis. SCFAs, for example, not only promote vasodilation by stimulating endothelial nitric oxide production but also modulate immune responses by reducing pro-inflammatory cytokine production. This immune modulation can affect sympathetic nervous system activity via the gut–brain axis, altering vascular tone and contributing to blood pressure regulation. Additionally, microbial metabolites like TMAO can exacerbate vascular inflammation and fibrosis, leading to increased vascular resistance and elevated blood pressure. The gut–kidney axis also plays a role, as SCFAs activate receptors such as GPR41/43 in the kidneys to enhance natriuresis and reduce sodium retention, thereby helping to lower blood pressure. These interconnected pathways highlight the multifactorial nature of hypertension, suggesting that altering one mechanism, such as increasing SCFAs, can affect multiple systems involved in blood pressure control, from the vasculature to the nervous system and kidneys. Understanding these interactions points to the need for integrated therapeutic approaches that target multiple pathways simultaneously.

Therapeutic Strategies and Future Directions

Given the multifactorial role of the gut microbiota in hypertension pathogenesis, targeting the intestinal microecosystem has emerged as a promising therapeutic approach. Current interventions focus on restoring microbial diversity, enhancing beneficial metabolites such as SCFAs, and suppressing pro-inflammatory or pro-hypertensive pathways. These strategies include probiotics and prebiotics, dietary modulation, FMT, and pharmacological–microbiota interactions, which together represent the evolving frontier of microbiota-based therapy for hypertension.

Probiotics, Prebiotics, and Dietary Interventions

Numerous clinical and experimental studies have demonstrated that probiotics can modestly but significantly reduce blood pressure, especially in patients with mild hypertension or metabolic syndrome. Supplementation with strains such as Lactobacillus plantarum, L. helveticus, and Bifidobacterium breve has been shown to improve endothelial function, enhance SCFA production, and reduce oxidative stress [20]. However, the effects of probiotics are strain-specific, and the colonization of beneficial bacteria is often transient, which limits their long-term efficacy. Moreover, the effects observed in clinical trials are often modest compared to conventional pharmacological treatments. Meta-analyses suggest that multi-strain probiotic formulations administered for more than eight weeks yield the most pronounced antihypertensive effects. Yet, there is significant variability in the outcomes, and the long-term safety of these interventions remains unclear. Prebiotics—mainly nondigestible fibers like inulin and fructooligosaccharides—promote the growth of beneficial bacteria and increase SCFA synthesis, indirectly contributing to vasodilation and improved metabolic homeostasis [12]. Although prebiotics show promise, their effects can be influenced by diet and individual microbiome composition, making the outcomes more variable. Dietary interventions emphasizing high fiber, polyphenol-rich foods (e.g., fruits, vegetables, whole grains), and reduced salt intake have similarly been associated with favorable microbial remodeling and improved blood pressure control, further supporting the role of diet–microbiota interactions in hypertension management [21]. However, these dietary interventions are not universally effective, as some individuals may not respond adequately due to differences in gut microbiome composition or metabolic factors.

FMT

FMT represents a direct and powerful method for restoring gut microbial diversity. Clinical trials and animal studies have shown that transferring microbiota from normotensive donors to hypertensive recipients can reduce both systolic and diastolic blood pressure. Mechanistically, FMT reestablishes a balanced microbial community, increases SCFA-producing taxa, and decreases pro-inflammatory species such as Eggerthella lenta and Erysipelatoclostridium ramosum [22]. However, the effects of FMT are variable, and the therapeutic benefits observed in some trials have not been consistently reproduced in others. The transient nature of its effects, as seen in the first multicenter, randomized, placebo-controlled trial of FMT capsules, suggests that FMT may not provide long-term blood pressure control, and the observed reductions in systolic blood pressure (~4 mmHg) may be modest compared to conventional antihypertensive therapies. Despite these challenges, the trial demonstrated transient reductions in systolic blood pressure and improvements in microbial diversity, supporting the concept of microbiota manipulation as a viable therapeutic strategy [6]. Nonetheless, the clinical applicability of FMT is limited by several factors, including the complexity of donor-recipient matching, the safety concerns regarding long-term use, and the potential ethical issues surrounding the procedure. Future research should focus on optimizing FMT protocols, such as donor selection, delivery route, dosing frequency, and the development of next-generation standardized microbial consortia for targeted and reproducible effects. Additionally, further studies are needed to establish the long-term safety, efficacy, and clinical relevance of FMT in diverse patient populations.

Pharmacological–Microbiota Interactions

An emerging area of research highlights the bidirectional interactions between antihypertensive drugs and gut microbiota. Several medications, including angiotensin receptor blockers (e.g., irbesartan) and calcium channel blockers, have been found to modulate microbial composition by enriching beneficial genera like Lactobacillus and Akkermansia, potentially augmenting their blood pressure–lowering effects [23]. However, the effects of antihypertensive drugs on microbiota

composition are not fully understood, and the long-term consequences of these changes remain uncertain. Additionally, while some studies suggest that these microbiota changes could amplify the blood pressure–lowering effects of medications, the overall clinical impact is still debated, as microbiota modulation could also lead to unexpected side effects. Conversely, gut microbiota can metabolize and alter the bioavailability or efficacy of certain antihypertensive drugs through enzymatic modifications. For example, certain microbial populations may enhance or reduce the absorption of specific medications, thus influencing their therapeutic outcomes. These reciprocal interactions suggest that combining pharmacological treatments with microbiota-targeted approaches may yield synergistic therapeutic outcomes [24]. Nevertheless, these interactions are highly individual, and the variability in patient responses due to differences in microbiota composition poses a challenge for the widespread clinical implementation of microbiota-targeted therapies. Understanding these interactions at the metabolic and genomic levels will be essential for developing precision medicine strategies tailored to individual microbial profiles.

Personalized Microbiota-Based Therapies and Future Outlook

The heterogeneity of gut microbiota across individuals and populations poses both challenges and opportunities for personalized hypertension management. Advances in metagenomics, metabolomics, and artificial intelligence–driven modeling now allow the identification of microbial biomarkers predictive of therapeutic response. However, the variability in microbiota profiles between individuals complicates the development of standardized interventions, and the predictive power of microbial biomarkers for treatment outcomes remains inconsistent. Integration of multi-omics data can help design individualized interventions combining probiotics, diet, and pharmacotherapy to achieve sustained blood pressure control. Moreover, sex-specific differences in microbiota composition and hormonal influences on microbial metabolism warrant further exploration to refine personalized treatment strategies. These differences could affect how individuals respond to both dietary and pharmacological interventions, highlighting the need for gender-specific therapeutic approaches. Future research should also investigate the long-term safety, efficacy, and regulatory frameworks for microbiota-based therapies, as well as addressing ethical concerns related to microbiota manipulation, such as donor-recipient matching for FMT. Ensuring their clinical translation into standardized care for hypertension will require rigorous clinical trials and evidence-based guidelines to overcome the challenges associated with individual variability and treatment consistency.

Conclusion

In conclusion, gut microbiota represent a dynamic and modifiable determinant of blood pressure regulation. Restoring microbial homeostasis through dietary, probiotic, and microbial transplantation strategies provides a novel avenue for hypertension management beyond traditional pharmacological approaches. While current evidence underscores promising short-term benefits, the long-term efficacy of these interventions remains uncertain, and significant individual variability complicates the establishment of universal treatment protocols. Long-term safety, optimal dosage, and the risk of adverse effects in different populations require further investigation. Additionally, the mechanistic complexities of how gut microbiota influence blood pressure, including their interactions with other physiological systems and the host's genetic and environmental factors, remain to be fully understood. The integration of microbiome science with precision medicine and systems biology will be instrumental in developing targeted, sustainable, and patient-specific therapeutic solutions for hypertension, ultimately contributing to improved cardiovascular outcomes and global health. However, to translate these findings into clinical practice, future research must address the gaps in our understanding of microbiota-based therapies and overcome the challenges of individual variability, therapeutic consistency, and long-term clinical validation.

Abbreviations

Fecal microbiota transplantation: FMT; Hypothalamic-pituitary-adrenal: HPA; Lipopolysaccharide: LPS; Nitric oxide: NO; Short-chain fatty acid: SCFA; Toll-like receptor 4: TLR4; Trimethylamine-N-oxide: TMAO.

Author Contributions

HaiTao Yang drafted and revised the manuscript. JingKun Liu conceived the idea, supervised the study, and provided critical revisions. All authors read and approved the final version of the manuscript.

Acknowledgements

The authors thank the Department of Cardiology, The First Affiliated Hospital of Xinjiang Medical University, and the Department of Thoracic and Abdominal Radiotherapy, The Affiliated Tumor Hospital of Xinjiang Medical University, for their support.

Funding Information

Not applicable.

Ethics Approval and Consent to Participate

Not applicable. This article does not contain any studies with human participants or animals performed by any of the authors.

Competing Interests

The authors declare that they have no competing interests.

Data Availability

The authors declare that they have no existing or potential commercial or financial relationships that could create a conflict of interest at the time of conducting this study.

References

[1] Mishra SR, Satheesh G, Khanal V, Nguyen TN, Picone D, Chapman N, et al. Closing the Gap in Global Disparities in Hypertension Control. Hypertension. 2025 Mar;82(3):407-410. https://doi.org/10.1161/HYPERTENSIONAHA.124.24137

[2] Marques FZ, Mackay CR, Kaye DM. Beyond gut feelings: how the gut microbiota regulates blood pressure. Nat Rev Cardiol. 2018 Jan;15(1):20-32. https://doi.org/10.1038/nrcardio.2017.120

[3] Bartolomaeus H, Balogh A, Yakoub M, Homann S, Markó L, Höges S, et al. Short-Chain Fatty Acid Propionate Protects From Hypertensive Cardiovascular Damage. Circulation. 2019 Mar 12;139(11):1407-1421. https://doi.org/10.1161/CIRCULATIONAHA.118.036652

[4] Richards EM, Li J, Stevens BR, Pepine CJ, Raizada MK. Gut Microbiome and Neuroinflammation in Hypertension. Circ Res. 2022 Feb 4;130(3):401-417. https://doi.org/10.1161/CIRCRESAHA.121.319816

[5] Yang HT, Jiang ZH, Yang Y, Wu TT, Zheng YY, Ma YT, et al. Faecalibacterium prausnitzii as a potential Antiatherosclerotic microbe. Cell Commun Signal. 2024 Jan 19;22(1):54. https://doi.org/10.1186/s12964-023-01464-y

[6] Fan L, Chen J, Zhang Q, Ren J, Chen Y, Yang J, et al. Fecal microbiota transplantation for hypertension: an exploratory, multicenter, randomized, blinded, placebo-controlled trial. Microbiome. 2025 May 23;13(1):133. https://doi.org/10.1186/s40168-025-02118-6

[7] Li J, Wang SY, Yan KX, Wang P, Jiao J, Wang YD, et al. Intestinal microbiota by angiotensin receptor blocker therapy exerts protective effects against hypertensive damages. Imeta. 2024 Jul 18;3(4):e222. https://doi.org/10.1002/imt2.222

[8] Guo Y, Li X, Wang Z, Yu B. Gut Microbiota Dysbiosis in Human Hypertension: A Systematic Review of Observational Studies. Front Cardiovasc Med. 2021 May 14;8:650227. https://doi.org/10.3389/fcvm.2021.650227

[9] Hsu CN, Yu HR, Chan JYH, Lee WC, Wu KLH, Hou CY, et al. Maternal Acetate Supplementation Reverses Blood Pressure Increase in Male Offspring Induced by Exposure to Minocycline during Pregnancy and Lactation. Int J Mol Sci. 2022 Jul 18;23(14):7924. https://doi.org/10.3390/ijms23147924

[10] Wu X, Li Q, Cai J, Huang H, Ma S, Tan H. Longitudinal change of gut microbiota in hypertensive disorders in pregnancy: a nested case-control and Mendelian randomization study. Sci Rep. 2023 Oct 9;13(1):16986. https://doi.org/10.1038/s41598-023-43780-w

[11] Lewis-Mikhael AM, Davoodvandi A, Jafarnejad S. Effect of Lactobacillusplantarum containing probiotics on blood pressure: A systematic review and meta-analysis. Pharmacol Res. 2020 Mar;153:104663. https://doi.org/10.1016/j.phrs.2020.104663

[12] Zhao TX, Zhang L, Zhou N, Sun DS, Xie JH, Xu SK. Long-term use of probiotics for the management of office and ambulatory blood pressure: A systematic review and meta-analysis of randomized, controlled trials. Food Sci Nutr. 2022 Sep 20;11(1):101-113. https://doi.org/10.1002/fsn3.3069

[13] Dardi P, Dos Santos-Eichler RA, de Oliveira S, Vinolo MAR, Câmara NOS, Rossoni LV. Reduced intestinal butyrate availability is associated with the vascular remodeling in resistance arteries of hypertensive rats. Front Physiol. 2022 Sep 29;13:998362. https://doi.org/10.3389/fphys.2022.998362

[14] Xu L, Yu Q, Ma L, Su T, Zhang D, Yao D, et al. In vitro simulated fecal fermentation of mixed grains on short-chain fatty acid generation and its metabolized mechanism. Food Res Int. 2023 Aug;170:112949. https://doi.org/10.1016/j.foodres.2023.112949

[15] Joe B, McCarthy CG, Edwards JM, Cheng X, Chakraborty S, Yang T, et al. Microbiota Introduced to Germ-Free Rats Restores Vascular Contractility and Blood Pressure. Hypertension. 2020 Dec;76(6):1847-1855. https://doi.org/10.1161/HYPERTENSIONAHA.120.15939

[16] Kwon YN, Kim YJ. Gut-Brain-Microbiota Axis and Hypertension: A Literature Review. Curr Pharm Des. 2021;27(37):3939-3946. https://doi.org/10.2174/1381612827666210706161733

[17] Yang T, Maki KA, Marques FZ, Cai J, Joe B, Pepine CJ, et al. Hypertension and the Gut Microbiome: A Science Advisory From the American Heart Association. Hypertension. 2025 Sep;82(9):e160-e170. https://doi.org/10.1161/HYP.0000000000000247

[18] Jiang S, Shui Y, Cui Y, Tang C, Wang X, Qiu X, et al. Gut microbiota dependent trimethylamine N-oxide aggravates angiotensin II-induced hypertension. Redox Biol. 2021 Oct;46:102115. https://doi.org/10.1016/j.redox.2021.102115

[19] Tanaka M, Itoh H. Hypertension as a Metabolic Disorder and the Novel Role of the Gut. Curr Hypertens Rep. 2019 Jun 24;21(8):63. https://doi.org/10.1007/s11906-019-0964-5

[20] Robles-Vera I, de la Visitación N, Toral M, Sánchez M, Romero M, Gómez-Guzmán M, et al. Probiotic Bifidobacterium breve prevents DOCA-salt hypertension. FASEB J. 2020 Oct;34(10):13626-13640. https://doi.org/10.1096/fj.202001532R

[21] Zambrano AK, Cadena-Ullauri S, Ruiz-Pozo VA, Tamayo-Trujillo R, Paz-Cruz E, Guevara-Ramírez P, et al. Impact of fundamental components of the Mediterranean diet on the microbiota composition in blood pressure regulation. J Transl Med. 2024 May 3;22(1):417. https://doi.org/10.1186/s12967-024-05175-x

[22] Fan L, Ren J, Chen Y, Wang Y, Guo Z, Bu P, et al. Effect of fecal microbiota transplantation on primary hypertension and the underlying mechanism of gut microbiome restoration: protocol of a randomized, blinded, placebo-controlled study. Trials. 2022 Feb 24;23(1):178. https://doi.org/10.1186/s13063-022-06086-2

[23] Xiong Y, He Y, Chen Z, Wu T, Xiong Y, Peng Y, et al. Lactobacillus induced by irbesartan on spontaneously hyperten-

sive rat contribute to its antihypertensive effect. J Hypertens. 2024 Mar 1;42(3):460-470. https://doi.org/10.1097/HJH.0000000000003613

[24] Kyoung J, Atluri RR, Yang T. Resistance to Antihypertensive Drugs: Is Gut Microbiota the Missing Link? Hypertension. 2022 Oct;79(10):2138-2147. https://doi.org/10.1161/HYPERTENSIONAHA.122.19826

Research Article

Life Conflux

High-risk Factors and a Nomogram Prediction Model for Pulmonary Fungal Infection in Elderly Patients with Acute Exacerbation of Chronic Obstructive Pulmonary Disease

Authors

Tiantian Zhang, Siyu Sun, Yingying Zhu

Correspondence

yfy1361043@fy.ahmu.edu.cn (Y. Zhu)

Graphical Abstract

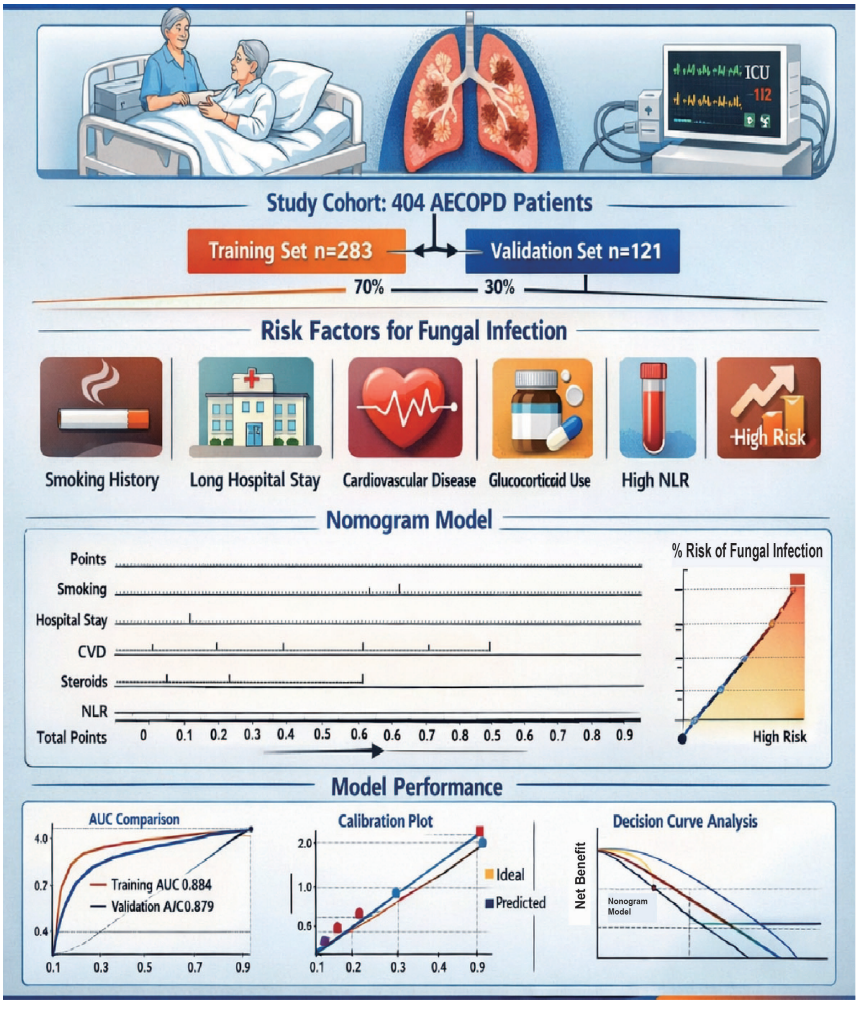

https://doi.org/10.71321/d3zf3339

Research Article

Life Conflux

High-risk Factors and a Nomogram Prediction Model for Pulmonary Fungal Infection in Elderly Patients with Acute Exacerbation of Chronic Obstructive Pulmonary Disease

Tiantian Zhang[1] **,** Siyu Sun[2] , Yingying Zhu[2*]

Received: 2025-12-05 | Accepted: 2026-02-13 | Published online: 2026-03-08

Abstract

Background: Pulmonary fungal infection is a major risk factor for death and prolonged hospitalization in elderly patients with acute exacerbation of chronic obstructive pulmonary disease (AECOPD). At present, early recognition of these infections remains difficult. This study therefore collected clinical data to develop an early-prediction model for fungal pneumonia complicating AECOPD.

Methods: We enrolled 404 elderly AECOPD patients admitted to the Department of Respiratory Medicine, First Affiliated Hospital of Anhui Medical University, from January to December 2023. The cohort was randomly split 7:3 into a training set (n =283) and a validation set (n =121). Univariate logistic regression was first performed in the training set; variables with $p < 0.05$ were entered into a multivariate model. Significant factors were used to construct a nomogram. Model performance was evaluated in both sets by the area under the receiver operating characteristic curve (AUC), calibration plots, and decision-curve analysis (DCA).

Results: Smoking history, length of hospital stay, concomitant cardiovascular disease, glucocorticoid use, and the neutrophil-to-lymphocyte ratio (NLR) were independent risk factors for fungal infection during AECOPD ($p < 0.05$). The nomogram achieved AUCs of 0.884[95% CI: 0.838–0.930] in the training set and 0.879 [95% CI: 0.795–0.962] in the validation set. Calibration and DCA curves indicated good clinical utility.

Conclusion: Smoking history, prolonged hospitalization, concurrent cardiovascular disease, glucocorticoid therapy, and elevated NLR are independent risk factors for fungal infection in AECOPD. The constructed nomogram exhibits strong predictive performance.

Keywords: elderly acute exacerbation of chronic obstructive pulmonary disease; fungal infection; risk factors; nomogram; prediction model

Introduction

Chronic obstructive pulmonary disease (COPD) is a heterogeneous disorder characterised by chronic respiratory symptoms—dyspnoea, cough and sputum production with acute exacerbations—resulting from persistent abnormalities of the airways (bronchitis/bronchiolitis) and / or alveoli (emphysema) that lead to progressive, irreversible airflow limitation [1]. An acute exacerbation of COPD (AECOPD) is defined as a worsening of dyspnoea, cough and/or sputum within <14 days, often accompanied by tachypnoea or tachycardia and usually triggered by respiratory infection, air pollution or parenchymal injury; it is associated with intensified local and systemic inflammation. Elderly patients with COPD are intrinsically more fragile, and consequently more prone to super-imposed infection. Recent data rank COPD as the fourth leading cause of death worldwide [2]; its high prevalence, disability and mortality impose a heavy clinical burden and profoundly affect disease trajectory and prognosis [3]. Pulmonary fungal infection is largely opportunistic: fungi colonising the upper airways or other sites invade the lower respiratory tract when host immunity wanes, producing a spectrum of disease that ranges from mild respiratory symptoms to respiratory failure or septic shock [4]. Compared with other pulmonary disorders, AECOPD is accompanied by longer hospital stay, broader-spectrum antibiotic exposure and more frequent invasive procedures—all recognised risk factors for invasive mycosis [5]. Personalised prediction models that integrate multidimensional data have proved powerful in clinical risk stratification and are now widely used in contemporary medicine [6].Although several independent risk factors for AECOPD complicated by pulmonary fungal infection have been identified, robust prognostic models remain scarce, especially for the elderly. Most previous studies have relied on single peripheral-blood indices; comprehensive models incorporating readily available inflammatory markers have rarely been reported. Against this background we sought to develop and validate a pragmatic prediction tool that quantifies the risk of concomitant fungal infection during hospitaliza-

1 Department of General Practice, The First Affiliated Hospital of Anhui Medical University, Hefei, 230000, China.

2 Department of Geriatric Respiratory and Critical Care Medicine, The First Affiliated Hospital of Anhui Medical University, Hefei, 230000, China.

* Corresponding Author.

tion in elderly patients with AECOPD, thereby facilitating timely empirical antifungal therapy and potentially improving clinical outcomes [7].

Study Population

A retrospective cohort design was adopted. From January to December 2023, 500 elderly patients admitted to the Department of Respiratory Medicine, the First Affiliated Hospital of Anhui Medical University, for acute exacerbation of chronic obstructive pulmonary disease (AECOPD) were consecutively screened. After application of inclusion and exclusion criteria, 404 cases were ultimately enrolled. The cohort was randomly split into a training set (n = 283) and a validation set (n = 121) in a 7:3 ratio using a computer-generated random-number sequence (Figure 1). The study protocol was approved by the Hospital Ethics Committee approval (No. PJ-2025-01-18) and was conducted in accordance with the principles of the Declaration of Helsinki.

Figure 1. Flow chart of patient selection and cohort allocation for model development and validation.

The diagram illustrates the derivation of the study population. Among 500 screened patients aged >65 years who met the diagnostic criteria for AECOPD, 96 were excluded (severe dysfunction of major organs, n=8; severe psychiatric or cerebrovascular disease, n=5; incomplete medical records, n=83). The remaining 404 eligible patients were randomly divided into a training set (n=283) for nomogram construction and a validation set (n=121) for internal validation.

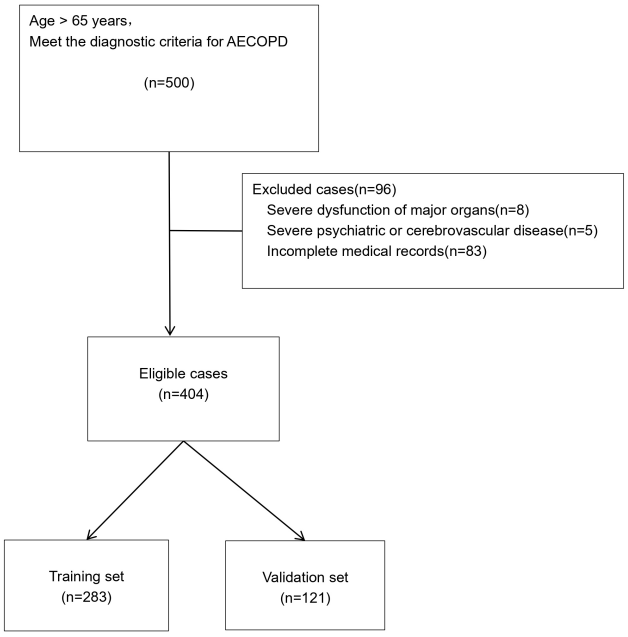

Inclusion and Exclusion Criteria

Inclusion criteria: (1) Age greater than 65 years; (2) Patients diagnosed with acute exacerbation of chronic obstructive pulmonary disease (AECOPD) according to the 2023 revised Chinese expert consensus on the diagnosis and treatment of AECOPD and confirmed by spirometry.(4) Complete medical record.

Exclusion criteria:(1) Severe dysfunction of any major vital organ; (2) Severe psychiatric or cerebrovascular disease; (3) Insufficient clinical data.

Diagnostic Methodology for Fungal Infection

Diagnosis of fungal infection was based on the Expert Consensus on the Diagnosis and Treatment of Pulmonary Mycoses issued by the Chinese Thoracic Society [8]and Internal Medicine (9th Edition), utilizing a three-tier diagnostic classification system (proven, probable, possible). Diagnosis was determined by a comprehensive assessment of clinical symptoms, imaging features, and microbiological findings in AECOPD patients. Suspected patients underwent imaging studies, and sputum samples were collected. For patients with an initial positive fungal sputum culture, a repeat sputum sample was collected for culture after 24-48 hours. Only cases with the same fungal species isolated in two or more consecutive cultures were included in further analysis. Multiple sputum cultures showing mixed fungal growth, in the absence of characteristic imaging changes or clinical symptom exacerbation, were considered contaminated and excluded. For patients with positive fungal sputum cultures but lacking definitive clinical symptoms or imaging evidence of pulmonary infection, antifungal treatment response was evaluated: cases were classified as fungal colonization (and excluded from the infection group) if there was no symptom progression or imaging deterioration without antifungal therapy, or if no improvement was observed following antifungal treatment. Only cases demonstrating clinical and radiological improvement in response to antifungal therapy were confirmed as pulmonary fungal infections.

Data collection

Baseline characteristics and comorbidities were systematically extracted from the electronic medical record, including age, sex, Body Mass Index (BMI), smoking history, alcohol consumption, and co-existing conditions such as hypertension, diabetes mellitus, and cardiovascular disease. The initial clinical presentation, physical findings, and the first available laboratory results obtained after admission were also recorded. Throughout hospitalization, all therapeutic interventions—specifically the administration of systemic corticosteroids and antimicrobial agents, as well as the use or non-use of mechanical ventilation—were prospectively logged. Clinical outcomes were subsequently evaluated in terms of total length of stay and the occurrence of in-hospital death.

Statistical analysis

All data processing, inferential statistics, and visualizations were performed with SPSS 27.0 and R 4.5.1. Two-sided tests were used throughout; statistical significance was set at $P < 0.05$. Continuous variables were first examined for normality. Normally distributed data are presented as mean ± SD ($\bar{x} \pm s$); non-normally distributed data are expressed as median [inter-quartile range, M (Q1, Q3)]. The entire cohort was randomly split 7:3, yielding a training set (n = 283) and a validation set (n = 121). In the training set, univariable logistic regression was applied to screen variables; those with $p < 0.05$ were entered into a multivariable logistic model. Significant predictors retained in the final model were used to construct a nomogram. Model performance was evaluated in both the training and validation sets with ROC curves, calibration plots, and decision-curve analysis (DCA).

Baseline characteristics of elderly patients presenting with acute exacerbation of chronic obstructive pulmonary disease and co-existing pulmonary fungal infections

A total of 404 patients were enrolled, including 311 males (77.0 %) and 93 females (23.0 %); 105 individuals (26.0 %) constituted the fungal-infection group (Table 1). Among the 105 patients with pulmonary fungal co-infection, Aspergillus fumigatus was the leading pathogen (n = 46, 43.8 %), followed by Candida albicans (n = 24, 22.9 %), Aspergillus flavus (n = 6, 5.7 %), Aspergillus niger (n = 5, 4.8%), Aspergillus sydowii (n = 1, 0.95 %), and Candida tropicalis (n = 1, 0.95 %); the causative organism remained unidentified in 22 cases (21.0 %). Among them, confirmed infections (83 cases, accounting for 79.0%) were diagnosed based on: (a) confirmation by histopathological examination, or (b) clinical manifestations consistent with infection, along with the same fungus detected in two or more consecutive sputum or bronchoalveolar lavage fluid cultures. Clinically diagnosed infections (22 cases, accounting for 21.0%, the " causative organism remained unidentified " group). These patients met all the following diagnostic criteria: although the specific pathogen could not be identified through consecutive cultures or histopathological examination, the diagnosis was established based on sufficient clinical, imaging, and indirect laboratory evidence. This study, adhering to the rigor of the predictive model, excluded suspected cases. That is, patients who only met the criteria for host factors combined with clinical or imaging features but lacked any mycological evidence (direct or indirect) were not included. The mean age was 75.97 years in the infection group versus 74.20 years in the non-infected group. Fever on admission was observed in 25.7 % of the fungal-infection group compared with 16.7 % of those without infection. Current or former smokers were more prevalent in the infected cohort (53.5 % and 37.1 %). Median length of stay was longer for infected patients (13 days and 10.25 days). Systemic corticosteroids were administered to 69.5 % of the infected group but only 13.7 % of the non-infected group, and antibiotic duration was likewise extended in the former. Mean BMI was lower in infected individuals (19.43 kg/m² and 23.92 kg/m²). Comorbid hypertension was reported in 42.9 % of infected and 47.1 % of non-infected patients; corresponding figures for diabetes were 18.1 % and 13.7 %, and for cardiovascular disease 52.4 % and 38.5 %.

Pulmonary Fungal Infection in Elderly Patients Hospitalized for Acute Exacerbation of Chronic Obstructive Pulmonary Disease

Univariable analysis of the training cohort revealed statistically significant differences ($p < 0.05$) between patients with and without concomitant fungal infection in the following variables: presence of fever, smoking history, length of hospital stay, co-existing cardiovascular disease, systemic corticosteroid use, duration of corticosteroid therapy, white-blood-cell count, neutrophil-to-lymphocyte ratio (NLR), C-reactive protein level, and blood glucose concentration. No significant differences were observed for any other parameters ($p > 0.05$) (Table 2).

Multivariable logistic regression analysis of risk factors for pulmonary fungal infection in elderly patients with acute exacerbation of chronic obstructive pulmonary disease

Multivariable logistic regression—using fungal infection as the dependent variable and all factors with $p < 0.05$ in Table 2 as covariates—identified smoking history, length of hospital stay, co-existing cardiovascular disease, systemic corticosteroid use, and NLR as independent predictors (all $p < 0.05$) (Table 3).

Prediction Model Development

Based on the multivariable logistic regression coefficients, the five independent risk factors (smoking history, length of hospital stay, concomitant cardiovascular disease, systemic corticosteroid use, and NLR) were each weighted and assigned corresponding points. Summing the points for an individual patient and locating the total on the lower axis of the

Table 1. Baseline characteristics of elderly patients presenting with acute exacerbation of chronic obstructive pulmonary disease and co-existing pulmonary fungal infections

Variable	Total n=404	Fungal Infection n=105	Without Fungal Infection n=299	χ^2/t	*P*-value
Age, years	74.8±9.70	75.97±9.42	74.23±9.79	-1.61	0.110
Fever	77(19.1%)	27(25.7%)	50(16.7%)	3.51	0.06
Hypertension	186(46.0%)	45(42.9%)	141(47.1%)	0.5	0.479
Diabetes Mellitus	60(14.9%)	19(18.1%)	41(13.7%)	0.86	0.354
Cardiovascular Disease	152(37.6%)	55(52.4%)	97(38.5%)	12,85	<0.001
Smoking history	167(41.3%)	56(53.3%)	111(37.1%)	7.77	0.05
BMI (kg/m²)	22.7 ± 16.0	19.43±6.64	23.92±18.24	2.08	0.05
Length of Hospital Stay, days	10.96 ± 7.91	13.00±12.28	10.25±5.63	-2.20	0.030
Duration of Glucocorticoid Use	114(28.2%)	73(69.5%)	41(13.7%)	11.67	<0.001
WBC, ×10 ^{9} /L	8.86 ± 4.22	10.75±5.75	8.19±3.54	-4.28	<0.001
NLR	10.33 ± 19.82	17.82±35.35	7.70±9.69	-2.87	0.01
CRP, mg/L	36.62 ± 56.1	45.18±59.63	33.62±54.85	-1.75	0.08
ALB, g/L	36.38 ± 5.44	35.63±5.53	36.64±5.41	1.62	0.11
PA, mg/L	164.5 ± 73.9	127.65±82.64	177.39±70.54	4.30	<0.001
Glu, mmol/L	6.95 ± 2.59	7.48±3.23	6.76±2.33	-2.08	0.04

nomogram yields the predicted probability of fungal infection (Figure 2). ROC curves (Figure 3) were nearly superimposable between the training and validation sets, with areas under the curve (AUC) of 0.884 [95 % CI 0.838–0.930] and 0.879 [95 % CI 0.796–0.962], respectively.Calibration plots (Figure 4) showed close agreement between predicted probabilities and observed event rates; Hosmer-Lemeshow tests yielded p > 0.05 in both cohorts. Decision-curve analysis (DCA, Figure 5) demonstrated favorable net clinical benefit across the full range of reasonable threshold probabilities.

Discussion

COPD is a heterogeneous disorder. GOLD 2025 classifies its determinants into genetic susceptibility, environmental exposures and events occurring across the life-course; together these insults destroy lung parenchyma and distort normal lung development or ageing. Acute exacerbations are frequently complicated by co-morbidities that further depress systemic immunity and predispose to secondary fungal infection. In the present series 105 of 404 eligible patients (26.0 %) acquired pulmonary mycoses, with Aspergillus spp. predominating—a distribution consistent with previous reports. Multivariable analysis identified five independent risk factors: current or past smoking, prolonged hospital stay, concomitant cardiovascular disease, systemic corticosteroid therapy and an elevated neutrophil-to-lymphocyte ratio (NLR).

Figure 2. Nomogram predicting the probability of pulmonary fungal infection in elderly patients hospitalized for AECOPD.
The model incorporates five independent risk factors identified by multivariable logistic regression: Systemic glucocorticoid therapy (yes = 1, no = 0) Neutrophil-to-lymphocyte ratio (NLR, continuous) Smoking history (yes = 1, no = 0) Length of hospital stay (days, continuous) Cardiovascular disease (yes = 1, no = 0) To obtain the predicted probability: Locate the patient's value on each variable axis → draw a vertical line up to the "Points" axis to determine points for that variable. Sum the points for all variables → locate the total on the "Total Points" axis. Drop a vertical line from the total-points value to the "Predicted value of infection" axis to read the probability (0–1).

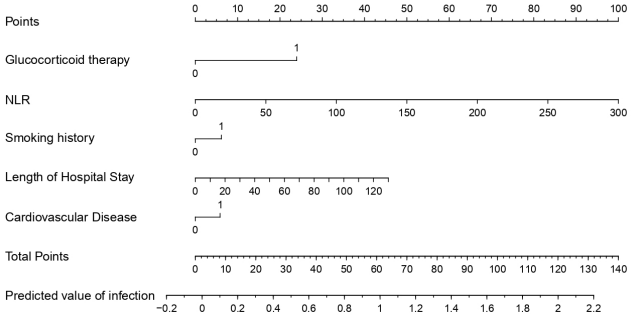

Table 2. Univariable Analysis of Risk Factors for Pulmonary Fungal Infection in Elderly Patients Hospitalized for Acute Exacerbation of Chronic Obstructive Pulmonary Disease.

Variable	OR-value	95%CI	*P*-value
Age, years	1.003	0.998~1.009	0.256
Gender, Male; Female	0.949	0.839~1.074	0.410
Fever	1.227	1.083~1.39	0.001
Hypertension	0.939	0.846~1.042	0.240
Diabetes Mellitus	1.054	0.908~1.224	0.492
Cardiovascular Disease	1.131	1.016~1.258	0.025
Smoking history	1.194	1.077~1.323	0.001
BMI (kg/m²)	1	0.994~1.006	0.996
Length of Hospital Stay, days	1.007	1.001~1.013	0.017
Duration of antibiotic therapy, days	1.003	0.996~1.01	0.351
Duration of Glucocorticoid Use	1.663	1.509~1.834	<0.001
Duration of Glucocorticoid Use, days	1.007	1.001~1.013	0.015
WBC, ×10 ^{9} /L	1.026	1.015~1.037	<0.001
NLR	1.008	1.005~1.01	<0.001
CRP, mg/L	0.987	0.977~0.997	0.011
ALB, g/L	1.000	1.000	0.107
PA, mg/L	0.858	0.735~1.002	0.054
Glu, mmol/L	1.399	1.209~1.619	<0.001

Table 3. Multivariable logistic regression analysis of risk factors for pulmonary fungal infection in elderly patients with acute exacerbation of chronic obstructive pulmonary.

Variable	OR-value	95%CI	*P*-value
Smoking history	1.194	1.077~1.323	0.001
Length of Hospital Stay	1.007	1.001~1.013	0.017
Cardiovascular Disease	1.131	1.016~1.258	0.025
systemic glucocorticoid therapy	1.663	1.509~1.834	<0.001
NLR	1.008	1.005~1.01	<0.001

Figure 3. ROC curves of the nomogram for predicting pulmonary fungal infection in elderly AECOPD patients.
The diagram displays the receiver operating characteristic (ROC) curves for both the training set and the validation set. Training set: AUC = 0.884 (95 % CI 0.838–0.930) Validation set: AUC = 0.879 (95 % CI 0.795–0.962) Statistical methods: ROC analysis was performed with the pROC package in R 4.5.1; 95 % confidence intervals were calculated by 2 000 bootstrap replications.

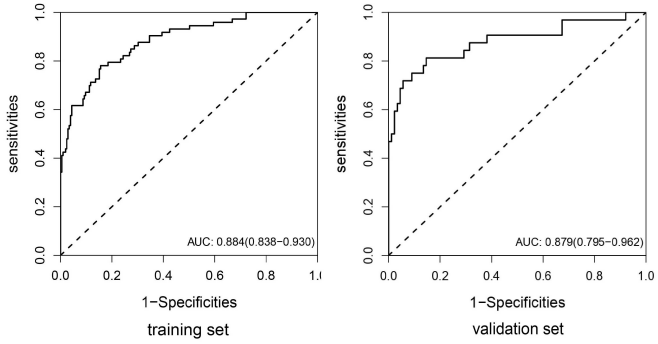

Figure 4. Calibration plots of the nomogram for predicting the probability of pulmonary fungal infection in elderly AECOPD patients.
The left and right panels display the agreement between predicted and observed probabilities in the training and validation sets, respectively. The diagonal gray dashed line represents perfect calibration (Ideal). The solid lines show the apparent (raw) calibration, while the dashed lines (Bias-corrected) are adjusted for overfitting using 1,000 bootstrap resamples. Points or curves closer to the Ideal line indicate better calibration.

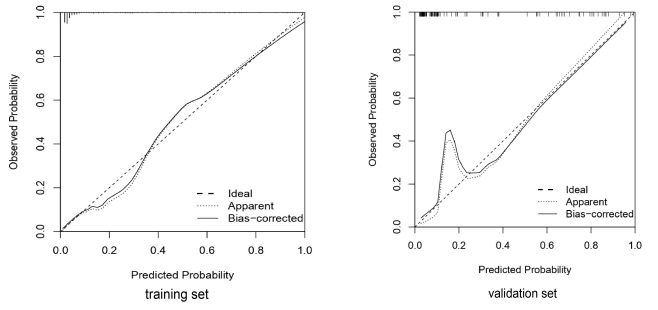

Figure 5. Decision curve analysis (DCA) for the nomogram predicting pulmonary fungal infection in elderly AECOPD patients.
The left and right panels display threshold probability versus net benefit curves for the training and validation sets, respectively. The blue "All" line assumes all patients are infected and treated; the gray "None" line assumes no treatment; the red "Nomogram Model" line represents the net clinical benefit of using the nomogram to guide treatment decisions. Across clinically relevant threshold probabilities (0–25%), the model maintains a positive net benefit, indicating superior clinical utility compared to treating all or no patients. Statistical methods: DCA was performed using the rmda package in R version 4.5.1; net benefit was calculated with 1,000 bootstrap resamples for bias correction.

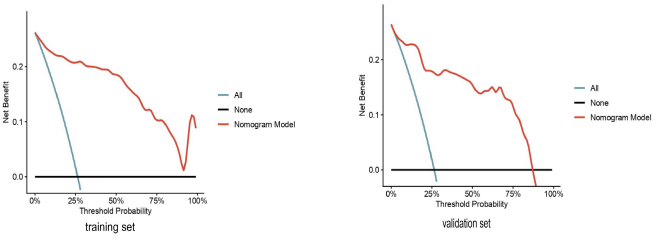

Smoking increases the risk of pulmonary fungal infection
Cigarette smoke exerts broad immunosuppressive effects. Nicotine, tar and other combustion products impair mucociliary clearance, damage airway epithelium and blunt phagocytic activity of alveolar macrophages and neutrophils while suppressing T- and B-cell responses [9]. These defects compromise respiratory barrier function and facilitate fungal colonisation and invasion, particularly during exacerbations when airway inflammation is most intense. The human respiratory tract harbors a complex ecosystem composed of bacteria, fungi, and viruses. Disruptions within this microbial community are closely associated with the onset and progression of various respiratory diseases. When the airways are exposed to external stimuli, the host mounts an abnormal immune response accompanied by persistent inflammation, which in turn reshapes the composition and structure of the airway microbiota. Smoking disrupts this ecological balance to some extent [10]. Our data confirm that smoking significantly increases the risk of invasive fungal disease in elderly AECOPD patients.

Prolonged hospital stay is a risk factor for co-existing pulmonary fungal infection
Length of hospital stay is a proxy for cumulative exposure to antibiotics, corticosteroids and invasive procedures such as intubation—each of which disrupts mechanical or immunological defences. We observed a direct relationship between duration of admission and probability of fungal infection, underscoring the need for heightened surveillance in long-stay patients. Prolonged hospitalization not only prolongs exposure to broad-spectrum antibiotics and invasive devices but also intensifies physiological stress and immunosuppression, all of which synergistically amplify the risk profile; consequently, the likelihood of acquiring pulmonary fungal infection rises substantially, especially in elderly or nutritionally depleted individuals.

Systemic corticosteroid use significantly increases the risk of pulmonary fungal infection
Systemic corticosteroids, while dampening harmful inflammation, simultaneously impair cell-mediated immunity. Experimental work demonstrates that glucocorticoids directly enhance fungal growth, morphological switching and virulence-factor expression in Aspergillus and Candida spp [11-13]. In our cohort, both corticosteroid use and longer courses were strongly associated with mycotic infection.
Finally, repeated or broad-spectrum antibiotic therapy eradicates bacterial competitors and allows fungal overgrowth [14]. We found that every additional day of antibiotic treatment incrementally increased infection odds, emphasising the importance of stringent antimicrobial stewardship in AECOPD management.

Co-existing cardiovascular disease is an independent risk factor for pulmonary fungal infection in AECOPD patients
The circulatory disorders enrolled in this study included coronary artery disease, chronic heart failure, valvular heart disease, and related conditions. The three most frequent cardiac comorbidities in COPD are atrial fibrillation (AF), heart failure (HF), and ischaemic heart disease (IHD), all of which—like COPD—present chiefly with dyspnoea. HF intensifies the respiratory symptoms of AECOPD by producing pulmonary con-

gestion, airway oedema and reduced exercise tolerance; it also disrupts the mucosal mechanical barrier, creating favourable conditions for fungal colonisation. Cardiovascular disease and fungal infection share common risk factors such as advanced age, smoking and diabetes. Conversely, the marked systemic inflammation during AECOPD increases the risk of acute coronary events, generating a "fungal infection–HF" vicious circle. Shared pathophysiological substrates—oxidative stress, endothelial dysfunction and immunosenescence—make cardiovascular disease the second leading cause of death in COPD patients with pulmonary disorders [15-16].

A higher neutrophil-to-lymphocyte ratio (NLR) is associated with an increased probability of pulmonary fungal infection in elderly AECOPD patients

Leukocytosis disrupts immune homeostasis by creating an inflammatory milieu in which pro-inflammatory cytokines suppress anti-fungal immunity. Bacterial super-infection triggers massive neutrophil recruitment and exuberant release of cytokines that impair macrophage-mediated killing of Aspergillus and Candida spp. The neutrophil-to-lymphocyte ratio (NLR), a composite inflammatory index derived from routine full blood count, offers rapid, inexpensive and reproducible quantification of this dysregulated response. In the present study, elevated NLR emerged as an independent risk factor for fungal infection in AECOPD. Previous work has shown that high NLR correlates with impaired pulmonary ventilation in exacerbated COPD, presumably by amplifying airway inflammation and parenchymal damage, thereby facilitating fungal colonisation and invasion [17].

Studies also show that serum albumin reflects overall nutritional reserve; lower concentrations indicate malnutrition, which negatively influences both survival and long-term prognosis [18]. Albumin itself maintains colloid oncotic pressure, transports endogenous and exogenous solutes (hormones, free fatty acids, drugs), and functions as a nitrogen reserve and acid–base buffer; its serum level is a central biochemical index of nutritional status, hepatic function, and systemic inflammation [18]. Chronic dysglycaemia induces systemic microangiopathy, reduces alveolar–capillary oxygen diffusion, and disrupts pulmonary parenchymal architecture—changes that collectively facilitate invasive fungal colonisation [19]. Additionally, elevated blood glucose exacerbates endothelial dysfunction [20], further compromising respiratory function and amplifying the likelihood of fungal infection. In this study, low protein levels and elevated blood glucose were also identified as risk factors for AECOPD complicated with pulmonary fungal infection. Although they were not included in the final predictive model, this may be attributed to the small sample size. Therefore, these two indicators also warrant additional attention in clinical practice.

Although the present study did not identify radiological features such as emphysema, bullae or old tuberculosis scars as independent risk factors, earlier reports have consistently linked these structural abnormalities to pulmonary mycosis. Whether their non-significance in our cohort reflects a true absence of effect or is attributable to limited statistical power remains uncertain; enlarging the sample size in future investigations will be necessary to clarify their contribution [21].

In addition, the single-centre, retrospective design inevitably introduces selection and information bias; future work should adopt prospective, multicentre protocols to enhance external validity and robustness.

Conclusion

In summary, pulmonary fungal infection is common in elderly patients hospitalized for AECOPD and is associated with poor outcomes. Early recognition is therefore essential. Smoking history, prolonged length of stay, pre-existing cardiovascular disease, systemic corticosteroid use (and its duration), and elevated NLR are independent correlates of mycotic complications. Clinicians should maintain a high index of suspicion for invasive fungal disease when any of these factors are present in an elderly AECOPD inpatient.

Abbreviations

AECOPD - Acute Exacerbation of Chronic Obstructive Pulmonary Disease; AF - Atrial Fibrillation; ALB - Albumin; AUC - Area Under the Curve; COPD - Chronic Obstructive Pulmonary Disease; CRP - C-Reactive Protein; DCA - Decision Curve Analysis; HF - Heart Failure; IHD - Ischaemic Heart Disease ; NLR - Neutrophil-to-Lymphocyte Ratio; PA - Prealbumin; ROC - Receiver Operating Characteristic; WBC - White Blood Cell.

Author Contributions

Tiantian Zhang: Conceptualization, Data curation, Formal analysis, Visualization, Writing – original draft, Writing – review & editing. Siyu Sun: Data curation, Formal analysis, Validation, Supervision, Writing – review & editing. Yingying Zhu: Conceptualization, Supervision, Writing – review & editing. All authors read and approved the final manuscript.

Acknowledgements

Not applicable.

Funding Information

This work was supported by the National Natural Science Foundation of China Youth Science Fund Cultivation Program (Grant No. 2019kj05).

Ethics Approval and Consent to Participate

The study protocol was approved by the Hospital Ethics Committee approval (No. PJ-2025-01-18).

Competing Interests

The authors declare that they have no existing or potential commercial or financial relationships that could create a conflict of interest at the time of conducting this study.

Data Availability

Not applicable.

Reference

[1] Maitre T, Cottenet J, Godet C, Roussot A, Abdoul Carime N, Ok V, et al. (2021). Chronic pulmonary aspergillosis: prevalence, favouring pulmonary diseases and prognosis. Eur Respir J, 58(2). https://doi.org/10.1183/13993003.03345-2020

[2] Wang YY, Wang J, Lu ZW, Zhou QQ, Cao YG, Du YJ, et al. (2025). Global, regional, and national burden of lower respiratory infections and chronic obstructive pulmonary disease, 1990-2021: a systematic analysis from the global burden of disease study 2021. Infection, 53(5), 2191-2202. https://doi.org/10.1007/s15010-025-02566-0

[3] Liu SX, M P, W L, QZ H, GF H, MX W, et al. (2023). Global, regional, and national burden of lower respiratory infections and chronic obstructive pulmonary disease. Chinese Journal of Gerontology, 43(04), 817-821. https://kns.cnki.net/kcms2/article/abstract?v=vQ2wnlBr1y6vbIErhuHCGdSON2euxkNxtOJ15W8ZKsIb6m0jGmg8hRXcJJPD3v2zVwFUOIC0-_pwdUd446TsZLSCFe04wlPmp2pfioFmHKaSLEOOitUnRwTvimSutigfjRYHnWQKgY1xAFrrt73OB4feNgGjfAY-50JRDvUA9ThERWVwhjCN1wu2cdwyo0Ze&uniplatform=NZKPT&language=CHS

[4] Leung JM, Tiew PY, Mac Aogáin M, Budden KF, Yong VF, Thomas SS, et al. (2017). The role of acute and chronic respiratory colonization and infections in the pathogenesis of COPD. Respirology, 22(4), 634-650. https://doi.org/10.1111/resp.13032

[5] Shen H, Wu HB, & Y C. (2023). Risk factors for pulmonary fungal infection in elderly patients with acute exacerbation of chronic obstructive pulmonary disease. Chinese Journal of Gerontology, 43(19), 4687-4690. https://kns.cnki.net/kcms2/article/abstract?v=vQ2wnlBr1y7s60nL-dyCsSQ3zFSN3lMmQDsCdZhcjfg3aYk_bUhx5PGIz5riDPrLP9cl_Mj3FgQrS4iAuqpNFwNS4qVkcdVOMlykzo6P339lfOARWrQ2NTKmmUyUoxxH0fDqnAUvuQTcSeVhGt2E-ASM7gT9eeiNzraC4F4zcsZG4dhnDMWZvR1pr8l25Uvi&uniplatform=NZKPT&language=CHS

[6] Yu YL, Lin CK, Zhu CS, & Y W. (2024). Development of a nomogram-based risk prediction model and web calculator for acute exacerbation of chronic obstructive pulmonary disease. Journal of Practical Cardio-Cerebro-Pulmonary Vascular Disease, 32(06), 16-21. https://kns.cnki.net/kcms2/article/abstract?v=vQ2wnlBr1y7GzGDW0xORGsVFn1liQ2LEipg-07rgnn7dtMHF_awAH2cRHg6piewzFEXsYO87oEkxklftN7uBIEtvKxVypTlhX68nfqjFKhRoOekPtMYRPaCBdyUj3gGRiw7EsIa2duF1iiGJ5C2aLButMfbnqMqDZtOZ8xSDUUSTRyFpdtDdU0MrFSEz08H0&uniplatform=NZKPT&language=CHS

[7] Lin X, & N H. (2024). A nomogram prediction model for secondary pulmonary fungal infection in acute exacerbation of chronic obstructive pulmonary disease. Chinese Journal of Respiratory and Critical Care Medicine, 23(02), 77-85. https://kns.cnki.net/kcms2/article/abstract?v=vQ2wnlBr1y4NvgGQDBl7ny3HJaG6RxQXoN9BYqBQaQII3c4hpOQCXaIPCMwxrxjF5wYnQbY-VwTMk_FhG5Ph3tuDzpW_gqxnYMIXKrCUXIiYSr9hq2GmyD3nrQtjLKZh3-zRWd3dJ7E2CGDr_CCxpGIUMj_t9aNPWWBY5nLWPkOackiWYzDXAtfro9lpvqto&uniplatform=NZKPT&language=CHS

[8] Expert Panel Consensus on the Diagnosis and Treatment of Pulmonary Fungal Disease. (2007). Chinese Journal of Tuberculosis and Respiratory Diseases, 30(11), 821-834. https://kns.cnki.net/kcms2/article/abstract?v=vQ2wnlBr1y53kDiZwO-TuwoDCoYVkNCo8dD7j5RucNX65emn3Er-YO0fF8t2b-awEBUTv5cxYuJnSKNkQprYgek22ILQAeK0hDzVURmkw1AWnzQ3a7rOKr9HTRuOaSRIZYsEiFpYCP7XEi_G7gg_OTTfu6JhVxs9KIsF1xYruhHKFeU1-Eobbg==&uniplatform=NZKPT&language=CHS

[9] Lugg ST, Scott A, Parekh D, Naidu B, & Thickett DR. (2022). Cigarette smoke exposure and alveolar macrophages: mechanisms for lung disease. Thorax, 77(1), 94-101. https://doi.org/10.1136/thoraxjnl-2020-216296

[10] Lin L, Yi X, Liu H, Meng R, Li S, Liu X, et al. (2023). The airway microbiome mediates the interaction between environmental exposure and respiratory health in humans. Nat Med, 29(7), 1750-1759. https://doi.org/10.1038/s41591-023-02424-2

[11] Razia DEM, Gao C, Wang C, An Y, Wang F, Liu L, et al. (2025). Targeting Non-Eosinophilic Immunological Pathways in COPD and AECOPD: Current Insights and Therapeutic Strategies. Int J Chron Obstruct Pulmon Dis, 20, 511-532. https://doi.org/10.2147/copd.S506616

[12] Fardet L, Petersen I, & Nazareth I. (2016). Common Infections in Patients Prescribed Systemic Glucocorticoids in Primary Care: A Population-Based Cohort Study. PLoS Med, 13(5), e1002024. https://doi.org/10.1371/journal.pmed.1002024

[13] Diaz-Jimenez D, Kolb JP, & Cidlowski JA. (2021). Glucocorticoids as Regulators of Macrophage-Mediated Tissue Homeostasis. Front Immunol, 12, 669891. https://doi.org/10.3389/fimmu.2021.669891

[14] Chen HD, Fu HQ, & YG N. (2024). Development and validation of a nomogram for predicting prognosis in COPD patients complicated with pulmonary infection. Anhui Medical Journal, 45(05), 598-602. https://link.cnki.net/urlid/34.1077.R.20240514.1704.038

[15] Rabe KF, Hurst JR, & Suissa S. (2018). Cardiovascular disease and COPD: dangerous liaisons? Eur Respir Rev, 27(149). https://doi.org/10.1183/16000617.0057-2018

[16] McMurray JJ, Packer M, Desai AS, Gong J, Lefkowitz MP, Rizkala AR, et al. (2014). Angiotensin-neprilysin inhibition versus enalapril in heart failure. N Engl J Med, 371(11), 993-1004. https://doi.org/10.1056/NEJMoa1409077

[17] Liu Y, Xu J, Ma L, Cao GY, & FD Z. (2024). Association of peripheral blood eosinophils, D-dimer and neutrophil-to-lymphocyte ratio with pulmonary ventilatory function in AECOPD patients. Tianjin Medical Journal, 52(12), 1261-1265. https://link.cnki.net/urlid/12.1116.R.20240929.1023.004

[18] Manolis AA, Manolis TA, Melita H, Mikhailidis DP, & Manolis AS. (2022). Low serum albumin: A neglected predictor in patients with cardiovascular disease. Eur J Intern Med, 102, 24-39. https://doi.org/10.1016/j.ejim.2022.05.004

[19] Y C. (2017). Effect of blood glucose management on pul-

monary fungal infection in patients with diabetes mellitus and chronic obstructive pulmonary disease. Diabetes New World, 20(03), 142-144. https://doi.org/10.16658/j.cnki.1672-4062.2017.03.142

[20] Zhang L, Jiang F, Xie Y, Mo Y, Zhang X, & Liu C. (2023). Diabetic endothelial microangiopathy and pulmonary dysfunction. Front Endocrinol (Lausanne), 14, 1073878. https://doi.org/10.3389/fendo.2023.1073878

[21] Han XY, Jin XY, & LH C. (2020). Relationship between high-resolution CT phenotypes and airway inflammation in chronic obstructive pulmonary disease. Journal of Dalian Medical University. Journal of Dalian Medical University, 42(01), 27-31.https://kns.cnki.net/kcms2/article/abstract?v=vQ2wnlBr1y4RWp9v061V9ZG0TTusuymF9nfPhEPQPanIB2o6exgBvxcLm8wQ2jQZXzECXhqsp-J1avxqXS2-CziPNkkOi2Ymu6BGMCAL0G1W8DkIfs6DXKQ0QhZHi9VuiteXW3xXqqSc2zTmilz-EDcVOC69eYSLMJ2izES_mHKVrNHFJVMmHLjA1uLBcyFl&uniplatform=NZKPT&language=CHS

Regulatory T Cells in Precision Immunotherapy: Mechanistic Insights and Translational Advances of Low-dose Interleukin-2

Authors

Ruiling Feng, Bo Huang, Xia Zhang, Jing He

Correspondence

hejing@pkuph.edu.cn (J. He)

Graphical Abstract

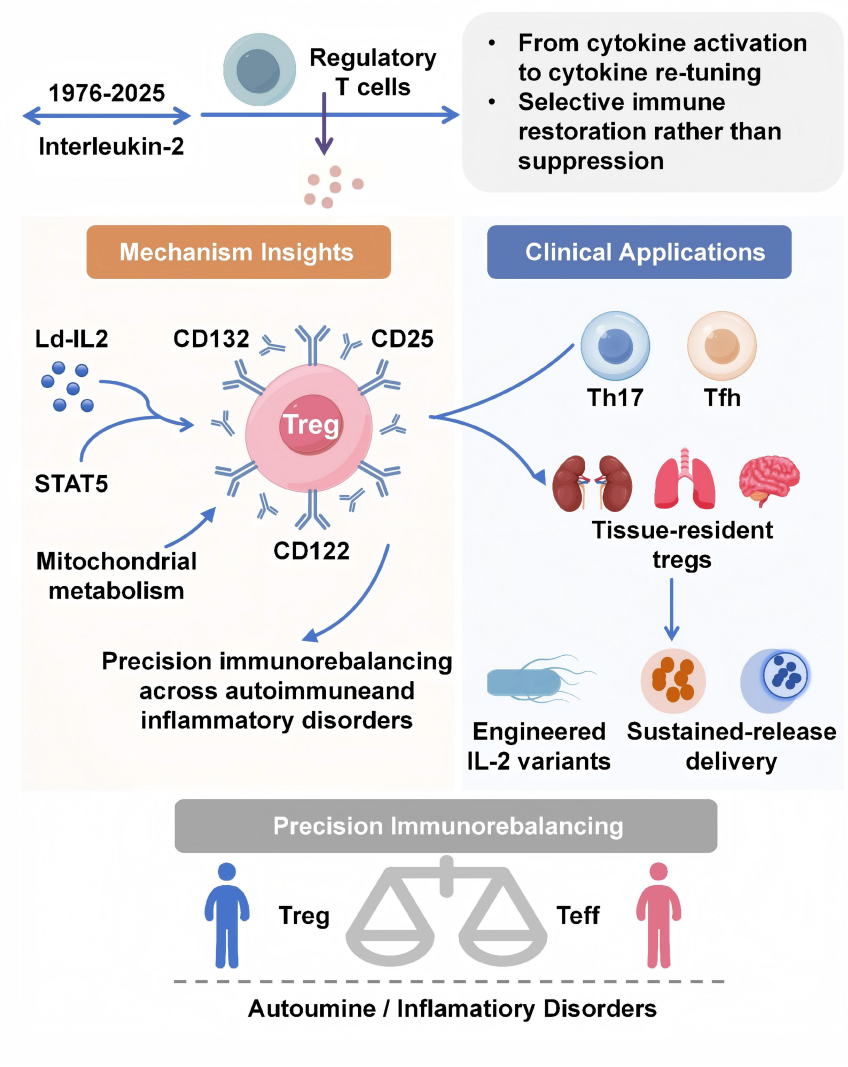

https://doi.org/10.71321/xk8wzt47

Review Article Life Conflux

Regulatory T Cells in Precision Immunotherapy: Mechanistic Insights and Translational Advances of Low-dose Interleukin-2

Ruiling Feng [1], Bo Huang [1], Xia Zhang [1], Jing He [1*]

Received: 2025-10-23 | Accepted: 2026-01-15 | Published online: 2026-03-10

Abstract

Regulatory T cells (Tregs) are the central guardians of immune tolerance, safeguarding against autoimmune and inflammatory damage through Foxp3-dependent transcriptional programs. Recent breakthroughs in precision immunotherapy have revived interest in low-dose interleukin-2 (Ld-IL-2), a cytokine-based strategy that selectively expands and activates Tregs via the high-affinity IL-2 receptor (CD25). This review summarizes emerging mechanistic insights into how Ld-IL-2 orchestrates multilevel immune rebalancing and highlights its translational progress from molecular engineering to clinical applications across autoimmune diseases. We integrated recent findings from cellular, metabolic, and systems immunology studies, together with our own multi-center clinical trial data, to outline the dynamic networks linking IL-2 signaling, Treg plasticity, and immune homeostasis. Ld-IL-2 exerts a dose-dependent biphasic effect on the immune system, selectively enhancing Treg survival and function while restraining pathogenic Th17, Tfh, and Teff subsets. Beyond classical STAT5-FOXP3 activation, recent studies reveal that IL-2 reprograms Treg metabolism toward oxidative phosphorylation, stabilizes Foxp3 epigenetic landscapes, and coordinates intercellular communication through exosomal and tissue-resident networks. Innovations in topologically engineered IL-2 variants and sustained-release delivery systems (e.g., polylactic-acid microsphere–exosome composites) further extend the precision and durability of Treg-directed therapy. Clinical evidence from SLE, Sjögren's disease, and relapsing polychondritis confirms robust immune restoration and favorable safety profiles within defined dose windows. By selectively activating the Treg axis and reprogramming immune homeostasis, low-dose IL-2 represents a paradigm for precision immunotherapy. Integrating molecular engineering and targeted delivery strategies will enable next-generation cytokine therapies to achieve durable immune tolerance across autoimmune and inflammatory disorders.

Keywords: Regulatory T cells; Low-dose Interleukin-2; Foxp3; Immune tolerance; Precision immunotherapy; Translational medicine

Introduction

Interleukin-2 (IL-2) was first identified in 1976 as a potent T-cell growth factor that sustains clonal expansion of activated lymphocytes and fuels effector immunity [1]. During the early decades of cytokine research, IL-2 was considered primarily as a molecule that amplifies cytotoxic T-cell and natural killer (NK) cell activity, leading to its clinical application in high-dose regimens for metastatic cancer and chronic viral infection [2]. However, the subsequent identification of a distinct $CD4^+$ T cell subset expressing high levels of the IL-2 receptor α-chain (CD25) and the transcription factor Forkhead box protein 3 (Foxp3) challenged this view. These cells—now known as regulatory T cells (Tregs)—were shown to depend critically on IL-2 for their development, survival, and suppressive function [3]. This paradigm shift transformed IL-2 from a mere activator of immune responses into a master regulator of immune tolerance.

In the decades since Shimon Sakaguchi and colleagues defined Tregs as essential for preventing spontaneous autoimmunity, IL-2 has emerged as the key cytokine linking effector and regulatory immunity [4]. Whereas high-dose IL-2 promotes effector proliferation through intermediate-affinity βγ (CD122/CD132) receptor signaling, low-dose IL-2 (Ld-IL-2) preferentially engages the high-affinity αβγ (CD25/CD122/CD132) receptor complex that is constitutively expressed on Tregs [5-6]. This receptor hierarchy provides a unique therapeutic window in which Ld-IL-2 selectively expands and stabilizes Tregs without activating pathogenic effector T cells or inducing generalized inflammation. Previous experimental and clinical studies have demonstrated robust Treg reconstitution and immune restoration across autoimmune conditions such as Systemic lupus erythematosus (SLE), primary Sjögren's disease (SjD), type 1 diabetes, and graft-versus-host disease [7-10].

Despite great advances in molecular immunology, treatment of autoimmune diseases still largely relies on broad immunosup-

1 Department of Rheumatology & Immunology, Peking University People's Hospital, Beijing, 100044, China.

* Corresponding Author.

pressive agents—glucocorticoids, calcineurin inhibitors, or cytotoxic drugs—that indiscriminately suppress both protective and pathogenic immunity. Although these regimens can alleviate symptoms, their long-term administration is associated with infection risk, metabolic toxicity, and incomplete disease remission. More importantly, they fail to address the underlying immune dysregulation characterized by the numerical and functional decline of Tregs and the overactivation of effector T cells. Thus, the unmet clinical requirement lies in restoring the physiological immune balance rather than merely dampening immune activation. Targeted Treg restoration through cytokine modulation represents a rational and biologically precise strategy to achieve this goal.

Consequently, the therapeutic strategy of "**precision immunorebalancing**" has been proposed. This approach aims to restore immune homeostasis by selectively modulating the immune system at cellular, molecular, and tissue levels. Ld-IL2 preferentially activates high-affinity receptors on Tregs to induce tolerance without global immunosuppression. Numerous researches revealed that its efficacy stems not only from Treg expansion but also from a fundamental reprogramming of Treg metabolism, epigenome, and transcriptome, which reinforces their suppressor identity and simultaneously attenuates Th17 and Tfh pathways. Additional modulation of NK and memory $CD8^+$ T cells further integrates to maintain immune homeostasis. Translationally, engineered IL-2 variants with extended half-life and controlled receptor selectivity, along with sustained-release delivery systems such as polylactic-acid microspheres or exosome-based nanocarriers, are further enhancing the precision and durability of Treg-targeted therapy.

In this review, we provide a comprehensive overview of the mechanistic underpinnings of Treg-centered IL-2 signaling and summarize recent translational advances that position Ld-IL-2 as a cornerstone of next-generation precision immunotherapy. By integrating molecular biology, systems immunology, and clinical evidence, we aim to delineate how IL-2 has evolved from a classic immunostimulant to a fine-tuned regulator of immune tolerance, opening new avenues for durable disease remission across autoimmune and inflammatory disorders.

Molecular Mechanisms of IL-2-Mediated Treg Regulation

IL-2 Receptor Signaling and the STAT5–FOXP3 Axis

The biological effects of IL-2 are determined by the composition and affinity of its trimeric receptor complex (Figure 1). Tregs constitutively express the high-affinity IL-2 receptor, composed of α (CD25), β (CD122), and γ (CD132) chains, enabling them to respond to picomolar concentrations of the cytokine [5]. In contrast, conventional $CD4^+$and $CD8^+$ T cells express only the intermediate-affinity βγ complex, which requires much higher IL-2 levels for activation [11-12]. This receptor hierarchy forms the molecular foundation for the selective responsiveness of Tregs to low-dose IL-2 (Ld-IL-2).

Upon IL-2 binding, JAK1 and JAK3 associated with CD122 and CD132 are activated, leading to phosphorylation of STAT5 [13-16]. Dimerized STAT5 translocates into the nucleus to bind FOXP3 and its enhancer regions, thereby reinforcing the transcriptional program that sustains Treg identity [17]. Concomitantly, PI3K–AKT and MAPK pathways undergo transient activation, delivering metabolic and pro-survival signals without converting Tregs into effector cells [18]. In contrast, excessive AKT activation—as induced by high-dose IL-2—can destabilize FOXP3 expression, highlighting the critical role of a controlled signaling amplitude [16].

Figure 1. Mechanisic network of low-dose IL-2 in immune regulation. Low-dose IL-2 preferentially signals through the high-affinity IL-2 receptor (IL-2Rαβγ) on regulatory T cells, engaging JAK–STAT and mTOR–AMPK signaling. These pathways sustain Foxp3 transcription and reprogram cellular metabolism, thereby stabilizing Treg identity and function. The resulting network suppresses Th17 and Tfh responses while maintaining $CD8^+$ T and NK cell homeostasis, collectively restoring immune balance.

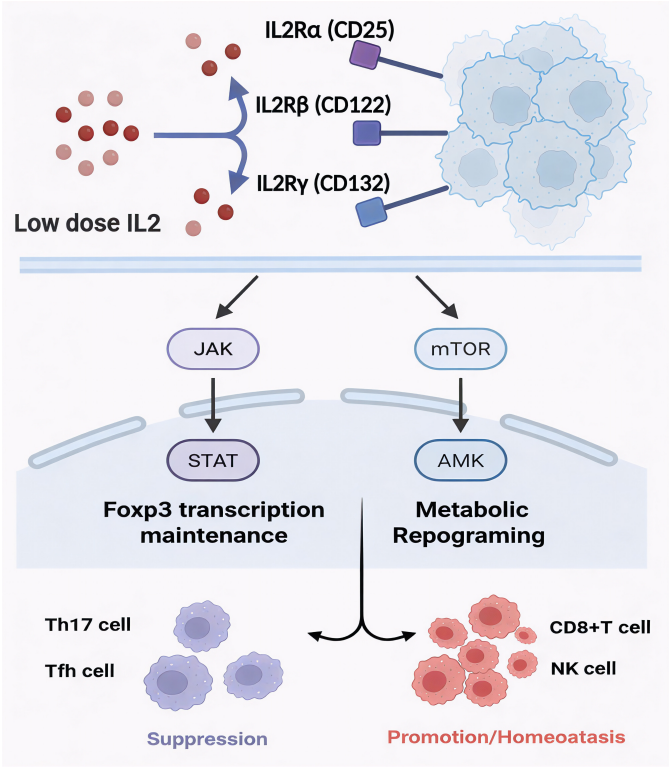

FOXP3 acts as the lineage-defining transcription factor that suppresses pro-inflammatory genes while promoting immunosuppressive mediators such as IL-10, TGF-β, and CTLA-4 [19-20]. Phosphorylated STAT5 not only initiates FOXP3 transcription but also maintains its epigenetic accessibility through recruitment of histone acetyltransferases [21]. Recent multi-omics analyses show that sustained, low-intensity STAT5 signaling preserves FOXP3 stability, whereas intermittent or excessive activation promotes Treg plasticity and loss of function [22]. Thus, Ld-IL-2 achieves an optimal signal-strength threshold that sustains suppressive potency while avoiding effector conversion.

Moreover, IL-2 signaling influences the composition of the Treg pool. Peripheral IL-2 availability regulates the balance between thymus-derived Tregs and peripherally induced Tregs (pTregs), both essential for maintaining tolerance [23]. Through up-regulation of B cell lymphoma 2 (Bcl-2) and down-regulation of pro-apoptotic Bim, IL-2 prolongs Treg survival and enhances their tissue persistence [24-25]. Collectively, these findings underscore that IL-2 is not merely a growth factor but the master

regulator orchestrating Treg lineage commitment, stability, and homeostatic renewal.

Epigenetic and Metabolic Reprogramming of Tregs

In addition to the canonical receptor signaling, IL-2 emerges as a critical regulator of the epigenetic and metabolic programs that determine Treg identity. At the chromatin level, Ld-IL-2 maintains demethylation of the Treg-specific demethylated region (TSDR) within the FOXP3 locus, which is the hallmark of stable, suppressive Tregs [26-29]. This demethylated configuration is stabilized by STAT5, which promotes the recruitment of TET demethylases and suppresses DNA methyltransferase (DNMT) activity, preventing the loss of FOXP3 expression under inflammatory conditions [30-32]. Single-cell ATAC-seq studies further reveal that IL-2 stimulation increases chromatin accessibility at genomic loci encoding critical Treg functional molecules, including IL2RA, CTLA4, and IKZF2 (Helios), reinforcing the transcriptional network sustaining Treg lineage fidelity [18, 33-35].

Metabolically, IL-2 signaling coordinates the balance between oxidative phosphorylation (OXPHOS) and glycolysis, a pivotal determinant of Treg function. In contrast to effector T cells that rely heavily on aerobic glycolysis, Tregs prefer fatty acid oxidation and mitochondrial respiration to support long-term survival and suppressive capacity [36-37]. Through controlled activation of the PI3K–AKT–mTOR axis, Ld-IL-2 enhances fatty-acid oxidation while limiting anabolic glycolysis [38]. Simultaneously, IL-2 up-regulates AMP-activated protein kinase (AMPK), promoting mitochondrial biogenesis and reactive-oxygen-species (ROS) detoxification [39-40]. Together, this IL-2-driven metabolic reprogramming enables Tregs to adapt to nutrient-poor or hypoxic microenvironments, which are frequently encountered in chronically inflamed tissues.

IL-2 signaling integrates with cellular metabolism to regulate the availability of epigenetic substrates, notably within one-carbon metabolism, which generates the universal methyl donor S-adenosylmethionine (SAM) [41-42]. This crosstalk ensures a sufficient supply of methyl-donor for sustaining FOXP3 chromatin marks [43]. Perturbation of this loop, for instance through mTOR hyperactivation or glucose overload, results in FOXP3 instability and Treg dysfunction [18, 44]. These insights explain why Ld-IL-2, but not higher doses, consistently promotes the expansion of functionally stable and long-lived Tregs.

Recent proteomic studies further indicate that IL-2 induces a shift toward an anti-inflammatory secretome, including soluble CD25 and adenosine-generating enzymes (CD39/CD73) [45]. Such extracellular metabolites contribute to a tolerogenic microenvironment that suppresses the activation of bystander effector T cells and antigen-presenting cell activation. Hence, IL-2 not only controls the intracellular transcriptional and metabolic programs of Tregs but also directs the remodeling of the extracellular immunological landscape, establishing a multilayered network of immune regulation.

Tissue Residency and Exosomal Communication

Emerging evidence indicates that IL-2 signaling extends beyond systemic immune regulation to spatially confined tissue microenvironments [46]. Tissue-resident Tregs (TR-Tregs) in non-lymphoid organs including salivary gland, lung, skin, and skeletal muscle exhibit distinct transcriptomic signatures characterized by high IL2RA and IL1RL1 (ST2) expression. These TR-Tregs not only suppress inflammation but also participate in tissue repair through secretion of amphiregulin and growth factors [47-50]. The density and functional activity of TR-Tregs are critically dependent on local IL-2 availability, which can be derived from tissue dendritic cells, natural killer (NK) cells, or exogenous low-dose IL-2 therapy. In murine models of Sjögren's-like exocrinopathy and arthritis, targeted delivery of IL-2 to glandular or joint tissues enhances Treg accumulation, reduces Th17 infiltration, and restores tissue integrity [51-53], highlighting the therapeutic potential of spatially restricted cytokine modulation.

A novel mechanism of IL-2-mediated communication involves extracellular vesicles (EVs) and exosomes. Activated T cells and stromal cells can package IL-2 and IL-2 receptor subunits into exosomes, forming a localized cytokine delivery system that extends the half-life and range of IL-2 signaling. Furthermore, Treg-derived exosomes carry immunoregulatory molecules such as CTLA-4, LAG-3, and miRNAs (miR-155, miR-21) that further suppress effector responses [54-56]. Recent studies suggest that Ld-IL-2 treatment enhances the production of these Treg exosomes, which can be detected in peripheral circulation and correlate with clinical remission in autoimmune diseases [57-60]. Such findings open a new dimension of intercellular communication where IL-2 not only acts as a soluble cytokine but also as a cargo within vesicular networks shaping the immune micro-environment.

These insights into tissue-specific IL-2 biology are informing the development of next-generation therapeutic formulations. Engineered delivery systems such as biomaterial-based slow-release microspheres and exosome-hybrid nanocarriers can deliver IL-2 directly to inflamed sites, maintaining effective local concentrations while minimizing systemic exposure [61]. This approach recapitulates the natural activity of IL-2 within tissue niches and enhances the functional persistence of resident Treg populations. Together, these mechanistic insights demonstrate that Ld-IL-2 acts not as a simple proliferative molecular but as a multidimensional signal integrating receptor affinity, epigenetic stability, metabolic fitness, and tissue-specific microenvironmental context to achieve precise immune rebalancing.

Systemic and Cellular Effects Beyond Tregs

The therapeutic efficacy of Ld-IL2 is initiated by its high-affinity binding to Tregs but culminates in the systemic recalibration of immunity. This stems from a coordinated reprogramming of the immune landscape, inhibiting effector T-cell and B-cell responses, while simultaneously regulating the homeostasis of innate and cytotoxic lymphocytes. The following discussion details how Ld-IL-2 integrates these multi-cellular processes to re-establish systemic immune tolerance (Table 1).

The Treg–Th17/Tfh Counter-regulatory Axis

The pathogenesis of autoimmune inflammation frequently involves a dysregulated balance between immunosuppressive regulatory T (Treg) cells and pathogenic T helper 17 (Th17) and T follicular helper (Tfh) cells. Th17 cells produce IL-17A, IL-21 and GM-CSF, driving tissue infiltration and neutrophil recruitment, whereas Tfh cells promote B-cell activation and autoantibody production [62-64]. The reciprocal relationship among these subsets is strongly regulated by interleukin-2 (IL-

2) signaling.

At the molecular level, IL-2 serves as a potent negative regulator of Th17 and Tfh differentiation. Low dose of IL-2 selectively activates STAT5, which competitively antagonizes STAT3 at key genomic loci, including the promoters of IL17A and the Tfh master regulator BCL6, thereby suppressing the transcriptional programs for inflammatory cytokines and Tfh lineage genes [65-67]. Consequently, Ld-IL-2 not only promotes Treg stability but also actively constrains the differentiation of Th17 and Tfh lineages. This dual mechanism yields a synergistic anti-inflammatory effect: Treg-derived IL-10 and TGF-β suppress residual Th17 activity, while the concomitant reduction in Tfh-derived IL-21 reduces B-cell stimulation and autoantibody generation [68-69].

Clinical and pre-clinical evidence consistently support this mechanistic framework. In patients with systemic lupus erythematosus (SLE) and Sjögren's disease (SjD), Ld-IL-2 therapy consistently increases circulating Treg numbers while concomitantly reducing the frequencies of Th17 and T follicular helper (Tfh) cells, resulting in improvements in disease activity [8-9, 70-71]. Corresponding observations in various mouse models demonstrate that these changes correlate with suppressed germinal center reactions and decreased autoantibody titers [72-73]. Thus, by modulating the Treg–Th17/Tfh axis, Ld-IL-2 effectively redirects the adaptive immune response from a pathogenic inflammatory state toward controlled tolerance.

The suppression of Th17/Tfh pathways exhibits a clear dose-dependency. At an optimal low dose (approximately 1 million IU), IL-2 robustly expands the Treg compartment without significantly activating effector T cells (Teffs) [7, 60, 74]. In contrast, higher doses (> 3 M IU) can lead to the partial activation of effector pathways, reflecting the biphasic response to IL-2 that has been documented in clinical dose-related studies [10]. Therefore, precise dose decision is essential to retain the desired balance between regulatory and effector immunity.

CD8$^+$ T-cell Regulation and Memory-like Differentiation

Beyond CD4$^+$ T cells, IL-2 also plays a crucial role in the cytotoxic compartment. Ld-IL-2 preferentially expands a distinct population of CD8$^+$CD122$^+$ memory-like T cells that express intermediate-affinity IL-2 receptors (CD25) [75-76]. This subset is transcriptionally defined by the concurrent upregulation of Eomesodermin (Eomes) and the anti-apoptotic protein Bcl-2, a molecular signature that supports their long-term persistence and confers a regulated cytotoxic potential, without inducing excessive tissue damage [77-79].

Mechanistically, Ld-IL-2 engages the βγ receptor complex (CD122/CD132) on these cells to promote homeostatic proliferation and IL-10 production, contributing to the resolution of inflammation [80-82]. Furthermore, IL-2 modulates the memory differentiation pathway of CD8$^+$ cells. Continuous low-level signaling via STAT5 favors a central-memory phenotype (CD62L$^+$CCR7$^+$) over short-lived effector cells [83-84]. This phenotype ensures a rapid but non-pathogenic response upon secondary antigen exposure, which is especially relevant for patients with chronic viral infections or immune deficiency associated with autoimmunity. Collectively, these findings illustrate how Ld-IL-2 fine-tunes the cytotoxic arm of immunity to support immune equilibrium rather than immunosuppression.

Modulation of NK Cell Activity and Innate Immunity

Natural killer (NK) cells represent a pivotal innate immune target of IL-2. Constitutively expressing the intermediate-affinity IL-2 receptor βγ complex (CD122/CD132), NK cells respond to both high- and low-dose IL-2, albeit with divergent functional consequences [85-86]. At low doses, IL-2 preferentially enhances the CD56^{bright} regulatory NK subset that produces IL-10 and modulates antigen-presenting cells [85, 87-90]. These cells exhibit reduced cytotoxic activity but increased immunoregulatory potential, providing an additional layer of immune control.

Experimental studies show that Ld-IL2 upregulates the expression of inhibitory receptors such as NKG2A and CD94 on NK cells, thereby raising the threshold for activation and preventing excessive cytolytic activity, while preserving critical antiviral functions like interferon-gamma (IFN-γ) secretion [91-92]. This "calibrated activation" state supports tissue repair and homeostasis as high-dose IL-2 triggers the expansion of CD56^{dim} cytolytic NK cells, which can exacerbate tissue damage and cytokine toxicity [93]. Thus, the NK cell response mirrors the dose-dependent duality of IL-2 seen in T cells.

Furthermore, IL-2 indirectly modulates innate immunity through Treg-educated mechanisms. Tregs expanded by Ld-IL-2 secrete copious amounts of IL-10 and TGF-β, which skew macrophage polarization toward an M2-like, tissue-reparative phenotype and restrain the pro-inflammatory capacity of dendritic cells [94-95]. This cascade establishes a positive feedback loop in which innate cells further support Treg maintenance and local IL-2 availability, stabilizing the immunological microenvironment.

Such innate re-education may explain the clinically favorable infection profile associated with Ld-IL-2 therapy. Unlike

Table 1. Differential effects of IL-2 on immune cell subsets and functional outcomes.

Cell Subset	IL-2 Receptor Expression	Response to Low-dose IL-2	Functional Effect	Impact on Immune Homeostasis
Treg (CD4$^+$ CD25$^+$ FOXP3$^+$)	CD25 high CD122$^+$ CD132$^+$	Strong activation (↑ STAT5)	↑ Suppressive cytokines (IL-10, TGF-β)	Restores tolerance
Teff (CD4$^+$ effector)	CD25 low	Minimal effect	↓ IFN-γ production	Reduces inflammation
Th17	CD25 low	Indirect inhibition via Treg	↓ IL-17 output	Prevents autoimmunity
Tfh	CD25 low	Suppressed	↓ B cell help	Decreases autoantibody
CD8$^+$ memory-like T	CD122 high	Moderate activation	↑ Cytotoxic homeostasis	Enhances infection control
NK cells	CD122 high	↑ Survival and cytotoxicity	Balanced innate response	Maintains immune surveillance

broad-spectrum immunosuppressants which increase susceptibility to opportunistic infections, Ld-IL-2 has not been linked to elevated infection rates in clinical trials [73, 96-98]. It enhances mucosal barrier immunity and NK-mediated viral clearance. These observations underscore that precision cytokine therapy can restore tolerance without compromising host defense.

Integrated Network of Immune Homeostasis

Ld-IL2 develops a coordinated recalibration of the immune system by engaging regulatory T cells (Tregs), effector T cells, cytotoxic lymphocytes, and innate subsets within an integrated network of homeostatic control [99]. Rather than acting as a generalized immunosuppressant, Ld-IL-2 restores a dynamic equilibrium that preserves immune surveillance while restraining autoimmunity. This fine-tuned network operates through multiple interdependent layers.

At the signaling level, regulatory T cells (Tregs) express high-affinity IL-2Rαβγ complexes, which allow them to efficiently respond to low concentrations of IL-2 and establish a hierarchical access to this cytokine [4, 16, 100]. Through this preferential capture of IL-2, Tregs act as a critical sink that shapes the cytokine landscape and modulates effector cell activation thresholds. In parallel, feedback mechanisms reinforce this dominance as Tregs secrete IL-10 and generate adenosine through the CD39/CD73 axis, suppressing effector and antigen-presenting cell (APC) activation while limiting IL-2 consumption by competing lymphocyte subsets [101]. These negative feedback loops sustain the regulatory pool and prevent exhaustion of the cytokine niche. Beyond local regulation, cross-compartmental communication connects systemic and tissue-localized tolerance programs [102]. Tregs communicate with innate immune cells via cytokines, exosomes, and metabolites, thereby synchronizing peripheral and organ-specific tolerance.

Through these integrated mechanisms, low-dose IL-2 acts as a biological "immune thermostat," recalibrating the immune setpoint toward tolerance rather than non-selective suppression, in contrast to conventional immunosuppressive strategies that broadly inhibit immune activity [12].

Conceptual Implications

The systemic immunomodulatory effects of Ld-IL-2 suggests that regulatory immunity is not confined to a single cell type but arises from a dynamically integrated network of interdependent signals. Ld-IL-2 operates by coordinately stabilizing the regulatory T cell (Treg) compartment while concurrently reprogramming the function of effector T cells and innate immune populations [4, 12]. This understanding has shifted the therapeutic paradigm from cytokine replacement to cytokine re-tuning, using low and precisely calibrated doses to activate selective pathways that restore systemic balance [103].

The consistent clinical benefits observed with Ld-IL-2 across a spectrum of autoimmune diseases, from systemic lupus erythematosus to alopecia areata, provide compelling translational validation for this network-centric view of immune homeostasis [104-108]. Consequently, Ld-IL-2 is rationally viewed as the foundational therapeutic agent in the emerging discipline of precision immunorebalancing, a field dedicated to the targeted restoration of immune homeostasis rather than its broad suppression.

Clinical Translation of Low-dose IL-2 Therapy

Dose-dependent biphasic responses and therapeutic window

The translational development of Ld-IL2 is rooted in its biphasic dose-response immunobiology. Pioneering oncology studies using high-dose IL2 (> 10 MIU/day) demonstrated potent anti-tumor immunity but were hampered by severe toxicity, including vascular leak syndrome, due to excessive activation of effector T and NK cells. In contrast, experimental immunology revealed that picomolar concentrations (0.3–3 MIU) selectively expand Tregs without activating pro-inflammatory Teff activation or systemic inflammation (Figure 2) [10]. This bell-shaped relationship defines a narrow therapeutic window that is central to precision cytokine therapy [103, 109].

Figure 2. Dose-dependent biphasic effects of IL-2 on Treg cells.
Low-dose IL-2 induces a selective, dose-dependent expansion of $CD4^{+}$ $CD25^{hi}$ $Foxp3^{+}$ Tregs through engagement of the high-affinity IL-2Rαβγ complex, with maximal response at approximately 1×10^{6} IU. Higher doses may activate conventional T (Tconv) and NK cells, thereby diminishing Treg selectivity and shifting the immune balance toward activation.

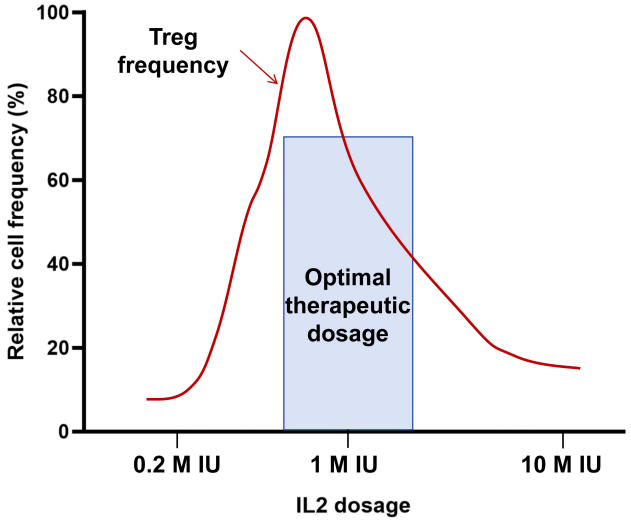

This selective effect is mechanistically controlled by differential sensitivity to IL-2. Tregs, owing to their constitutive expression of the high-affinity IL-2 receptor α-chain (CD25) and a primed JAK-STAT signaling apparatus, activate STAT5 at concentrations 100- to 300-fold lower than those required by Teffs [110-111]. Clinically, trials comparing 1 MIU versus 3 MIU dosing confirm this principle, demonstrating that a dose of 1 MIU optimally expands Tregs and yields clinical improvement with minimal adverse events, whereas a 3 MIU dose can induce transient Teff activation and associated side effects like fatigue [8, 10, 105, 112]. Importantly, pharmacodynamic analyses further demonstrate that serum IL-2 concentrations return to baseline within hours after Ld-IL-2 administration, allowing physiologic cycling of Treg signaling without receptor desensitization.

Longitudinal data reveal that the degree of Treg expansion is a strong predictor of clinical efficacy, with patients achieving a doubling (≥200%) in Treg frequency typically exhibiting sustained disease remission, supporting Treg frequency as a phar-

macodynamic biomarker for dose optimization [60, 71, 113]. These quantitative data provide a foundation for precision dosing models integrating IL-2 pharmacokinetics, baseline Treg status, and cytokine network feedback.

Clinical evidence across autoimmune diseases

Systemic Lupus Erythematosus (SLE)

SLE represents the prototype disease in which Ld-IL2 therapy has demonstrated consistent efficacy. Multiple open-label and randomized trials have reported significant improvements in SLEDAI scores accompanied by marked Treg expansion. In our multicenter double-blind phase IIb trial (NCT04077684), patients receiving 1 MIU IL-2 for 5 consecutive days per cycle showed a 2.2-fold increase in Treg frequency and a mean 4-point reduction in SLEDAI after 12 weeks [8, 60, 108, 114-115]. Transcriptomic profiling revealed down-regulation of type-I interferon-responsive genes and normalization of IL-21 and CXCL13 signatures, reflecting suppression of Tfh-driven autoantibody production [72, 116]. The favorable safety profile was confirmed, with only mild adverse events (fatigue, transient erythema < 5%) and no increased infection risk.

Primary Sjögren's Disease (SjD)

In Sjögren's disease, Ld-IL-2 has shown promise as a disease-modifying therapy capable of restoring immune balance and exocrine gland function. A prospective study in 30 patients demonstrated that treatment significantly increased the Treg/Th17 ratio and improved unstimulated salivary flow rates following two cycles [9]. Flow cytometric analysis showed preferential expansion of $CCR4^{+}$ $CXCR5^{-}$ Tregs and reduction of circulating Tfh cells. These immunological changes were associated with clinical benefit, as evidenced by a >3-point reduction in ESSDAI scores in 70% of participants. These findings suggest that Ld-IL2 can effectively modulate the local immune microenvironment in target tissues, consistent with tissue-resident Treg accumulation observed in experimental models. Importantly, the improvements in lacrimal and salivary function were correlated with molecular signatures of reduced IL-17 and BAFF pathways.

Relapsing Polychondritis (RP)

Relapsing polychondritis (RP), a rare autoimmune disorder characterized by steroid-dependent cartilage inflammation, presents a compelling target for Ld-IL-2 therapy [117]. In our exploratory open-label trial (n = 9), 1 MIU IL-2 for 5 days per cycle led to rapid symptom improvement within two weeks, with normalization of C-reactive protein (CRP) levels and Relapsing Polychondritis Disease Activity Index (RPDAI) scores in the majority of patients. Immunological responses confirmed selective Treg expansion and a concomitant reduction in activated $CD4^{+}CD69^{+}$ T cells. These findings provide initial clinical proof-of-concept that Ld-IL-2 can effectively control autoimmune-mediated cartilaginous inflammation without inducing broad immunosuppression.

Type 1 Diabetes and Other Conditions

The application of Ld-IL-2 extends to other autoimmune contexts. In new-onset type 1 diabetes, therapy aims to preserve residual β-cell function, with studies showing that Ld-IL-2 can increase Treg frequency and stabilize C-peptide levels [10, 118]. Promising pilot data in autoimmune vasculitis and hepatitis further underscore its potential as a broad-spectrum immunomodulator [119-120]. Collectively, across this spectrum of diseases, Ld-IL-2 consistently achieves a quantifiable restoration of Treg populations (typically a 150–250% increase) and delivers clinically meaningful disease amelioration with a minimal toxicity profile.

Safety and tolerability profile

The collective safety data from over 600 patients treated with Ld-IL-2 worldwide reveal an exceptionally favorable profile (Table 2). The most common adverse events are mild and transient, including injection-site reactions, fatigue, and mild nausea, with an incidence generally below 10%. Critically, no grade ≥2 cytokine-release syndrome or treatment-related serious infections have been consistently reported, and routine laboratory parameters (e.g., hepatic and renal function) remain stable. Immune monitoring confirms that Ld-IL-2 does not compromise protective immunity, as evidenced by preserved antiviral NK-cell function and vaccine responses [121]. These results contrast with that of conventional immunosuppressants and underscores the fundamental distinction between precise immune recalibration and generalized immunosuppression.

Innovative formulations and delivery strategies

Topologically engineered IL-2 variants

Advances in protein engineering have yielded a newly developed IL-2 variants designed to achieve superior cellular selectivity [122-124]. These molecules are engineered by our group to retain high affinity for the CD25 (IL-2Rα) subunit while attenuating binding to CD122 (IL-2Rβ), thereby favoring signaling through the high-affinity receptor complex predominantly expressed on Tregs. This design not only enhances Treg selectivity but also often extends serum half-life, mitigating the need for frequent dosing. Preclinical studies with such variants have demonstrated sustained Treg expansion for over five days, positioning them as promising second-generation candidates for long-acting immune recalibration.

Sustained-release biomaterial platforms

To address the inherently short plasma half-life of native IL-2, significant efforts have been directed toward developing sustained-release delivery systems. Biodegradable polylactic-acid (PLA) microspheres can encapsulate IL-2 and provide controlled release of the bioactive cytokine over 72 to 96 hours, maintaining stable, physiologic concentrations and avoiding the peaks associated with toxicity [125]. Further sophistication is achieved by combining these microspheres with Treg-targeting exosomes to create hybrid complexes, which can facilitate the targeted delivery of IL-2 to inflamed tissues such as salivary glands or joints. This approach achieves localized Treg reconstitution and tissue repair with negligible systemic exposure. Pre-clinical data demonstrate marked reduction of inflammatory cell infiltration and enhanced tissue integrity in models of Sjögren-like syndrome and arthritis.

Localized delivery and minimally invasive routes

Given the emerging importance of tissue-resident Tregs, local subcutaneous or periglandular administration is being explored. Preliminary clinical studies from our group indicate that parotid region micro-injection achieves regional Treg accumulation and amelioration of glandular inflammation in SjD patients. Such approaches leverage physiological IL-2 gradients within tissue niches and hold the potential to reduce systemic dose requirements. Together, these formulation and delivery innovations represent the translational frontier of precision cytokine therapy.

Biomarkers and precision monitoring

The translational development of Ld-IL2 has been greatly facilitated by the evolution of quantitative immunomonitoring assays. Flow cytometric measurement of $CD25^+CD127^{low}FOXP3^+$ Tregs remains the gold-standard biomarker, but emerging omics approaches providing unprecedented resolution [126-127]. Single-cell RNA and TCR sequencing have identified distinct Treg clonotypes expanding after therapy, while epigenetic analyses of FOXP3 locus demethylation (e.g., TSDR methylation status) allow for longitudinal tracking of Treg lineage stability [128-130]. Circulating exosomal IL-2 and microRNA signatures (miR-155, miR-21) correlate with clinical response and may serve as minimally invasive surrogate biomarkers [131]. The integration of these multidimensional data into AI-driven models is poised to enable personalized dose optimization and prediction of long-term treatment efficacy.

Comparative advantages over traditional immunosuppression

Ld-IL-2 possesses distinct mechanistic and clinical advantages over conventional broad-spectrum immunosuppressants. Unlike these agents, which non-specifically inhibit lymphocyte activation or proliferation, Ld-IL-2 acts by selectively regulating the immune system. This mechanistic precision underlies several distinct clinical advantages as Ld-IL2 restored physiological tolerance through a normalized Treg-to-effector T cell balance and preserved antimicrobial immunity stemming from maintained NK and memory $CD8^+$ T cell activity. The re-establishment of a stable immune set-point underpins the potential for achieving drug-free remission in certain individuals. These distinctive properties collectively position Ld-IL-2 not as a mere immunosuppressant, but as a pioneering agent for immune reconstruction.

Future perspectives in translational design

The future trajectory of Ld-IL-2 therapy lies in the development of integrated platforms that synergize engineered cytokine variants, advanced biomaterial-based delivery systems, and

Table 2. Major clinical trials and observational studies of low-dose IL-2 in autoimmune diseases.

Disease	Study Type / Year	Sample Size	Dose (million IU) / Schedule	Clinical Outcome	Safety Profile
SLE	Double-blind RCT [8] (NCT02465580 and NCT02932137)	60	1×every other day for 2 weeks and followed by a 2-week break /cycle	Improved SRI-4 response rate	Lower incidence of infection
SLE	Multicenter Phase II RCT [108] (NCT02955615)	100	1.5 daily × 5 days, then weekly	SLEDAI −5.1; reduced flares	Transient fatigue (5%)
SLE	Ongoing Phase II (Unpublished; NCT04077684)	80	0.2–1 dose every other day × 12 weeks, then weekly for 12 weeks	Improved SRI-4 response	Well tolerated
pSS	Randomized trial [9]	30	1×every other day for 2 weeks and followed by a 2-week break /cycle	ESSDAI −3	No serious AEs and lower infection risk
RP	Pilot RCT (Unpublished; NCT04077736)	10	1 × 5 days, then weekly	RPDAI −9;	No AEs
T1DM	DILT1D trial (NCT01827735)[112]	40	0.04×106 to 1.5×106 IU/m2 daily	Increases in Treg frequencies	None reported
T1DM	Phase I/II RCT (DILfrequency, NCT01353833) [10]	24	0.3–3 × 5 days, adaptive dosing	↑ β-cell function; ↓ HbA1c	no serious AEs
GVHD	open-label (NCT01517347) [152]	90	1.0 × 106 IU/ m2 daily× 14 days	Minimal residual disease-positive	None reported
GVHD	observational cohort (NCT00529035) [7]	29	0.3/ 1/3× 106 IU/ m2 × 8 weeks	preferential, sustained Treg cell expansion	None reported
Alzheimer's disease	Phase 2a RCT (NCT06096090) [153]	38	1.0 × 106 IU/day×21 weeks	CSF Aβ42 levels ↑	None reported
Amyotrophic lateral sclerosis	MIROCALS study (NCT03039673) [154]	304	2 × 106 IU/day× 5 days	Decrease in risk of death	No serious AEs
Bullous pemphigoid	Perspective study (ChiCTR2000028707) [97]	43	half million IU every other day × 8 weeks	Shorter disease control time	No serious infections

digital immunomonitoring (Figure 3 and Table 3). Multi-omics profiling can define patient-specific immune signatures that predict responsiveness to IL-2. Strategic combinations of Ld-IL-2 with other immunomodulators [75, 96, 132-134] including JAK inhibitors, microbiome-derived metabolites, or belimumab may achieve synergistic efficacy by concurrently targeting complementary pathways. Ultimately, the goal is to develop a personalized immunotherapy ecosystem where cytokine dosing is dynamically optimized based on real-time immune feedback, thereby transforming Ld-IL-2 from a disease-specific intervention into a universal platform for restoring immune homeostasis across autoimmunity, chronic inflammation, and transplantation medicine.

Treg modification and clinical practice

Maintaining long-term Treg stability

The durability of Treg-mediated immune tolerance depends on the sustained expression and epigenetic stability of FOXP3. Under inflammatory or metabolic stress, Tregs can undergo functional reprogramming—often termed "Treg plasticity"—characterized by loss of FOXP3 expression and acquisition of pro-inflammatory, effector-like properties [135-136]. In chronic autoimmune diseases, pro-inflammatory cytokines such as IL-6, IL-1β, and TNF-α contribute to this instability by disrupting STAT5 signaling and modifying the chromatin landscape at the FOXP3 locus, thereby impairing its transcription [137]. Consequently, a subset of expanded Tregs may adopt pathogenic effector or Th17-like phenotypes, ultimately compromising the durability of therapeutic responses.

To address this challenge, several strategies are under exploration. Optimized dosing regimens, such as periodic administration of Ld-IL-2, may better support Treg lineage stability than continuous exposure, as intermittent pulses mimic physiological cytokine exposure [8, 59, 70]. Combining Ld-IL-2

Figure 3. Engineered IL-2 variants and targeted delivery strategies. (**A**) Topological Engineered IL2 Variants. Rational IL2 mutation to reduce IL-2Rβ affinity while preserving IL-2Rα binding, achieving CD25-biased agonists with enhanced Treg selectivity, prolonged half-life, and higher stability. (**B**) Targeted Delivery for Sustained Release. A hybrid nanoparticle platform combining PLA microspheres and exosomes enables designed for controlled IL-2 release, maintaining therapeutic concentrations within the selective window. (**C**) Tissue-Selective Immunomodulation. Local injection including salivary, gland and joint concentrates IL-2 at sites of inflammation, maximizing Treg enrichment and resulting in reduced inflammation with limited systemic toxicity.

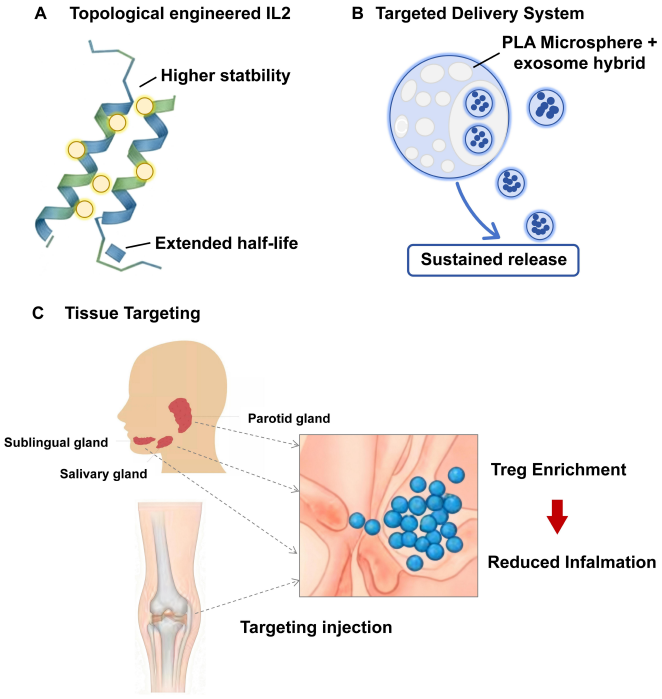

Table 3. Summary of engineered IL-2 variants and delivery systems.

Approach	Design Feature	Mechanistic Advantage	Pre-clinical Outcome	Translational Potential *1
Topological engineered IL-2	Reduced CD122 binding, retained CD25 affinity	Enhanced Treg selectivity	Prolonged half-life (> 48 h)	Phase I preparation
PEGylated IL-2 [122]	PEG chain modification	Reduced renal clearance	Improved AUC × 3	Safety proven
IL2-4M-PEG [155]	Substitute amino acids and implement site-directed PEGylation	reduced CD25 binding activity and an extended half-life	Amplify effector cells	Enhance combined cancer therapies
IL-2/anti-IL-2 complex	Transient complex with anti-IL-2 mAb	Directed Treg bias	↑ Treg/Teff ratio	Translatable
Pegylated rhIL-2 (SAR444336) [156]	Site-specifically pegylated form	enhanced PK and induced Tregs	reduced stimulation of off-target effector T and NK cells	Reduced inflammation in a delayed-type hypersensitivity model
PD1-IL2v [61]	Antibody-cytokine fusion proteins	Expansion of CD8+ and Tconv cells	↑ cytotoxic CD8+ T cells	Next-generation immunocytokines
PLA microsphere system [157]	Slow-release (>72h)	Sustained serum level	Stable Treg expansion	Ready for pilot test
IL-2 mutein [158]	Fc-fused homodimer	reduced potency and enhanced Treg cell selectivity	Preferential Treg cell enrichment	Strong future potential
Exosome nanocarrier	Natural membrane vector	Targeted tissue delivery	Localized immunomodulation	Strong future potential

with therapies that reinforce FOXP3 stability—such as low-dose rapamycin, histone deacetylase (HDAC) inhibitors, or metabolic modulators targeting the AMPK-mTOR pathway—has shown synergistic effects in preclinical studies. Advances in synthetic biology also allow enforced FOXP3 expression or CRISPR-mediated editing of important enhancer regions to generate functionally stabilized Treg cells. These engineered cellular therapies, while technically demanding, hold promise for achieving durable immune tolerance that persists beyond transient cytokine stimulation.

Inter-individual variability and biomarker-guided precision dosing

Substantial inter-individual heterogeneity in response to standardized Ld-IL2 regimens has emerged as a key challenge in the clinic. This variability is influenced by genetic and immunological factors, including polymorphisms in genes such as IL2RA, STAT5B, and PTPN2, which can alter IL-2 receptor sensitivity and downstream signaling fidelity [138-141]. Furthermore, baseline immunological responses including the frequency and activation state of regulatory T cells (Tregs) vary considerably across different autoimmune diseases, contributing to divergent therapeutic outcomes [7, 106, 109].

Addressing this variability requires the development of quantitative biomarkers for real-time dose adjustment. The Treg/Teff ratio and absolute Treg counts serve as practical, short-term pharmacodynamic markers. These include the analysis of FOXP3 Treg-specific demethylated region (TSDR) methylation status, measurement of serum IL-2 trough levels, and assessment of phospho-STAT5 induction dynamics in responsive cell populations. Integrating these measurements into algorithm-driven dosing models could enable personalized treatment cycles that maintain each patient within their optimal "immune tolerance window." Ultimately, artificial intelligence platforms that synthesize longitudinal immunophenotyping, cytokine pharmacokinetics, and clinical data are expected to make precision dosing a practical reality.

Optimization of cytokine delivery and tissue targeting

The therapeutic application of native interleukin-2 (IL-2) is constrained by its rapid clearance from plasma, with a half-life of merely 5-10 minutes, and its non-specific tissue distribution. These properties limit its efficacy in autoimmune conditions where pathology is confined to specific organs. A central objective in the field is, therefore, to achieve sustained, localized cytokine exposure while minimizing systemic diffusion and associated off-target effects. Innovative biomaterial-based delivery systems offer a promising strategy to overcome these limitations. Platforms such as poly (lactic acid) (PLA) microspheres, hydrogel depots, and exosome-hybrid nanocarriers are designed to provide controlled release of IL-2, thereby extending its in vivo bioavailability, reducing the frequency of administration, and facilitating enhanced accumulation at target sites [142-143].

A more advanced approach involves the development of formulations engineered for local activity within particular organs [144]. Periglandular injection of microsphere-encapsulated IL-2 has been shown to enrich Tregs locally and restore salivary function in models of Sjögren's disease, while intra-articular delivery holds potential for managing rheumatoid arthritis by modulating the joint microenvironment [145-147]. Combining spatial targeting with molecular engineering like topological IL-2 variants exhibiting selective CD25 binding could maximize therapeutic precision and minimize systemic effects [124]. The successful clinical translation of these sophisticated bio-engineered biologics will be closely tied to the ongoing evolution of regulatory frameworks tailored to assess their unique profiles.

Balancing immune tolerance and host defense

An inherent challenge of all immunomodulatory strategies is preserving protective immunity while inducing tolerance. Although clinical trials have not reported increased infection rates with Ld-IL-2, long-term surveillance is warranted, particularly in immunocompromised patients. Maintaining the functional capacity of natural killer (NK) cell and memory $CD8^+$ T cell activity is crucial for robust antiviral and anti-tumor surveillance [76, 77, 82, 86]. Future therapeutic protocols could incorporate adaptive dosing strategies informed by real-time biomarkers of these effector functions, such as NK cell interferon-gamma (IFN-γ) production or $CD8^+$ T cell granzyme B levels, to dynamically ensure that host defense remains uncompromised.

In parallel, the interplay between Ld-IL-2 and other immunotherapeutic modalities, such as vaccination and cancer immunotherapy, presents a compelling area for future investigation [4]. Emerging evidence suggests that intermittent Ld-IL2 could enhance vaccine responses by preserving immune memory, while engineered IL-2 antagonists or dual-function molecules may allow temporal toggling between tolerance and activation depending on clinical context [124].

Integrating multi-omics and system immunology

The complexity of IL-2 signaling networks calls for comprehensive multi-omics approaches to fully delineate its impact on the immune system. Single-cell transcriptomics, chromatin accessibility mapping, and proteomics have already delineated the cellular heterogeneity of Treg and Teff subsets responding to Ld-IL-2 [148]. Integrating these datasets with metabolomic profiles and microbiome analysis will yield a more holistic understanding of the cytokine-induced remodeling of immune homeostasis. Subsequently, systems immunology frameworks can leverage this integrated information to identify predictive molecular modules associated with clinical response and resistance, thereby informing the development of rational combination therapies and novel biomarker discovery [149].

This systems-level insight paves the way for rationally designed combination strategies. As co-administration of Ld-IL-2 with microbiota-derived short-chain fatty acids, which are known to promote Treg generation and function through epigenetic and metabolic mechanisms, could synergistically enhance immune tolerance [150]. Similarly, combining Ld-IL-2 with agents that neutralize type I interferon signaling may suppress the inflammatory condition that undermines Treg stability in certain autoimmune diseases [151]. Such "rational combination immunotherapies" embody the principle of precision immunorebalancing, aiming to recalibrate entire pathological networks rather than isolated targets.

Future design of next-generation IL-2 therapeutics

The future of IL-2-based therapy is set to be defined by the convergence of advanced protein engineering, computational design, and intelligent delivery. Next-generation IL-2 variants

are being engineered with structural modifications that precisely control receptor subunit bias—favoring CD25 for Treg selectivity—while simultaneously improving pharmacokinetic profiles and enabling effective signaling at near-physiological concentrations. Conjugation with antibody fragments or Fc domains may extend half-life, while fusion with targeting moieties (e.g., chemokine receptors, integrins) could direct cytokine activity to inflamed tissues.

Beyond protein modifications, novel delivery platforms using programmable RNA or DNA vectors encoding the IL-2 sequence present a transformative approach. These systems could enable endogenous, in vivo production of the cytokine under the regulation of tunable promoters, offering a pathway for sustained yet reversible immune modulation. The ultimate integration of these sophisticated molecular tools with biocompatible delivery systems and real-time immune monitoring is poised to give rise to a new class of "smart cytokines," capable of dynamically adapting their activity to the evolving immunological state of the patient.

Conclusion

Low-dose IL-2 has transformed from a conventional cytokine into precision immunomodulation, demonstrating that immune responses can be selectively and restoratively recalibrated rather than broadly suppressed. The coming decade will likely see this approach mature into a mainstream clinical modality. Its sustained success will rest on three critical pillars: a deepening mechanistic understanding of Treg biology, relentless technological innovation in cytokine design and delivery, and the implementation of data-driven personalization strategies. By systematically addressing the remaining challenges including stability, variability, and precise tissue targeting, Ld-IL-2 has the potential to evolve from a promising biological therapy into a cornerstone of immune-tolerance medicine, reshaping therapeutic strategies across autoimmunity, transplantation, and chronic inflammatory diseases.

Abbreviation

Tregs: Regulatory T cells; pTregs: peripherally induced Tregs; TR-Tregs: Tissue-resident Tregs; Ld-IL-2: low-dose interleukin-2; NK cell: natural killer cell; Th17: T helper 17; Tfh: T follicular helper; Teffs: effector T cells; SLE: Systemic lupus erythematosus; Bcl-2; B cell lymphoma 2; TSDR: Treg-specific demethylated region; DNMT: DNA methyltransferase; OXPHOS: oxidative phosphorylation; AMPK: AMP-activated protein kinase; ROS: reactive-oxygen-species; SAM: S-adenosylmethionine; EVs: extracellular vesicles; IFN-γ: interferon-gamma; APC: antigen-presenting cell; RP: Relapsing polychondritis; CRP: C-reactive protein; RPDAI: Relapsing Polychondritis Disease Activity Index; PLA: polylactic-acid; HDAC: histone deacetylase.

Author Contributions

Ruiling Feng: writing original draft, prepare, create, or express the content for publication, especially in writing the initial draft. Bo Huang and Xia Zhang: writing review and editing, prepare, create, or express the content for publication, especially in writing the initial draft. Jing He: supervision, supervise and lead the planning and execution of research activities.All authors read and approved the final manuscript.

Acknowledgements

Not Applicable.

Funding Information

This study was funded by National Key Research and Development Program of China (2022YFE0131700), National Natural Science Foundation of China (82271835, 82071813).

Ethics Approval and Consent to Participate

Not Applicable.

Competing Interests

The authors declare that they have no known competing financial interests or personal relationships that could have appeared to influence the work reported in this paper.

Data Availability

All data needed to evaluate the conclusions in the paper are present in the paper. Additional data related to this paper may be requested from the authors.

References

[1] Morgan DA, Ruscetti FW, & Gallo R. (1976). Selective in vitro growth of T lymphocytes from normal human bone marrows. Science, 193(4257), 1007-1008. https://doi.org/10.1126/science.181845

[2] Rosenberg SA. (2014). IL-2: the first effective immunotherapy for human cancer. J Immunol, 192(12), 5451-5458. https://doi.org/10.4049/jimmunol.1490019

[3] Hu W, Dolsten GA, Wang EY, Beroshvili G, Wang ZM, Ghelani AP, et al. (2025). Temporal and context-dependent requirements for the transcription factor Foxp3 expression in regulatory T cells. Nat Immunol, 10.1038/s41590-025-02295-4. https://doi.org/10.1038/s41590-025-02295-4

[4] Boyman O, & Sprent J. (2012). The role of interleukin-2 during homeostasis and activation of the immune system. Nat Rev Immunol, 12(3), 180-190. https://doi.org/10.1038/nri3156

[5] Wang X, Rickert M, & Garcia KC. (2005). Structure of the quaternary complex of interleukin-2 with its alpha, beta, and gammac receptors. Science, 310(5751), 1159-1163. https://doi.org/10.1126/science.1117893

[6] Overwijk WW, Tagliaferri MA, & Zalevsky J. (2021). Engineering IL-2 to Give New Life to T Cell Immunotherapy.

Annu Rev Med, 72, 281-311. https://doi.org/10.1146/annurev-med-073118-011031
[7] Koreth J, Matsuoka K, Kim HT, McDonough SM, Bindra B, Alyea EP, 3rd, et al. (2011). Interleukin-2 and regulatory T cells in graft-versus-host disease. N. Engl. J. Med., 365(22), 2055-2066. https://doi.org/10.1056/NEJMoa1108188
[8] He J, Zhang R, Shao M, Zhao X, Miao M, Chen J, et al. (2020). Efficacy and safety of low-dose IL-2 in the treatment of systemic lupus erythematosus: a randomised, double-blind, placebo-controlled trial. Ann. Rheum. Dis., 79(1), 141-149. https://doi.org/10.1136/annrheumdis-2019-215396
[9] He J, Chen J, Miao M, Zhang R, Cheng G, Wang Y, et al. (2022). Efficacy and Safety of Low-Dose Interleukin 2 for Primary Sjögren Syndrome: A Randomized Clinical Trial. JAMA Netw Open, 5(11), e2241451. https://doi.org/10.1001/jamanetworkopen.2022.41451
[10] Hartemann A, Bensimon G, Payan CA, Jacqueminet S, Bourron O, Nicolas N, et al. (2013). Low-dose interleukin 2 in patients with type 1 diabetes: a phase 1/2 randomised, double-blind, placebo-controlled trial. Lancet Diabetes Endocrinol, 1(4), 295-305. https://doi.org/10.1016/S2213-8587(13)70113-X
[11] Mitra S, & Leonard WJ. (2018). Biology of IL-2 and its therapeutic modulation: Mechanisms and strategies. J Leukoc Biol, 103(4), 643-655. https://doi.org/10.1002/jlb.2ri0717-278r
[12] Abbas AK, Trotta E, D RS, Marson A, & Bluestone JA. (2018). Revisiting IL-2: Biology and therapeutic prospects. Sci Immunol, 3(25). https://doi.org/10.1126/sciimmunol.aat1482
[13] Johnston JA, Kawamura M, Kirken RA, Chen YQ, Blake TB, Shibuya K, et al. (1994). Phosphorylation and activation of the Jak-3 Janus kinase in response to interleukin-2. Nature, 370(6485), 151-153. https://doi.org/10.1038/370151a0
[14] Ghoreschi K, Laurence A, & O'Shea JJ. (2009). Janus kinases in immune cell signaling. Immunol Rev, 228(1), 273-287. https://doi.org/10.1111/j.1600-065X.2008.00754.x
[15] Lin JX, Li P, Liu D, Jin HT, He J, Ata Ur Rasheed M, et al. (2012). Critical Role of STAT5 transcription factor tetramerization for cytokine responses and normal immune function. Immunity, 36(4), 586-599. https://doi.org/10.1016/j.immuni.2012.02.017
[16] Chinen T, Kannan AK, Levine AG, Fan X, Klein U, Zheng Y, et al. (2016). An essential role for the IL-2 receptor in T(reg) cell function. Nat Immunol, 17(11), 1322-1333. https://doi.org/10.1038/ni.3540
[17] Feng Y, van der Veeken J, Shugay M, Putintseva EV, Osmanbeyoglu HU, Dikiy S, et al. (2015). A mechanism for expansion of regulatory T-cell repertoire and its role in self-tolerance. Nature, 528(7580), 132-136. https://doi.org/10.1038/nature16141
[18] Ise W, Kohyama M, Nutsch KM, Lee HM, Suri A, Unanue ER, et al. (2010). CTLA-4 suppresses the pathogenicity of self antigen-specific T cells by cell-intrinsic and cell-extrinsic mechanisms. Nat Immunol, 11(2), 129-135. https://doi.org/10.1038/ni.1835
[19] Zheng Y, Josefowicz SZ, Kas A, Chu TT, Gavin MA, & Rudensky AY. (2007). Genome-wide analysis of Foxp3 target genes in developing and mature regulatory T cells. Nature, 445(7130), 936-940. https://doi.org/10.1038/nature05563
[20] Wing K, Onishi Y, Prieto-Martin P, Yamaguchi T, Miyara M, Fehervari Z, et al. (2008). CTLA-4 control over Foxp3+ regulatory T cell function. Science, 322(5899), 271-275. https://doi.org/10.1126/science.1160062
[21] Yao Z, Kanno Y, Kerenyi M, Stephens G, Durant L, Watford WT, et al. (2007). Nonredundant roles for Stat5a/b in directly regulating Foxp3. Blood, 109(10), 4368-4375. https://doi.org/10.1182/blood-2006-11-055756
[22] Feng Y, Arvey A, Chinen T, van der Veeken J, Gasteiger G, & Rudensky AY. (2014). Control of the inheritance of regulatory T cell identity by a cis element in the Foxp3 locus. Cell, 158(4), 749-763. https://doi.org/10.1016/j.cell.2014.07.031
[23] Shevyrev D, & Tereshchenko V. (2019). Treg Heterogeneity, Function, and Homeostasis. Front Immunol, 10, 3100. https://doi.org/10.3389/fimmu.2019.03100
[24] Wang X, Szymczak-Workman AL, Gravano DM, Workman CJ, Green DR, & Vignali DA. (2012). Preferential control of induced regulatory T cell homeostasis via a Bim/Bcl-2 axis. Cell Death Dis, 3(2), e270. https://doi.org/10.1038/cddis.2012.9
[25] Barahona de Brito C, & Patra AK. (2022). NFAT Factors Are Dispensable for the Development but Are Critical for the Maintenance of Foxp3(+) Regulatory T Cells. Cells, 11(9). https://doi.org/10.3390/cells11091397
[26] Wieczorek G, Asemissen A, Model F, Turbachova I, Floess S, Liebenberg V, et al. (2009). Quantitative DNA methylation analysis of FOXP3 as a new method for counting regulatory T cells in peripheral blood and solid tissue. Cancer Res, 69(2), 599-608. https://doi.org/10.1158/0008-5472.Can-08-2361
[27] Chen Q, Kim YC, Laurence A, Punkosdy GA, & Shevach EM. (2011). IL-2 controls the stability of Foxp3 expression in TGF-beta-induced Foxp3+ T cells in vivo. J Immunol, 186(11), 6329-6337. https://doi.org/10.4049/jimmunol.1100061
[28] Bending D, Pesenacker AM, Ursu S, Wu Q, Lom H, Thirugnanabalan B, et al. (2014). Hypomethylation at the regulatory T cell-specific demethylated region in CD25hi T cells is decoupled from FOXP3 expression at the inflamed site in childhood arthritis. J Immunol, 193(6), 2699-2708. https://doi.org/10.4049/jimmunol.1400599
[29] Huss DJ, Mehta DS, Sharma A, You X, Riester KA, Sheridan JP, et al. (2015). In vivo maintenance of human regulatory T cells during CD25 blockade. J Immunol, 194(1), 84-92. https://doi.org/10.4049/jimmunol.1402140
[30] Toker A, Engelbert D, Garg G, Polansky JK, Floess S, Miyao T, et al. (2013). Active demethylation of the Foxp3 locus leads to the generation of stable regulatory T cells within the thymus. J Immunol, 190(7), 3180-3188. https://doi.org/10.4049/jimmunol.1203473
[31] Correa LO, Jordan MS, & Carty SA. (2020). DNA Methylation in T-Cell Development and Differentiation. Crit Rev Immunol, 40(2), 135-156. https://doi.org/10.1615/CritRevImmunol.2020033728
[32] Chen C, Wang Z, Ding Y, Wang L, Wang S, Wang H, et al. (2022). DNA Methylation: From Cancer Biology to Clinical Perspectives. Front Biosci (Landmark Ed), 27(12), 326.

https://doi.org/10.31083/j.fbl2712326
[33] Guo C, Liu Q, Zong D, Zhang W, Zuo Z, Yu Q, et al. (2022). Single-cell transcriptome profiling and chromatin accessibility reveal an exhausted regulatory CD4+ T cell subset in systemic lupus erythematosus. Cell Rep, 41(6), 111606. https://doi.org/10.1016/j.celrep.2022.111606
[34] Bonazzi S, d'Hennezel E, Beckwith REJ, Xu L, Fazal A, Magracheva A, et al. (2023). Discovery and characterization of a selective IKZF2 glue degrader for cancer immunotherapy. Cell Chem Biol, 30(3), 235-247.e212. https://doi.org/10.1016/j.chembiol.2023.02.005
[35] Xin Y, Yang M, Zhao Z, He Z, Mei Y, Xiong F, et al. (2025). AIM2 deficiency in CD4(+) T cells promotes psoriasis-like inflammation by regulating Th17-Treg axis via AIM2-IKZF2 pathway. J Autoimmun, 150, 103351. https://doi.org/10.1016/j.jaut.2024.103351
[36] McDonald-Hyman C, Aguilar EG, Compeer EB, Zaiken MC, Rhee SY, Mohamed FA, et al. (2025). Acetyl-CoA carboxylase-1 inhibition increases regulatory T-Cell metabolism and graft-vs-host disease treatment efficacy via mitochondrial fusion. J Clin Invest, 10.1172/jci182480. https://doi.org/10.1172/jci182480
[37] Han J, Zhou Z, Wang H, Chen Y, Li W, Dai M, et al. (2025). Dysfunctional glycolysis-UCP2-fatty acid oxidation promotes CTLA4(int)FOXP3(int) regulatory T-cell production in rheumatoid arthritis. Mol Med, 31(1), 310. https://doi.org/10.1186/s10020-025-01372-6
[38] Feng R, Xiao X, Wang Y, Huang B, Chen J, Cheng G, et al. (2024). Metabolic impact of low dose IL-2 therapy for primary Sjögren's Syndrome in a double-blind, randomized clinical trial. Clin Rheumatol, 43(12), 3789-3798. https://doi.org/10.1007/s10067-024-07165-2
[39] Duan W, Ding Y, Yu X, Ma D, Yang B, Li Y, et al. (2019). Metformin mitigates autoimmune insulitis by inhibiting Th1 and Th17 responses while promoting Treg production. Am J Transl Res, 11(4), 2393-2402.
[40] Pokhrel RH, Kang B, Timilshina M, & Chang JH. (2022). AMPK Amplifies IL2-STAT5 Signaling to Maintain Stability of Regulatory T Cells in Aged Mice. Int J Mol Sci, 23(20). https://doi.org/10.3390/ijms232012384
[41] De La Rosa J, Geller AM, LeGros HL, Jr., & Kotb M. (1992). Induction of interleukin 2 production but not methionine adenosyltransferase activity or S-adenosylmethionine turnover in Jurkat T-cells. Cancer Res, 52(12), 3361-3366.
[42] Sahin E, & Sahin M. (2019). Epigenetical Targeting of the FOXP3 Gene by S-Adenosylmethionine Diminishes the Suppressive Capacity of Regulatory T Cells Ex Vivo and Alters the Expression Profiles. J Immunother, 42(1), 11-22. https://doi.org/10.1097/cji.0000000000000247
[43] Field CS, Baixauli F, Kyle RL, Puleston DJ, Cameron AM, Sanin DE, et al. (2020). Mitochondrial Integrity Regulated by Lipid Metabolism Is a Cell-Intrinsic Checkpoint for Treg Suppressive Function. Cell Metab, 31(2), 422-437.e425. https://doi.org/10.1016/j.cmet.2019.11.021
[44] Zhang X, Wang G, Bi Y, Jiang Z, & Wang X. (2022). Inhibition of glutaminolysis ameliorates lupus by regulating T and B cell subsets and downregulating the mTOR/P70S6K/4EBP1 and NLRP3/caspase-1/IL-1β pathways in MRL/lpr mice. Int Immunopharmacol, 112, 109133. https://doi.org/10.1016/j.intimp.2022.109133
[45] Deaglio S, Dwyer KM, Gao W, Friedman D, Usheva A, Erat A, et al. (2007). Adenosine generation catalyzed by CD39 and CD73 expressed on regulatory T cells mediates immune suppression. J Exp Med, 204(6), 1257-1265. https://doi.org/10.1084/jem.20062512
[46] Arpaia N, Green JA, Moltedo B, Arvey A, Hemmers S, Yuan S, et al. (2015). A Distinct Function of Regulatory T Cells in Tissue Protection. Cell, 162(5), 1078-1089. https://doi.org/10.1016/j.cell.2015.08.021
[47] Zhang P, Wang J, Miao J, & Zhu P. (2025). The dual role of tissue regulatory T cells in tissue repair: return to homeostasis or fibrosis. Front Immunol, 16, 1560578. https://doi.org/10.3389/fimmu.2025.1560578
[48] Hilaire M, Mimoun A, Cagnet L, Villette R, Roubanis A, Sentenac H, et al. (2025). Neonatal regulatory T cells persist into adulthood across multiple tissues with high enrichment in the skin. Sci Adv, 11(40), eadx8037. https://doi.org/10.1126/sciadv.adx8037
[49] Fallegger A, Priola M, Artola-Borán M, Núñez NG, Wild S, Gurtner A, et al. (2022). TGF-β production by eosinophils drives the expansion of peripherally induced neuropilin(-) RORγt(+) regulatory T-cells during bacterial and allergen challenge. Mucosal Immunol, 15(3), 504-514. https://doi.org/10.1038/s41385-022-00484-0
[50] Zhou X, Tang J, Cao H, Fan H, & Li B. (2015). Tissue resident regulatory T cells: novel therapeutic targets for human disease. Cell Mol Immunol, 12(5), 543-552. https://doi.org/10.1038/cmi.2015.23
[51] Wang Y, Feng R, Cheng G, Huang B, Tian J, Gan Y, et al. (2022). Low Dose Interleukin-2 Ameliorates Sjögren's Syndrome in a Murine Model. Front Med (Lausanne), 9, 887354. https://doi.org/10.3389/fmed.2022.887354
[52] Xie F, Zhou X, Fang M, Li H, Su P, Tu Y, et al. (2019). Extracellular Vesicles in Cancer Immune Microenvironment and Cancer Immunotherapy. Adv Sci (Weinh), 6(24), 1901779. https://doi.org/10.1002/advs.201901779
[53] Xia Y, Jiang H, Wang C, Liu Z, Gao H, Yu JF, et al. (2025). Treg cell-derived exosomal miR-21 promotes osteogenic differentiation of periodontal ligament stem cells. BMC Oral Health, 25(1), 1465. https://doi.org/10.1186/s12903-025-06770-0
[54] Okoye IS, Coomes SM, Pelly VS, Czieso S, Papayannopoulos V, Tolmachova T, et al. (2014). MicroRNA-containing T-regulatory-cell-derived exosomes suppress pathogenic T helper 1 cells. Immunity, 41(1), 89-103. https://doi.org/10.1016/j.immuni.2014.05.019
[55] Rahmani M, Mohammadnia-Afrouzi M, Nouri HR, Fattahi S, Akhavan-Niaki H, & Mostafazadeh A. (2018). Human PBMCs fight or flight response to starvation stress: Increased T-reg, FOXP3, and TGF-β1 with decreased miR-21 and Constant miR-181c levels. Biomed Pharmacother, 108, 1404-1411. https://doi.org/10.1016/j.biopha.2018.09.163
[56] Gertel S, Polachek A, Elkayam O, & Furer V. (2022). Lymphocyte activation gene-3 (LAG-3) regulatory T cells: An evolving biomarker for treatment response in autoimmune diseases. Autoimmun Rev, 21(6), 103085. https://doi.org/10.1016/j.autrev.2022.103085
[57] Ravichandran R, Itabashi Y, Fleming T, Bansal S, Bowen S, Poulson C, et al. (2022). Low-dose IL-2 prevents murine chronic cardiac allograft rejection: Role for IL-2-induced T regulatory cells and exosomes with PD-L1 and CD73. Am J Transplant, 22(9), 2180-2194. https://doi.org/10.1111/

ajt.17101
[58] Churlaud G, Jimenez V, Ruberte J, Amadoudji Zin M, Fourcade G, Gottrand G, et al. (2014). Sustained stimulation and expansion of Tregs by IL2 control autoimmunity without impairing immune responses to infection, vaccination and cancer. Clin Immunol, 151(2), 114-126. https://doi.org/10.1016/j.clim.2014.02.003
[59] Feng M, Guo H, Zhang C, Wang Y, Liang Z, Zhao X, et al. (2019). Absolute reduction of regulatory T cells and regulatory effect of short-term and low-dose IL-2 in polymyositis or dermatomyositis. Int Immunopharmacol, 77, 105912. https://doi.org/10.1016/j.intimp.2019.105912
[60] Rosenzwajg M, Lorenzon R, Cacoub P, Pham HP, Pitoiset F, El Soufi K, et al. (2019). Immunological and clinical effects of low-dose interleukin-2 across 11 autoimmune diseases in a single, open clinical trial. Ann. Rheum. Dis., 78(2), 209-217. https://doi.org/10.1136/annrheumdis-2018-214229
[61] Fusi I, Serger C, Herzig P, Germann M, Sandholzer MT, Oelgarth N, et al. (2025). PD-1-targeted cis-delivery of an IL-2 variant induces a multifaceted antitumoral T cell response in human lung cancer. Sci Transl Med, 17(816), eadr3718. https://doi.org/10.1126/scitranslmed.adr3718
[62] Kehry MR, Yamashita LC, & Hodgkin PD. (1990). B-cell proliferation and differentiation mediated by Th-cell membranes and lymphokines. Res Immunol, 141(4-5), 421-423. https://doi.org/10.1016/0923-2494(90)90033-u
[63] Cen Z, Li Y, Wei B, Wu W, Huang Y, & Lu J. (2021). The Role of B Cells in Regulation of Th Cell Differentiation in Coxsackievirus B3-Induced Acute Myocarditis. Inflammation, 44(5), 1949-1960. https://doi.org/10.1007/s10753-021-01472-5
[64] Park E, & Ciofani M. (2025). Th17 cell pathogenicity in autoimmune disease. Exp Mol Med, 57(9), 1913-1927. https://doi.org/10.1038/s12276-025-01535-9
[65] Cheng H, Nan F, Ji N, Ma X, Zhang J, Liang H, et al. (2025). Regulatory T cell therapy promotes TGF-β and IL-6-dependent pro-inflammatory Th17 cell generation by reducing IL-2. Nat Commun, 16(1), 7644. https://doi.org/10.1038/s41467-025-62628-7
[66] Dold L, Kalthoff S, Frank L, Zhou T, Esser P, Lutz P, et al. (2024). STAT activation in regulatory CD4(+) T cells of patients with primary sclerosing cholangitis. Immun Inflamm Dis, 12(4), e1248. https://doi.org/10.1002/iid3.1248
[67] Kim S, Boehme L, Nel L, Casian A, Sangle S, Nova-Lamperti E, et al. (2022). Defective STAT5 Activation and Aberrant Expression of BCL6 in Naive CD4 T Cells Enhances Follicular Th Cell-like Differentiation in Patients with Granulomatosis with Polyangiitis. J Immunol, 208(4), 807-818. https://doi.org/10.4049/jimmunol.2001331
[68] Ballesteros-Tato A, León B, Graf BA, Moquin A, Adams PS, Lund FE, et al. (2012). Interleukin-2 inhibits germinal center formation by limiting T follicular helper cell differentiation. Immunity, 36(5), 847-856. https://doi.org/10.1016/j.immuni.2012.02.012
[69] Chaudhry A, Rudra D, Treuting P, Samstein RM, Liang Y, Kas A, et al. (2009). CD4+ regulatory T cells control TH17 responses in a Stat3-dependent manner. Science, 326(5955), 986-991. https://doi.org/10.1126/science.1172702
[70] Rosenzwajg M, Lorenzon R, Cacoub P, Pham HP, Pitoiset F, El Soufi K, et al. (2019). Immunological and clinical effects of low-dose interleukin-2 across 11 autoimmune diseases in a single, open clinical trial. Ann Rheum Dis, 78(2), 209-217. https://doi.org/10.1136/annrheumdis-2018-214229
[71] Miao M, Li Y, Xu D, Zhang R, He J, Sun X, et al. (2022). Therapeutic responses and predictors of low-dose interleukin-2 in systemic lupus erythematosus. Clin Exp Rheumatol, 40(5), 867-871. https://doi.org/10.55563/clinexprheumatol/1o6pn1
[72] Rose A, von Spee-Mayer C, Kloke L, Wu K, Kühl A, Enghard P, et al. (2019). IL-2 Therapy Diminishes Renal Inflammation and the Activity of Kidney-Infiltrating CD4+ T Cells in Murine Lupus Nephritis. Cells, 8(10). https://doi.org/10.3390/cells8101234
[73] Zhou P, Chen J, He J, Zheng T, Yunis J, Makota V, et al. (2021). Low-dose IL-2 therapy invigorates CD8+ T cells for viral control in systemic lupus erythematosus. PLoS Pathog, 17(10), e1009858. https://doi.org/10.1371/journal.ppat.1009858
[74] Kim N, Jeon YW, Nam YS, Lim JY, Im KI, Lee ES, et al. (2016). Therapeutic potential of low-dose IL-2 in a chronic GVHD patient by in vivo expansion of regulatory T cells. Cytokine, 78, 22-26. https://doi.org/10.1016/j.cyto.2015.11.020
[75] Wang F, Wang S, He B, Liu H, Wang X, Li C, et al. (2021). Immunotherapeutic strategy based on anti-OX40L and low dose of IL-2 to prolong graft survival in sensitized mice by inducing the generation of CD4(+) and CD8(+) Tregs. Int Immunopharmacol, 97, 107663. https://doi.org/10.1016/j.intimp.2021.107663
[76] Onyshchenko K, Luo R, Guffart E, Gaedicke S, Grosu AL, Firat E, et al. (2023). Expansion of circulating stem-like CD8(+) T cells by adding CD122-directed IL-2 complexes to radiation and anti-PD1 therapies in mice. Nat Commun, 14(1), 2087. https://doi.org/10.1038/s41467-023-37825-x
[77] Kalia V, Sarkar S, Subramaniam S, Haining WN, Smith KA, & Ahmed R. (2010). Prolonged interleukin-2Ralpha expression on virus-specific CD8+ T cells favors terminal-effector differentiation in vivo. Immunity, 32(1), 91-103. https://doi.org/10.1016/j.immuni.2009.11.010
[78] Shameli A, Yamanouchi J, Tsai S, Yang Y, Clemente-Casares X, Moore A, et al. (2013). IL-2 promotes the function of memory-like autoregulatory CD8+ T cells but suppresses their development via FoxP3+ Treg cells. Eur J Immunol, 43(2), 394-403. https://doi.org/10.1002/eji.201242845
[79] Li S, Xie Q, Zeng Y, Zou C, Liu X, Wu S, et al. (2014). A naturally occurring CD8(+)CD122(+) T-cell subset as a memory-like Treg family. Cell Mol Immunol, 11(4), 326-331. https://doi.org/10.1038/cmi.2014.25
[80] Horwitz DA, Zheng SG, & Gray JD. (2003). The role of the combination of IL-2 and TGF-beta or IL-10 in the generation and function of CD4+ CD25+ and CD8+ regulatory T cell subsets. J Leukoc Biol, 74(4), 471-478. https://doi.org/10.1189/jlb.0503228
[81] Minai Y, Hisatsune T, Nishijima K, Enomoto A, & Kaminogawa S. (1994). Activation via TCR or IL-2 receptor of a CD8+ suppressor T cell clone: effect on IL-10 production and on proliferation of the suppressor T cell. Cytotechnology, 14(2), 81-87. https://doi.org/10.1007/bf00758172
[82] Elrefaei M, Ventura FL, Baker CA, Clark R, Bangsberg DR, & Cao H. (2007). HIV-specific IL-10-positive CD8+ T cells suppress cytolysis and IL-2 production by CD8+ T cells. J Immunol, 178(5), 3265-3271. https://doi.org/10.4049/jim-

munol.178.5.3265
[83] Grange M, Giordano M, Mas A, Roncagalli R, Firaguay G, Nunes JA, et al. (2015). Control of CD8 T cell proliferation and terminal differentiation by active STAT5 and CDKN2A/CDKN2B. Immunology, 145(4), 543-557. https://doi.org/10.1111/imm.12471
[84] Qin Y, Qian Y, Zhang J, & Liu S. (2025). CD1d-Restricted NKT Cells Promote Central Memory CD8(+) T Cell Formation via an IL-15-pSTAT5-Eomes Axis in a Pathogen-Exposed Environment. Int J Mol Sci, 26(15). https://doi.org/10.3390/ijms26157272
[85] Caligiuri MA. (2008). Human natural killer cells. Blood, 112(3), 461-469. https://doi.org/10.1182/blood-2007-09-077438
[86] Harris KE, Lorentsen KJ, Malik-Chaudhry HK, Loughlin K, Basappa HM, Hartstein S, et al. (2021). A bispecific antibody agonist of the IL-2 heterodimeric receptor preferentially promotes in vivo expansion of CD8 and NK cells. Sci Rep, 11(1), 10592. https://doi.org/10.1038/s41598-021-90096-8
[87] Hirakawa M, Matos TR, Liu H, Koreth J, Kim HT, Paul NE, et al. (2016). Low-dose IL-2 selectively activates subsets of CD4(+) Tregs and NK cells. JCI Insight, 1(18), e89278. https://doi.org/10.1172/jci.insight.89278
[88] McQuaid SL, Loughran ST, Power PA, Maguire P, Szczygiel A, & Johnson PA. (2020). Low-dose IL-2 induces CD56(bright) NK regulation of T cells via NKp44 and NKp46. Clin Exp Immunol, 200(3), 228-241. https://doi.org/10.1111/cei.13422
[89] Li Z, Lim WK, Mahesh SP, Liu B, & Nussenblatt RB. (2005). Cutting edge: in vivo blockade of human IL-2 receptor induces expansion of CD56(bright) regulatory NK cells in patients with active uveitis. J Immunol, 174(9), 5187-5191. https://doi.org/10.4049/jimmunol.174.9.5187
[90] Lee M, Bell CJM, Rubio Garcia A, Godfrey L, Pekalski M, Wicker LS, et al. (2023). CD56(bright) natural killer cells preferentially kill proliferating CD4(+) T cells. Discov Immunol, 2(1), kyad012. https://doi.org/10.1093/discim/kyad012
[91] Gumá M, Angulo A, Vilches C, Gómez-Lozano N, Malats N, & López-Botet M. (2004). Imprint of human cytomegalovirus infection on the NK cell receptor repertoire. Blood, 104(12), 3664-3671. https://doi.org/10.1182/blood-2004-05-2058
[92] Chen J, Ren E, Tao Z, Lu H, Huang Y, Li J, et al. (2025). Orchestrating T and NK cells for tumor immunotherapy via NKG2A-targeted delivery of a de novo designed IL-2Rβγ agonist. Drug Deliv, 32(1), 2482195. https://doi.org/10.1080/10717544.2025.2482195
[93] Unger ML, Hokland M, Basse PH, Nannmark U, & Johansson BR. (1997). High dose IL-2-activated murine natural killer (A-NK) cells accumulate glycogen and granules, lose cytotoxicity, and alter target cell interaction in vitro. Scand J Immunol, 45(6), 623-636. https://doi.org/10.1046/j.1365-3083.1997.d01-437.x
[94] Tiemessen MM, Jagger AL, Evans HG, van Herwijnen MJ, John S, & Taams LS. (2007). CD4+CD25+Foxp3+ regulatory T cells induce alternative activation of human monocytes/macrophages. Proc Natl Acad Sci U S A, 104(49), 19446-19451. https://doi.org/10.1073/pnas.0706832104
[95] Moore KW, de Waal Malefyt R, Coffman RL, & O'Garra A. (2001). Interleukin-10 and the interleukin-10 receptor. Annu Rev Immunol, 19, 683-765. https://doi.org/10.1146/annurev.immunol.19.1.683
[96] Zhang X, Miao M, Zhang R, Liu X, Zhao X, Shao M, et al. (2022). Efficacy and safety of low-dose interleukin-2 in combination with methotrexate in patients with active rheumatoid arthritis: a randomized, double-blind, placebo-controlled phase 2 trial. Signal Transduct Target Ther, 7(1), 67. https://doi.org/10.1038/s41392-022-00887-2
[97] Xue R, Li G, Zhou Y, Wang B, Xu Y, Zhao P, et al. (2024). Efficacy and safety of low-dose interleukin 2 in the treatment of moderate-to-severe bullous pemphigoid: A single center perspective-controlled trial. J Am Acad Dermatol, 91(6), 1113-1117. https://doi.org/10.1016/j.jaad.2024.08.033
[98] Li ZG, He J, & Miao M. (2023). Low-dose interleukin-2 therapy in autoimmune and inflammatory diseases: facts and hopes. Sci. Bull., 68(1), 10-13. https://doi.org/10.1016/j.scib.2022.12.024
[99] Malek TR. (2008). The biology of interleukin-2. Annu Rev Immunol, 26, 453-479. https://doi.org/10.1146/annurev.immunol.26.021607.090357
[100] Lykhopiy V, Malviya V, Humblet-Baron S, & Schlenner SM. (2023). "IL-2 immunotherapy for targeting regulatory T cells in autoimmunity". Genes Immun, 24(5), 248-262. https://doi.org/10.1038/s41435-023-00221-y
[101] Shevach EM. (2009). Mechanisms of foxp3+ T regulatory cell-mediated suppression. Immunity, 30(5), 636-645. https://doi.org/10.1016/j.immuni.2009.04.010
[102] Panduro M, Benoist C, & Mathis D. (2016). Tissue Tregs. Annu Rev Immunol, 34, 609-633. https://doi.org/10.1146/annurev-immunol-032712-095948
[103] Klatzmann D, & Abbas AK. (2015). The promise of low-dose interleukin-2 therapy for autoimmune and inflammatory diseases. Nat Rev Immunol, 15(5), 283-294. https://doi.org/10.1038/nri3823
[104] Castela E, Le Duff F, Butori C, Ticchioni M, Hofman P, Bahadoran P, et al. (2014). Effects of low-dose recombinant interleukin 2 to promote T-regulatory cells in alopecia areata. JAMA Dermatol, 150(7), 748-751. https://doi.org/10.1001/jamadermatol.2014.504
[105] Dong S, Hiam-Galvez KJ, Mowery CT, Herold KC, Gitelman SE, Esensten JH, et al. (2021). The effect of low-dose IL-2 and Treg adoptive cell therapy in patients with type 1 diabetes. JCI Insight, 6(18). https://doi.org/10.1172/jci.insight.147474
[106] Lim TY, Perpinan E, Londono MC, Miquel R, Ruiz P, Kurt AS, et al. (2023). Low dose interleukin-2 selectively expands circulating regulatory T cells but fails to promote liver allograft tolerance in humans. J Hepatol, 78(1), 153-164. https://doi.org/10.1016/j.jhep.2022.08.035
[107] Le Duff F, Bouaziz JD, Fontas E, Ticchioni M, Viguier M, Dereure O, et al. (2021). Low-Dose IL-2 for Treating Moderate to Severe Alopecia Areata: A 52-Week Multicenter Prospective Placebo-Controlled Study Assessing its Impact on T Regulatory Cell and NK Cell Populations. J Invest Dermatol, 141(4), 933-936.e936. https://doi.org/10.1016/j.jid.2020.08.015
[108] Humrich JY, Cacoub P, Rosenzwajg M, Pitoiset F, Pham HP, Guidoux J, et al. (2022). Low-dose interleukin-2 therapy in active systemic lupus erythematosus (LUPIL-2): a multicentre, double-blind, randomised and placebo-con-

trolled phase II trial. Ann. Rheum. Dis., 81(12), 1685-1694. https://doi.org/10.1136/ard-2022-222501

[109] Koreth J, Kim HT, Jones KT, Lange PB, Reynolds CG, Chammas MJ, et al. (2016). Efficacy, durability, and response predictors of low-dose interleukin-2 therapy for chronic graft-versus-host disease. Blood, 128(1), 130-137. https://doi.org/10.1182/blood-2016-02-702852

[110] Farooq A, Trehan S, Singh G, Arora N, Mehta T, Jain P, et al. (2024). A Comprehensive Review of Low-Dose Interleukin-2 (IL-2) Therapy for Systemic Lupus Erythematosus: Mechanisms, Efficacy, and Clinical Applications. Cureus, 16(9), e68748. https://doi.org/10.7759/cureus.68748

[111] Malek TR, & Bayer AL. (2004). Tolerance, not immunity, crucially depends on IL-2. Nat Rev Immunol, 4(9), 665-674. https://doi.org/10.1038/nri1435

[112] Todd JA, Evangelou M, Cutler AJ, Pekalski ML, Walker NM, Stevens HE, et al. (2016). Regulatory T Cell Responses in Participants with Type 1 Diabetes after a Single Dose of Interleukin-2: A Non-Randomised, Open Label, Adaptive Dose-Finding Trial. PLoS Med, 13(10), e1002139. https://doi.org/10.1371/journal.pmed.1002139

[113] Miao M, Xiao X, Tian J, Zhufeng Y, Feng R, Zhang R, et al. (2021). Therapeutic potential of targeting Tfr/Tfh cell balance by low-dose-IL-2 in active SLE: a post hoc analysis from a double-blind RCT study. Arthritis Res. Ther., 23(1), 167. https://doi.org/10.1186/s13075-021-02535-6

[114] He J, Zhang X, Wei Y, Sun X, Chen Y, Deng J, et al. (2016). Low-dose interleukin-2 treatment selectively modulates CD4(+) T cell subsets in patients with systemic lupus erythematosus. Nat. Med., 22(9), 991-993. https://doi.org/10.1038/nm.4148

[115] Humrich JY, & Riemekasten G. (2019). Low-dose interleukin-2 therapy for the treatment of systemic lupus erythematosus. Curr Opin Rheumatol, 31(2), 208-212. https://doi.org/10.1097/bor.0000000000000575

[116] von Spee-Mayer C, Siegert E, Abdirama D, Rose A, Klaus A, Alexander T, et al. (2016). Low-dose interleukin-2 selectively corrects regulatory T cell defects in patients with systemic lupus erythematosus. Ann. Rheum. Dis., 75(7), 1407-1415. https://doi.org/10.1136/annrheumdis-2015-207776

[117] Hu FY, Wang J, Zhang SX, Su R, Yan N, Gao C, et al. (2021). Absolute reduction of peripheral regulatory T cell in patients with relapsing polychondritis. Clin Exp Rheumatol, 39(3), 487-493. https://doi.org/10.55563/clinexprheumatol/qndtvt

[118] Rosenzwajg M, Salet R, Lorenzon R, Tchitchek N, Roux A, Bernard C, et al. (2020). Low-dose IL-2 in children with recently diagnosed type 1 diabetes: a Phase I/II randomised, double-blind, placebo-controlled, dose-finding study. Diabetologia, 63(9), 1808-1821. https://doi.org/10.1007/s00125-020-05200-w

[119] Saadoun D, Rosenzwajg M, Joly F, Six A, Carrat F, Thibault V, et al. (2011). Regulatory T-cell responses to low-dose interleukin-2 in HCV-induced vasculitis. N. Engl. J. Med., 365(22), 2067-2077. https://doi.org/10.1056/NEJMoa1105143

[120] Wang D, Fu B, Shen X, Guo C, Liu Y, Zhang J, et al. (2021). Restoration of HBV-specific CD8(+) T-cell responses by sequential low-dose IL-2 treatment in non-responder patients after IFN-alpha therapy. Signal Transduct Target Ther, 6(1), 376. https://doi.org/10.1038/s41392-021-00776-0

[121] Zhou X, Wang Y, Huang B, Feng R, Zhou X, Li C, et al. (2023). Dynamics of T follicular helper cells in patients with rheumatic diseases and subsequent antibody responses in a three-dose immunization regimen of CoronaVac. Immunology, 168(1), 184-197. https://doi.org/10.1111/imm.13572

[122] Zhang B, Sun J, Wang Y, Ji D, Yuan Y, Li S, et al. (2021). Site-specific PEGylation of interleukin-2 enhances immunosuppression via the sustained activation of regulatory T cells. Nat. Biomed. Eng., 5(11), 1288-1305. https://doi.org/10.1038/s41551-021-00797-8

[123] Levin AM, Bates DL, Ring AM, Krieg C, Lin JT, Su L, et al. (2012). Exploiting a natural conformational switch to engineer an interleukin-2 'superkine'. Nature, 484(7395), 529-533. https://doi.org/10.1038/nature10975

[124] Sockolosky JT, Trotta E, Parisi G, Picton L, Su LL, Le AC, et al. (2018). Selective targeting of engineered T cells using orthogonal IL-2 cytokine-receptor complexes. Science, 359(6379), 1037-1042. https://doi.org/10.1126/science.aar3246

[125] Horwitz DA, Kim D, Kang C, Brion K, Bickerton S, & La Cava A. (2025). CD2-targeted nanoparticles encapsulating IL-2 induce tolerogenic Tregs and TGF-β-producing NK cells that stabilize Tregs for long-term therapeutic efficacy in immune-mediated disorders. Front Immunol, 16, 1587237. https://doi.org/10.3389/fimmu.2025.1587237

[126] Koh B, Oz STG, Sato R, Nguyen HN, Dunlap G, Mahony C, et al. (2025). Functional and dysfunctional T regulatory cell states in human tissues in RA and other autoimmune arthritic diseases. bioRxiv, 10.1101/2025.09.23.677874. https://doi.org/10.1101/2025.09.23.677874

[127] Raposo A, Paço S, Ângelo-Dias M, Rosmaninho P, Almeida ARM, & Sousa AE. (2025). The distinctive signature of regulatory CD4 T cells committed in the human thymus. Front Immunol, 16, 1553554. https://doi.org/10.3389/fimmu.2025.1553554

[128] Cheng Z, Wang LJ, Honaker Y, Cincotta SA, Page CE, Vollhardt S, et al. (2025). Transcriptional fingerprinting of regulatory T cells: ensuring quality in cell therapy applications. Front Immunol, 16, 1602172. https://doi.org/10.3389/fimmu.2025.1602172

[129] Arroyo-Olarte RD, Flores-Castelán JC, Armas-López L, Escobedo G, Terrazas LI, Ávila-Moreno F, et al. (2024). Targeted Demethylation of FOXP3-TSDR Enhances the Suppressive Capacity of STAT6-deficient Inducible T Regulatory Cells. Inflammation, 47(6), 2159-2172. https://doi.org/10.1007/s10753-024-02031-4

[130] Kressler C, Gasparoni G, Nordström K, Hamo D, Salhab A, Dimitropoulos C, et al. (2020). Targeted De-Methylation of the FOXP3-TSDR Is Sufficient to Induce Physiological FOXP3 Expression but Not a Functional Treg Phenotype. Front Immunol, 11, 609891. https://doi.org/10.3389/fimmu.2020.609891

[131] Xu K, Liu Q, Wu K, Liu L, Zhao M, Yang H, et al. (2020). Extracellular vesicles as potential biomarkers and therapeutic approaches in autoimmune diseases. J Transl Med, 18(1), 432. https://doi.org/10.1186/s12967-020-

02609-0
[132] Feng R, Xiao X, Huang B, Zhang K, Zhang X, Li Z, et al. (2024). Predictive biomarkers for low-dose IL-2 therapy efficacy in systemic lupus erythematosus: a clinical analysis. Arthritis Res Ther, 26(1), 180. https://doi.org/10.1186/s13075-024-03388-5
[133] Friedberg JW, Neuberg D, Gribben JG, Fisher DC, Canning C, Koval M, et al. (2002). Combination immunotherapy with rituximab and interleukin 2 in patients with relapsed or refractory follicular non-Hodgkin's lymphoma. Br J Haematol, 117(4), 828-834. https://doi.org/10.1046/j.1365-2141.2002.03535.x
[134] Zhou H, Zhao X, Zhang R, Miao M, Pei W, Li Z, et al. (2023). Low-dose IL-2 mitigates glucocorticoid-induced Treg impairment and promotes improvement of SLE. Signal Transduction and Targeted Therapy, 8(1). https://doi.org/10.1038/s41392-023-01350-6
[135] Cases M, Ritter N, Rincon-Arevalo H, Kroh S, Adam A, Kirchner M, et al. (2025). Novel non-coding FOXP3 transcript isoform associated to potential transcriptional interference in human regulatory T cells. RNA Biol, 22(1), 1-20. https://doi.org/10.1080/15476286.2025.2502719
[136] Ramón-Vázquez A, Flood P, Cashman TL, Patil P, & Ghosh S. (2025). T lymphocyte plasticity in chronic inflammatory diseases: The emerging role of the Ikaros family as a key Th17-Treg switch. Autoimmun Rev, 24(3), 103735. https://doi.org/10.1016/j.autrev.2024.103735
[137] Lu Y, & Man XY. (2025). Diversity and function of regulatory T cells in health and autoimmune diseases. J Autoimmun, 151, 103357. https://doi.org/10.1016/j.jaut.2025.103357
[138] Bothur E, Raifer H, Haftmann C, Stittrich AB, Brüstle A, Brenner D, et al. (2015). Antigen receptor-mediated depletion of FOXP3 in induced regulatory T-lymphocytes via PTPN2 and FOXO1. Nat Commun, 6, 8576. https://doi.org/10.1038/ncomms9576
[139] Long SA, Cerosaletti K, Wan JY, Ho JC, Tatum M, Wei S, et al. (2011). An autoimmune-associated variant in PTPN2 reveals an impairment of IL-2R signaling in CD4(+) T cells. Genes Immun, 12(2), 116-125. https://doi.org/10.1038/gene.2010.54
[140] Lin JX, Ge M, Liu CY, Holewinski R, Andresson T, Yu ZX, et al. (2024). Tyrosine phosphorylation of both STAT5A and STAT5B is necessary for maximal IL-2 signaling and T cell proliferation. Nat Commun, 15(1), 7372. https://doi.org/10.1038/s41467-024-50925-6
[141] Santarlasci V, Mazzoni A, Capone M, Rossi MC, Maggi L, Montaini G, et al. (2017). Musculin inhibits human T-helper 17 cell response to interleukin 2 by controlling STAT5B activity. Eur J Immunol, 47(9), 1427-1442. https://doi.org/10.1002/eji.201746996
[142] Li Y, Lin D, Chen J, Zhang W, Jin H, Feng S, et al. (2025). Alkaline phosphatase-responsive hydrogel for efficient management of autoimmune intraocular inflammation. J Control Release, 387, 114229. https://doi.org/10.1016/j.jconrel.2025.114229
[143] Wahbi M, Wen Y, Kontopoulou M, & De France KJ. (2025). Modification of cellulose nanocrystals with epoxidized canola oil for enhancing interfacial compatibility with poly(lactic acid). Carbohydr Polym, 370, 124471. https://doi.org/10.1016/j.carbpol.2025.124471
[144] Shin H, Kang S, Won C, & Min DH. (2023). Enhanced Local Delivery of Engineered IL-2 mRNA by Porous Silica Nanoparticles to Promote Effective Antitumor Immunity. ACS Nano, 17(17), 17554-17567. https://doi.org/10.1021/acsnano.3c06733
[145] Jeon EY, Choi DS, Choi S, Won JY, Jo Y, Kim HB, et al. (2023). Enhancing adoptive T-cell therapy with fucoidan-based IL-2 delivery microcapsules. Bioeng Transl Med, 8(1), e10362. https://doi.org/10.1002/btm2.10362
[146] Wang J, Zhou L, & Liu B. (2020). Update on disease pathogenesis, diagnosis, and management of primary Sjögren's syndrome. Int J Rheum Dis, 23(6), 723-727. https://doi.org/10.1111/1756-185x.13839
[147] Streckfus C, Bigler L, Navazesh M, & Al-Hashimi I. (2001). Cytokine concentrations in stimulated whole saliva among patients with primary Sjögren's syndrome, secondary Sjögren's syndrome, and patients with primary Sjögren's syndrome receiving varying doses of interferon for symptomatic treatment of the condition: a preliminary study. Clin Oral Investig, 5(2), 133-135. https://doi.org/10.1007/s007840100104
[148] Zhao Z, Zhang X, Su L, Xu L, Zheng Y, & Sun J. (2018). Fine tuning subsets of CD4(+) T cells by low-dosage of IL-2 and a new therapeutic strategy for autoimmune diseases. Int Immunopharmacol, 56, 269-276. https://doi.org/10.1016/j.intimp.2018.01.042
[149] Villani AC, Sarkizova S, & Hacohen N. (2018). Systems Immunology: Learning the Rules of the Immune System. Annu Rev Immunol, 36, 813-842. https://doi.org/10.1146/annurev-immunol-042617-053035
[150] Smith PM, Howitt MR, Panikov N, Michaud M, Gallini CA, Bohlooly YM, et al. (2013). The microbial metabolites, short-chain fatty acids, regulate colonic Treg cell homeostasis. Science, 341(6145), 569-573. https://doi.org/10.1126/science.1241165
[151] Verra N, Jansen R, Groenewegen G, Mallo H, Kersten MJ, Bex A, et al. (2003). Immunotherapy with concurrent subcutaneous GM-CSF, low-dose IL-2 and IFN-alpha in patients with progressive metastatic renal cell carcinoma. Br J Cancer, 88(9), 1346-1351. https://doi.org/10.1038/sj.bjc.6600915
[152] Zhao XY, Zhao XS, Wang YT, Chen YH, Xu LP, Zhang XH, et al. (2016). Prophylactic use of low-dose interleukin-2 and the clinical outcomes of hematopoietic stem cell transplantation: A randomized study. Oncoimmunology, 5(12), e1250992. https://doi.org/10.1080/2162402x.2016.1250992
[153] Faridar A, Gamez N, Li D, Wang Y, Boradia R, Thome AD, et al. (2025). Low-dose interleukin-2 in patients with mild to moderate Alzheimer's disease: a randomized clinical trial. Alzheimers Res Ther, 17(1), 146. https://doi.org/10.1186/s13195-025-01791-x
[154] Bensimon G, Leigh PN, Tree T, Malaspina A, Payan CA, Pham HP, et al. (2025). Efficacy and safety of low-dose IL-2 as an add-on therapy to riluzole (MIROCALS): a phase 2b, double-blind, randomised, placebo-controlled trial. Lancet, 405(10492), 1837-1850. https://doi.org/10.1016/s0140-6736(25)00262-4
[155] Tong B, Leong SG, Jian T, Niu G, Gai Y, Meng X, et al. (2024). Site-specific pegylated IL2 mutein with biased IL2 receptor binding for cancer immunotherapy. Int Im-

munopharmacol, 136, 112359. https://doi.org/10.1016/j.intimp.2024.112359
[156] Karakus U, Sahin D, Mittl PRE, Mooij P, Koopman G, & Boyman O. (2020). Receptor-gated IL-2 delivery by an anti-human IL-2 antibody activates regulatory T cells in three different species. Sci. Transl. Med., 12(574). https://doi.org/10.1126/scitranslmed.abb9283
[157] Chen X, Wang L, Liu Q, Jia J, Liu Y, Zhang W, et al. (2014). Polycation-decorated PLA microspheres induce robust immune responses via commonly used parenteral administration routes. Int Immunopharmacol, 23(2), 592-602. https://doi.org/10.1016/j.intimp.2014.10.010
[158] Khoryati L, Pham MN, Sherve M, Kumari S, Cook K, Pearson J, et al. (2020). An IL-2 mutein engineered to promote expansion of regulatory T cells arrests ongoing autoimmunity in mice. Sci Immunol, 5(50). https://doi.org/10.1126/sciimmunol.aba5264